

University of Southampton Research Repository ePrints Soton

Copyright © and Moral Rights for this thesis are retained by the author and/or other copyright owners. A copy can be downloaded for personal non-commercial research or study, without prior permission or charge. This thesis cannot be reproduced or quoted extensively from without first obtaining permission in writing from the copyright holder/s. The content must not be changed in any way or sold commercially in any format or medium without the formal permission of the copyright holders.

When referring to this work, full bibliographic details including the author, title, awarding institution and date of the thesis must be given e.g.

AUTHOR (year of submission) "Full thesis title", University of Southampton, name of the University School or Department, PhD Thesis, pagination

UNIVERSITY OF SOUTHAMPTON

FACULTY OF ENGINEERING AND THE ENVIRONMENT

National Centre for Advanced Tribology at Southampton (nCATS)

Thick Film Sensors For Engine Oil Acidity Detection

by

Mostafa Soleimani



Thesis for the degree of Doctor of Philosophy

March 2014

This page is intentionally left blank

UNIVERSITY OF SOUTHAMPTON

ABSTRACT

FACULTY OF ENGINEERING AND THE ENVIRONMENT

Tribology

Thesis for the degree of Doctor of Philosophy

THICK FILM SENSORS FOR ENGINE OIL ACIDITY DETECTION

By Mostafa Soleimani

Engine oil condition monitoring has attracted considerable interests from industries and general public over the years due to its critical role in maintaining the performance and longevity of cars and industrial engines. Lubricants degrade during the course of operation and can be costly or detrimental to the engine if oil change intervals are not optimised. However, on-line robust monitoring for oils has been very challenging since oil degradation process is often complicated and influenced by a number of parameters, such as the operating temperature and contamination.

Due to the complexity of the oil chemistry and their degradation processes, there have not been any commercially available on-line sensors for oil chemical property monitoring reported. Oil acidity is traditionally measured through potentiometric or photometric/colorimetric titration methods. Recent attempts at miniaturising infrared (IR) and chronopotentiometric (CP) sensors based on solid-state devices for acidity/alkalinity determination of oil have not been very successful since the CP technology suffers from sensitivity and stability issues and IR sensors are still bulky and adversely susceptible to the engine's harsh environment.

This project, sponsored by Shell Global Solutions, aims to develop robust chemical sensors that can detect oil acidity due to oil degradation. The initial comprehensive literature review has identified that thick film (TF) sensor technology offers compact and low cost mass production solutions and have been proved to be robust with good reproducibility for aqueous solutions acidity measurements. Their feasibility in detecting oil acidity was thus investigated in this study and experimental work has been carried out to fabricate TF electrodes and evaluate them in a range of oils to explain their performance in detecting acid content. Based on their performance in aqueous solutions in previous studies, this study has investigated the performance of one type of TF working electrode (Ruthenium Oxide (RuO_2)) combined with various TF reference electrodes in order to develop the most suitable electrodes for oils. To simulate oil ageing, a fully formulated engine oil and a base oil were oxidised under controlled conditions. Also, different amount of nitric acid was added to a fully formulated oil to simulate the oil acidity changes. Acid number (AN) of the oil samples was obtained using conventional titration methods and viscosity and conductivity of the oil samples were measured using laboratory-based equipment in order to validate TF sensor measurements and

establish a relationship between different properties of oil samples during their degradation process. Temperature effects on thick film electrodes as well as their long-term stability and repeatability were also investigated.

The results show that, for the first time, TF sensors respond to the acidity changes in all oil types tested and linear correlation between the TF responses and the AN was found in the oxidised oils within certain ranges at the tested temperatures (50 °C and 80 °C). TF sensors can detect oil acidity up to AN of 28 mgKOH/g. Although oil conductivity and viscosity were affected by the oil oxidation process, but no direct relationship was found between them and the TF responses. Based on the experimental results, sensing mechanisms of the TF electrodes in oils are proposed.

Contents

ABSTRACT.....	III
CONTENTS.....	V
LIST OF TABLES	VIII
LIST OF FIGURES	IX
DECLARATION OF AUTHORSHIP	XIII
LIST OF PUBLICATIONS	XV
NOMENCLATURE.....	XVII
ACKNOWLEDGEMENTS	XIX
CHAPTER 1. INTRODUCTION.....	1
1.1 Background	2
1.2 Aims & objectives.....	3
1.3 Thesis Structure	4
CHAPTER 2. LITERATURE REVIEW	5
2.1 Maintenance Strategies	6
2.1.1 Condition Monitoring	7
2.1.2 Oil Condition Monitoring	8
2.2 Lubricating Oil.....	9
2.2.1 Base oil	9
2.2.2 Fully formulated oil	10
2.2.3 Oil additives.....	10
2.2.4 Oil properties	15
2.2.5 Oil degradation processes	23
2.3 Sensing technologies for oil condition monitoring.....	31
2.3.1 Techniques for oil viscosity analysis	31
2.3.2 Techniques for chemical analysis	35
2.3.3 Electrical property measurement	40
2.3.4 Indirect Methods	46
2.3.5 Integrated sensors	47
2.4 Summary.....	49

CHAPTER 3. THICK FILM TECHNOLOGY.....	51
3.1 Introduction.....	52
3.2 Screen printing technology (sensor fabrication).....	53
3.3 TF ion-selective electrodes for chemical sensing.....	57
3.4 Reference Electrode.....	59
3.5 Summary.....	62
CHAPTER 4. EXPERIMENTAL METHODOLOGIES.....	63
4.1 Introduction.....	64
4.2 Thick Film Electrodes for Oil Acidity Measurement.....	66
4.2.1 Electrode Design & Construction Process.....	66
4.2.2 Electronics and circuitry.....	71
4.2.3 Hydration and Calibration of the electrodes.....	72
4.3 Acid Number (AN) measurement.....	72
4.4 Conductivity measurement.....	73
4.5 Viscosity measurement.....	74
4.6 Oil samples.....	75
4.6.1 Oxidised base & fully formulated engine oil samples.....	75
4.6.2 Adding nitric acid into fresh fully formulated engine oil.....	77
4.7 Sensor evaluation tests.....	77
4.7.1 Temperature effects test.....	78
4.7.2 Stability and repeatability test.....	78
CHAPTER 5. RESULTS AND DISCUSSIONS.....	79
5.1 Introduction.....	80
5.2 Hydration and pH testing in buffer solutions.....	81
5.3 Oxidised base oil samples.....	84
5.3.1 AN, viscosity and EIS results.....	84
5.3.2 Electrochemical Impedance Spectroscopy (EIS):.....	84
5.3.3 Measurements using TF sensors.....	88
5.3.4 TF sensors vs. AN, viscosity, conductivity & water content.....	91
5.3.5 Conclusions.....	95
5.4 Oxidised engine oil samples.....	97
5.4.1 TF sensors responses.....	97
5.4.2 AN, Viscosity and conductivity measurements.....	99
5.4.3 Correlations between the TF sensors responses and AN, viscosity & conductivity.....	101

5.5	Oxidised base and fully formulated oil comparison	105
5.5.1	Conductivity	105
5.5.2	Viscosity	106
5.5.3	Acid Number (AN)	107
5.6	Adding nitric acid into fresh engine oil	108
5.6.1	Conductivity, Viscosity and AN measurements	108
5.6.2	TF sensors responses	109
5.6.3	Low acid concentration (0-200 ppm).....	112
5.6.4	Higher acid concentration (200-2000 ppm)	113
5.6.5	Summary.....	115
CHAPTER 6. THICK FILM SENSORS PERFORMANCE AND MECHANISM		117
6.1	Introduction.....	118
6.2	Temperature effects	119
6.2.1	Aqueous buffer solutions	119
6.2.2	Oxidised base oil samples	121
6.2.3	Oxidised fully formulated oil samples	125
6.3	Stability test	129
6.4	Repeatability test.....	130
6.5	REs type and design influence	131
6.6	Effects on the sensitivities of the TF electrodes	135
6.7	Proposed sensing mechanisms of TF electrodes.....	138
CHAPTER 7. CONCLUSIONS AND FURTHER WORK.....		141
7.1	Introduction.....	142
7.2	Conclusions.....	142
7.3	Future work.....	146
REFERENCES.....		149

List of Tables

Table 2-1: API Base oil categories	9
Table 2-2: Lubricant contaminants type and sources	24
Table 2-3: Viscometers and their characteristics	33
Table 4-1: List of reference electrodes used for the experiments	70
Table 4-2: Drying and curing temperatures for the pastes used for thick film electrodes fabrication	70
Table 4-3: Detail of the case studies and oil samples	75
Table 4-4: Oxidised base and fully formulated oil samples	76
Table 4-5 Details of the Oil samples.....	77
Table 5-1: Details of the oxidised oil samples.....	84
Table 5-2: Summary of the oxidised base oil samples test.....	96
Table 5-3: Summary of the oxidised fully formulated oil samples test.....	104
Table 5-4: Oxidised base and fully formulated oil samples and their equivalent numbers...	105
Table 5-5 summarises the TF sensors performance and other oil properties.	115
Table 5-6: Summary of the ' added acid to fresh engine oil' test.....	116
Table 6-1: Performance of TF RuO ₂ WE vs. different REs in oxidised base oil test.....	133
Table 6-2: Performance of TF RuO ₂ WE vs. different REs in oxidised fully formulated oil test.....	133
Table 6-3: Performance of TF RuO ₂ WE vs. different REs in nitric acid added to fresh engine oil test.....	134

List of Figures

Figure 2-1: A schematic of oil monitoring systems.....	8
Figure 2-2: A mode of an overbased detergent'	11
Figure 2-3: Acid neutralisation of overbased detergent.....	12
Figure 2-4: Acid and base reactions suggested by Hone et al.	12
Figure 2-5: A schematic showing the mechanism of dispersant molecule preventing soot formation.....	13
Figure 2-6: Viscosity-temperature plots of a number of particular oils.....	16
Figure 2-7: Electrode response versus pH value (pH-Voltage plot).....	19
Figure 2-8: AN, BN and iron content trend in a used lubricant (adopted from).....	20
Figure 2-9: Viscometer examples: a) Capillary, b) Rotational, and c) Cone on Plate.....	32
Figure 2-10: (a) Eitzen Visgage viscometer, (b) Viscolite 700 by Hydramotion Ltd.	33
Figure 2-11: Kittiwake (FG-K25197-KW) AN measurement device	35
Figure 2-12: Glass membrane electrode (a) pH meter (b) WE structure(c) RE structure (d) pH meter amplifier circuit.....	36
Figure 2-13: Output of iridium oxide sensors vs. acid number values in diesel oil samples...38	
Figure 2-14: IR sensor a) sensor design, and b) the sensor prototype ⁴⁶	39
Figure 2-15: A schematic of a two-electrode EIS sensor showing the equivalent circuits ⁴⁹ ...41	
Figure 2-16: An impedance spectrum for fresh and oxidised oils ⁴⁹	41
Figure 2-17: A schematic diagram of the platinum and RTD sensor ⁵⁵	43
Figure 2-18: The plot of sensor outputs versus the mileage driven after the oil change ⁵⁵	44
Figure 2-19: The conductometric sensor: polymer covering the inter-digital electrodes	45
Figure 2-20 Tan-delta dielectric sensor	46
Figure 2-21: Integrated oil sensor developed by Hella limited.....	47
Figure 3-1: A Silicon pressure sensor integrated with thick film integrated circuits	53
Figure 3-2: Schematic of different materials (inks and pastes) used, to produce conductors and other components of a thick film circuit	54
Figure 3-3: Cross-section of the open weave section of a thick film screen	55
Figure 3-4: (a) Thick film printing process, (b) squeegee pushing the ink through the porous area of the screen	55
Figure 3-5: A thick-film furnace parts	56
Figure 3-6: particle structure of a thick-film paste after firing	56

Figure 3-7: Two electrodes electrochemical cell configuration	57
Figure 3-8: Schematic of a silver-silver chloride reference electrode	61
Figure 3-9: Commercial (Beckman Coulter) silver-silver chloride reference electrode	62
Figure 4-1: Schematic demonstrating the overall test methodology	65
Figure 4-2: Schematic demonstrating the thick film electrode fabrication process.....	66
Figure 4-3: Top-view and cross section of glass Ag/AgCl thick film reference electrode.....	68
Figure 4-4: Top-view and cross section of polymer Ag/AgCl thick film reference electrode	68
Figure 4-5: Top-view and cross section of bare silver thick film reference electrode	69
Figure 4-6: Top-view and cross section of ruthenium oxide thick film working electrode	69
Figure 4-7: DEK 1209 infrared mini dryer	69
Figure 4-8: Schematic of the experimental setup for oil acidity measurement	71
Figure 4-9: Three different pH buffer solutions (250 ml in glass container) used for calibration of the electrodes	72
Figure 4-10: The EIS test cell configuration, (A) side view; (B) top view (excluding the top electrode).....	74
Figure 4-11: Brookfield CAP2000 viscometer	75
Figure 4-12: Shell oxidised base oil samples.....	76
Figure 5-1: The hydration response of TF electrodes in aqueous buffer solution (pH 7)	82
Figure 5-2: The hydration response of TF electrodes in aqueous buffer solution (pH 7)	82
Figure 5-3: Graph of working electrode vs. different reference electrodes and a commercial reference electrode in different pH buffer solutions	83
Figure 5-4: Calibration graph for each reference electrode	83
Figure 5-5: Bode plot of the oxidised oil samples at 50 °C	85
Figure 5-6: Bode plot of the oxidised oil samples at 80 °C	85
Figure 5-7: Capacitance magnitude of the oxidised oil samples (1-1000 Hz),.....	86
Figure 5-8: Nyquist plots of the oxidised oil samples at 50 °C	87
Figure 5-9: Nyquist plots of the oxidised oil samples at 80 °C	87
Figure 5-10: Effective conductivity of the oxidised oil samples at 50 and 80 °C	88
Figure 5-11: TF sensors output in oxidised oil samples, a) at 50 °C and b) at 80 °C	90
Figure 5-12: SEM results and the EDX analysis (shown in the tables below the figures) from fresh and used TF RuO ₂ working electrodes: (a) surface of the fresh electrode (X200), (b) surface of the used electrode (X170)	90
Figure 5-13: Thick-film electrodes output alongside AN, viscosity and conductivity graphs at 50 °C.....	93

Figure 5-14: Thick-film electrodes output alongside AN, viscosity and conductivity graphs at 80 °C.....	93
Figure 5-15: TF vs. AN of the oxidised oil samples, a) at 50 °C and b) at 80 °C.....	94
Figure 5-16: TF vs. viscosity of the oxidised oil samples, a) at 50 °C and b) at 80 °C	94
Figure 5-17: TF vs. conductivity of the oxidised oil samples, a) at 50 °C and b) at 80 °C.....	94
Figure 5-18: TF RuO ₂ WE vs. Polymer RE at 50 °C and 80 °C (left hand-side Y-axis) alongside water content plot (right hand-side Y-axis) of the oxidised oil samples (measured at room temperature (RT)).....	95
Figure 5-19: TF sensors output in oxidised fully formulated oil samples at 50 °C.....	98
Figure 5-20: TF sensors output in oxidised fully formulated oil samples at 80 °C.....	98
Figure 5-21: AN, conductivity and viscosity plots of the oxidised oil samples at 50 °C.....	100
Figure 5-22: AN, conductivity and viscosity plots of the oxidised oil samples at 80 °C.....	100
Figure 5-23: TF electrodes output alongside AN, viscosity and conductivity graphs at 50 °C	102
Figure 5-24: TF electrodes output alongside AN, viscosity and conductivity graphs at 80 °C	102
Figure 5-25: TF sensor responses vs. AN of the fully formulated oxidised oil samples, a) at 50 °C, and b) at 80 °C	103
Figure 5-26: Conductivity of oxidised fully formulated and base oil samples, a) at 50 °C, and b) at 80 °C	106
Figure 5-27: Viscosity of oxidised fully formulated and base oil samples, a) at 50 °C, and b) at 80 °C.....	107
Figure 5-28: AN of the oxidised fully formulated and base oil samples at room temperature	107
Figure 5-29 AN measurements of the degraded oil samples at room temperature combined with conductivity graphs at 50 and 80 °C.....	108
Figure 5-30: TF acidity sensors output in artificially degraded oil samples at 50 °C	109
Figure 5-31: TF acidity sensors output in artificially degraded oil samples at 80 °C	110
Figure 5-32: Acidity sensors output in oil samples (left y-axis) and the AN and conductivity of the oil samples (right y-axes).....	111
Figure 5-33: TF sensors output (left y-axis) and conductivity (right y-axis) of the oil samples at low acid concentration range.	111
Figure 5-34: TF sensors output (left y-axis) and conductivity (right y-axis) of the oil samples at low acid concentration range at 50 °C	112

Figure 5-35: TF sensors output (left y-axis) and conductivity (right y-axis) of the oil samples at low acid concentration range at 80 °C	113
Figure 6-1: Temperature effects on thick film RuO ₂ WE vs. Ag/AgCl glass reference electrode in pH 4, 7 and 10 buffer solutions	120
Figure 6-2: Temperature effects on thick film RuO ₂ WE vs. bare Ag reference electrode in pH 4, 7 and 10 buffer solutions.....	120
Figures 6-3: Temperature effects on thick film RuO ₂ WE vs. Ag/AgCl polymer reference electrode in pH 4, 7 and 10 buffer solutions	121
Figure 6-4: TF electrodes in 4 hours oxidised base oil sample tested at five temperatures ..	122
Figure 6-5: TF electrodes in 20 hours oxidised base oil sample tested at five temperatures	122
Figure 6-6: Temperature effect on conductivity of the oxidised base oil samples	123
Figure 6-7: Temperature effect on viscosity of the oxidised base oil samples	124
Figure 6-8: Temperature effect on TF electrodes, viscosity and conductivity of the 4 hours oxidised base oil sample	124
Figure 6-9: Temperature effect on TF electrodes, viscosity and conductivity of the 20 hours oxidised base oil sample	125
Figure 6-10: TF electrodes in 48 hours oxidised fully formulated oil sample tested at five temperatures.....	126
Figure 6-11: TF electrodes in 120 hours oxidised fully formulated oil sample tested at five temperatures.....	126
Figure 6-12: Temperature effect on conductivity of the oxidised fully formulated oil samples	127
Figure 6-13: Temperature effect on viscosity of the oxidised fully formulated oil samples.	127
Figure 6-14: Temperature effect on TF electrodes, viscosity and conductivity of the 48 hours oxidised fully formulated oil sample	128
Figure 6-15: Temperature effect on TF electrodes, viscosity and conductivity of the 120 hours oxidised fully formulated oil sample	128
Figure 6-16: Long term stability test of the TF electrodes in 24 hours oxidised oil at 50 °C	129
Figure 6-17: Repeatability test of the acidity sensors in oxidised base oil samples, a) at 50 °C, and b) at 80 °C	130
Figure 6-18: Response of TF RuO ₂ WE vs. glass RE at: a) 50 °C and b) 80 °C.....	137
Figure 6-19: Response of TF RuO ₂ WE vs. Bare Ag RE at: a) 50 °C and b) 80 °C	137
Figure 6-20: Response of TF RuO ₂ WE vs. polymer RE at: a) 50 °C and b) 80 °C	137
Figure 7-1: Design suggested for portable or on-line deployment of TF sensor	147

Declaration of Authorship

I, Mostafa Soleimani, declare that this thesis entitled '*Thick Film Sensors For Engine Oil Acidity Detection*' and the work presented in it are my own and has been generated by me as the result of my own original research. I confirm that:

- this work was done wholly or mainly while in candidature for a research degree at this University;
- where any part of this thesis has previously been submitted for a degree or any other qualification at this University or any other institution, this has been clearly stated;
- where I have consulted the published work of others, this is always clearly attributed;
- where I have quoted from the work of others, the source is always given. With the exception of such quotations, this thesis is entirely my own work;
- I have acknowledged all main sources of help;
- where the thesis is based on work done by myself jointly with others, I have made clear exactly what was done by others and what I have contributed myself;
- parts of this work have been published and these publications are listed in the following page.

Signed:.....

Date: 25th March 2014

This page is intentionally left blank

List of Publications

Journal publications:

- M. Soleimani, M. Sophocleous, M. Glanc, J. Atkinson, L. Wang, R.J.K. Wood, R.I. Taylor, *Engine oil acidity detection using solid state ion selective electrodes*, The Journal of Tribology International, Volume 65, Pages 48-56, 2013.
<http://www.sciencedirect.com/science/article/pii/S0301679X13000819>
- M. Soleimani, M. Sophocleous, L. Wang, J. Atkinson, I.L. Hosier, A. S. Vaughan, R. I. Taylor, R. J. K. Wood, *Base oil oxidation detection using novel chemical sensors and impedance spectroscopy measurements*, Sensors and Actuators B: Chemical, 2014.
<http://www.sciencedirect.com/science/article/pii/S0925400514003529>
- M. Soleimani, L. Wang, J. Atkinson, R. I. Taylor, R. J. K. Wood, *Degradation analysis of fully formulated and base oil samples by in-situ acidity sensors and off-line techniques*, in preparation to be submitted to Sensors and Actuators B: Chemical, 2014.

Conference papers:

- M. Soleimani, L. Wang, J. Atkinson, R. I. Taylor, R. J. K. Wood, *Lubricating oil condition monitoring using thick film acidity sensors*, Proc. of World Tribology Congress, Torino, Italy, 2013.
- M. Soleimani, L. Wang, J. Atkinson, I. L. Hosier, R. I. Taylor, R. J. K. Wood, A. S. Vaughan, *Oil condition monitoring using novel chemical sensors and impedance measurements*, Proc. of Condition Monitoring (CM) & MFPT, Kraków, Poland, 2013.
- M. Soleimani, L. Wang, J. Atkinson, R. I. Taylor, R. J. K. Wood, *Oil degradation monitoring using chemical and electrical sensing techniques*, STLE 68th Annual Meeting, Detroit, USA, 2013.
- M. Soleimani, L. Wang, R. J. K. Wood, R. I. Taylor, *Engine oil acidity detection using solid state ion selective electrodes*, 39th Leeds-Lyon Conference on Tribology Challenges, Leeds, UK, 2012.
- M. Soleimani, L. Wang, R. J. K. Wood, R. I. Taylor, *Engine Oil Age Detection Using Integrated Smart Sensors*. Conference Proc. in Post Graduate Research Conference (PGR), Southampton, UK, 2011.

This page is intentionally left blank

Nomenclature

ε_0	Electric constant of air ($\approx 8.854 \times 10^{-12} \text{ Fm}^{-1}$)
ε	Relative permittivity or dielectric constant
ρ	Density
η	Dynamic viscosity
A	cross section area
AC	Alternating Current
Ag/AgCl	Silver/Silver-Chloride
AN	Acid number
API	The American Petroleum Institute
ASTM	American Society for Testing and Materials
ATR	Attenuated Total Reflection
BN	Base number
CBM	Condition based maintenance
CP	Chronopotentiometric
CV	Cyclic Voltammetry
d	Distance between the two conductor plates (capacitor)
EC	Equivalent Circuit
ECU	Engine Control Unit
EGR	Exhaust Gas Recirculation
EIS	Electrochemical Impedance Spectroscopy
EMS	Engine Management System
E-nose	Electronic nose
I	Electrical Current
IC	Integrated Circuits
IM	Improvement Maintenance
IR	Infrared Spectroscopy
IS	Impedance Spectroscopy
ISE	Ion Selective Electrodes
ISFET	Ion-Sensitive Field-Effect Transistor
JASO	Japanese Automobile Standard Organisation

k	electrical conductivity
l	length
MEMS	Micro Electro-Mechanical Systems
MOSFET	metal-oxide-semiconductor FET
PAO	Polyalphaolefin
PD	Potential Difference
PDM	Predictive Maintenance
PM	Preventive Maintenance
QCM	Quartz Crystal Microbalance
QDM	Quantitative Debris Monitor
R	Electrical Resistance
RTD	Resistance Temperature device
RTF	Run to Failure Maintenance
RuO ₂	Ruthenium Oxide
SAE	The Society of Automotive Engineers
SIEs	Specific Ion Electrodes
T	Absolute temperature
TF	Thick Film
V	Electrical Voltage
VII	Viscosity index improvers
WE	Working Electrode
RE	Reference Electrode
ZnDTPs	Zinc dithiophosphates

Acknowledgements

I would like to express gratitude towards my supervisors, Dr Ling Wang and Professor Robert Wood for their supervision and guidance through the years of my PhD, and for introducing me to an exciting field of Tribology, unknown to me before starting my research. The completion of this thesis would not have been possible without their persistent support.

I would like to thank Shell Global Solutions (UK) for providing me with a generous studentship for the PhD. Extra and very important thanks go to Dr Ian Taylor at Shell for his visits and invaluable assistance with the project. Special thanks go to Brian Papke at Shell Technology Centre Houston for preparing and providing the oxidised oil samples.

I am also thankful to Dr John Atkinson for allowing me to use the Thick Film facilities and for enthusiastically sharing his knowledge and expertise on TF sensing which greatly influenced the steering of this project. Special thanks go to Marios Sophocleous for the useful discussions and Monika Glanc for her help with the fabrication of the TF sensors.

Many thanks to Professor Alun Vaughn, Dr Ian Hosier and their colleagues at Tony Davies High Voltage Lab (TDHV, ECS) for allowing me to use the material laboratory and the impedance spectroscopy facilities. I am also thankful to Graham Hearn (Wolfson Electrostatics) for his assistance on electrical measurements and providing the conductivity meter. Very special thanks go to Professor Harvey Ruth (Head of ECS) for that one hour meeting in January 2011, introducing me to related research groups at TDHV lab and asking his son to provide used oil samples at the local garage.

I am also thankful to Dr Terry Harvey and Dr Mengyan Nie for all their assistance in the practical aspects of the project. Special thanks to Mohammad Vaezi and Dr Hamed Shahidipour for their support and giving me the time whenever needed. I am also thankful to my past and present officemates (7/4035), Dr Maria Salta, Dr Amir Rmaile, Dr Robert Hanzel, Natalya Doroshenko, Lianne Niehaus, Vanesa Martinez and Stefania Fabbri, who were encouraging and supportive during my PhD life.

Thanking the special ones is far broader a matter to fit into the context of a PhD thesis. Yet it is more than appropriate that I express most heartfelt gratitude towards my loving and beloved family for their truly unwavering support in all senses of the matter.

This page is intentionally left blank

Chapter 1. **Introduction**

1.1 Background

Lubrication is a major requirement for most applications that involve moving parts. Lubricating oils are employed in machineries to minimise friction, remove heat and wear particles, protect against corrosion, etc. The quality of lubrication has a huge effect on the efficiency of production processes. Lubricants degrade during the course of operation and the degradation process is governed by many parameters such as the operating temperature, pressure, contaminants etc. Lubricant deterioration leads to undesired consequences such as system malfunction, damage and failure. To avoid severe damages and reduce repair cost, it is desirable for all machineries to have an appropriate maintenance strategy to keep the quality of the lubricants above acceptable levels. Although a number of on-line and off-line sensing technologies such as single property sensors have been developed to measure various oil properties for oil monitoring, in practice, engine oil changes still largely rely on their mileage, drivers' driving style and habit, driving routines (city or highway) etc. For instance, the recommended oil change interval for gasoline cars is 2 years or 20,000 miles whilst for diesel cars, it is typically 1 year or 10,000 miles. These practices are not based on real condition of the oils thus have economic and environmental implications due to premature changing and can cause damages to engines owing to overdue changes. To correctly predict oil age, sophisticated methods that can provide information on lubricant conditions are demanded by a wide range of industries such as car and lubricant manufacturers. This project, sponsored by Shell Global Solutions, studied the current development in oil sensing and developed a novel sensing technique toward on-line oil condition monitoring.

1.2 Aims & objectives

The overall aim of this project is to develop robust sensors that can detect oil degradation. In order to accomplish this, initially, feasibility of fabricating different types of physical, chemical and electrical sensors was explored through literature review and preliminary laboratory experiments. Sensor fabrication using screen printing (thick film) technique was selected due to their significant advantages and robustness in chemical sensing of aqueous solutions. Although these types of sensors have been applied in the measurement of aqueous solutions, their application in oil acidity measurements have not been investigated before. Experiments have been carried out to examine their ability in determining oil ageing process.

The objectives of this research are to:

- study the state-of-the-art of the lubricants, their degradation process, current lubricant sensing methods and recent technological advances in oil condition monitoring
- design and fabricate novel thick film ion selective working electrodes (chemical sensors) for acidity determination of oil samples
- test the performance of the developed thick film electrodes in a variety of artificially degraded oil samples
- develop an understanding in oil degradation process and establish correlations between oil ageing and sensor outputs
- validate the chemical sensors results by testing the same oil samples by other laboratory-based devices (viscometers, impedance spectroscopy etc.)

1.3 Thesis Structure

This thesis is divided into seven chapters. This chapter is followed by a review on the main theory and relevant literature of lubricant condition monitoring. Chapter 2 starts with an overview on maintenance schemes and a detailed analysis of lubricants which includes the lubricant's composition, properties, additives, ageing and oxidation process. Condition monitoring techniques for lubricants are investigated in the next section detailing the important techniques for oil sensor fabrication and recent developments in the field of oil condition monitoring. Chapter 3 reviews the thick film (TF) technology used in this study to develop the novel acidity sensors and also discusses the details of TF working and reference electrodes.

Chapter 4 provides a description of the research methodologies and experimental details in this study. Initially, TF acidity sensor design, development and fabrication for this project, are discussed followed by preparation and calibration of the sensors for oil testing. Laboratory based devices (e.g. impedance spectroscopy and viscometers) which were used to validate acidity sensors results are also discussed in this chapter. The detail of the systematically degraded oil samples by either adding nitric acid or oxidation at Shell's Houston laboratories and other tests carried out such as temperature effect, stability and repeatability tests will be presented too.

Chapter 5 presents the experimental results of the TF acidity sensors in different degraded oil samples alongside other off-line measurements. The correlations between acidity sensors results and oil ageing as well as different oil properties are also discussed in this chapter. The performance of the TF acidity sensors is further analysed in Chapter 6 and the effects of temperature on the sensors as well as the results from stability and repeatability tests are presented. Also in this chapter, sensing mechanisms of the TF electrodes in aqueous solutions and oil samples are proposed and discussed.

Chapter 7 presents the overall conclusions from this study and suggestions for future work.

Chapter 2. Literature Review

2.1 Maintenance Strategies

Maintenance is defined as¹:

“The combination of all technical and administrative actions, intended to retain an item in, or restore it to, a state in which it can perform a required function.”

Before the Second World War, maintenance was thought of as an unnecessary extra cost to factories with no added value to finished products and thus repairing the broken component was the cheapest alternative (*Run to Failure Maintenance (RTF)*). After the Second World War and with emergence of novel engineering and scientific technologies, *Preventive Maintenance (PM)* proved to be more efficient and became part of the production system. The PM scheme is based on maintenance of systems and equipment before fault occurrence and is divided into *planned maintenance* and *condition-based maintenance*.

The maintenance evolution has since continued and it has become one of the most important functions in any industry alongside environment safety, quality of product and services². The foremost objective of maintenance is to keep the machines and facilities in their best condition while maximising the performance at the lowest cost. Other types of maintenance (after RTF and preventive) include Corrective Maintenance, Improvement Maintenance (IM) and Predictive Maintenance (PDM). Apart from Corrective Maintenance which is carried out after the occurrence of a failure, IM and PDM aim to find and eliminate the cause of the failure e.g. by redesigning the vulnerable equipment. PDM is different to preventive maintenance in the sense that it takes a step further by monitoring the actual condition of the desired equipment by looking for signs of failure. This method is implemented by either Condition or Statistical based predictive maintenance techniques. In the latter technique, failure predictive models, based on the statistical data collected from components, are developed. However, in condition based maintenance (CBM), diagnostic devices are employed to continuously or intermittently monitor the state of the machine, looking for signs of change, during operation^{2,3}.

Among other techniques, CBM has become popular due to indistinct advantage of monitoring the actual state of machine using sensors and other diagnostic devices.

2.1.1 Condition Monitoring

Condition monitoring is defined as⁴:

“...a type of maintenance inspection where an operational asset is monitored and the data obtained analysed to detect signs of degradation, diagnose cause of faults, and predict for how long it can be safely or economically run.”

Generally, condition monitoring increases the performance of a machine and its life-time, lowers the operating costs, reduces the downtime cost and prevents failures. Condition monitoring strategies play an important role in many machine based technologies and systems maximising machine reliability, availability and maintainability. The conventional condition monitoring approach is the observation of an apparatus condition based on sensing main properties/parameters, monitoring system performance and making confident assessments of degradation⁵.

Lubrication is a major requirement for most applications involving moving parts. The quality of lubrication affects the efficiency of production processes alongside the type and condition of the lubricant. Lubricants degrade during use and the degradation process is governed by many parameters in the system such as pressure, applied loads, operating temperature, contamination, wear, fuel interaction etc. Lubricant deterioration leads to a number of undesired consequences. Primarily the system efficiency decreases in addition to progressive deterioration of the lubricant which involves its chemical decomposition. The process of lubricant degrading will continue and if necessary actions are not taken, it can cause system delays, malfunctions, damage and even failure. Furthermore, to avoid these and the resultant high repair costs, maintenance programmes are employed to anticipate the life time of the lubricants. Determining oil state has been progressively revolutionised and is carried out via different practices such as predicted change intervals (e.g. annually) and laboratory-based analysis. However, these methods suffer from clear drawbacks including premature oil changes with obvious economical and environmental issues associated with the new and disposal of old lubricants and short maintenance intervals. Overdue exchange, on the other hand, will lead to the aforementioned complications. Therefore, the interest in developing a more sophisticated method in determining the condition of the lubricant (for oil changes) has grown amid automotive, industrial and lubricant companies.

2.1.2 Oil Condition Monitoring

Oil condition monitoring can be carried out either off-line, on-line or in-line (real-time), as can be seen in Figure 2-1. Off-line oil analysis involves taking oil samples in regular intervals, e.g. minutes, hours, days or months depending on the machine, analysing relevant oil properties in an onsite or off-site laboratory, and providing information on oil age for maintenance plans. The laboratory techniques include viscosity measurements, wear debris detection, elemental/chemical analysis etc.

Sample extraction out of the system and analysis in laboratory has clear limitations and disadvantages such as long delays, inaccuracy due to handling of samples/late measurements, expenses of shipment and analysis, safety issues, etc. Thus on-line/in-line condition monitoring systems are preferable as they measure the actual lubricants properties and produce outputs based on a wide range of data. Real-time monitoring systems consist of sensors and data acquisition devices which collect measurements for condition monitoring. The main advantage of such a system is its proactive and predictive approach in maintaining the quality of oil and avoids the reactive maintenance practice which causes system damages and failures to the system and its components.

Sensing techniques that have been used in oil condition monitoring can be based on lubricant properties measurement and measurement of oil contaminations. Before discussing different oil condition monitoring techniques, it is essential to review lubricant composition, oil degradation processes and sensing techniques.

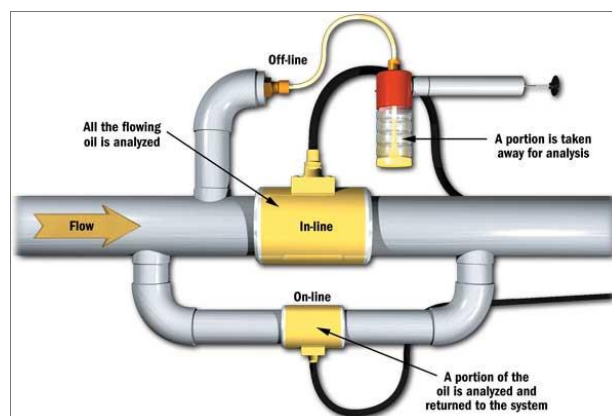


Figure 2-1: A schematic of oil monitoring systems⁶

2.2 Lubricating Oil

Lubrication technology dates back to 3,000 years ago when animal fats and vegetable oils were used before petroleum-based oils became common. The evolution of petroleum-based lubricating oil has seen many phases in order to improve base oil quality; from early processes such as acid treating and solvent extraction, which removed unnecessary molecules from the oil such as aromatics, to advanced processes e.g. hydrotreating and catalytic dewaxing improving specific lubricating qualities.

2.2.1 Base oil

Lubricating oils are employed in machinery to minimise friction, remove heat and wear particles, protect against corrosion, sealing, etc. Depending on their base stock composition and their sources, the base oils are classified into mineral and synthetic oils. Mineral oils have base oils, which are derived from natural crude oils from distillation process while synthetic oils are artificially manufactured by chemical processes⁷. Mineral oils mainly contain hydrocarbons such as Alkanes (also known as paraffins, major compound in crude oils), Cycloalkanes (also known as naphthenes, second most common) and aromatics (small proportion 2 to 8%); they are more commonly used due to the advantages of being relatively inexpensive, high stability and good availability. The American Petroleum Institute (API) has divided mineral oils into five main groups depending on volume of sulphur, saturates and viscosity index, as shown in Table 2-1⁸.

Group	Sulphur % wt.		Saturates %	Viscosity Index
I	> 0.03	and/ or	< 90	80 to 120
II	≤ 0.03	and	≥ 90	80 to 120
III	≤ 0.03	and	≥ 90	≥ 120
IV	100% poly-alpha-olefin (PAO)			
V	All other base oils not included in Groups I-IV (naphthenics, esters and polyglycols)			

Table 2-1: API Base oil categories

Unlike group I to III base oils which are derived from natural crude oils, synthetic oils are typically assembled from purified single chemicals by breaking down crude oil. There are four main types of synthetic base oil: Synthesised Hydrocarbons such as XHVI and PAO, Polyglycols, Organic esters and Phosphate esters. Other base oils include Silicones, silicate

esters and polphenyl esters. Most common synthetic lubricating oil is Polyalphaolefins (PAOs) based, which have been widely used in aerospace and space as well as automotive applications. Synthetic lubricants can also be made by further processing of mineral base oils (not just manufactured by separate processes). Group II and Group III base oils are often described as being synthetic (e.g. XHVI is a Group III base oil), whilst PAOs are Group IV and various other synthetics are Group V. Synthetic oils tend to have higher viscosity index than mineral oils thus are suitable for a larger temperature range⁹.

2.2.2 Fully formulated oil

Evolution of sophisticated machineries (e.g. car engines) has increased the demand for improved lubricating oil. Oil additives are used to improve the performance and to prolong the life of base oils. Oils are used in a wide variety of applications such as in gears, hydraulic systems, compressors, metal working and combustion engines. Amount and type of additives may vary depending on the application. Fully formulated lubricants are organic polymeric liquids produced by complexly blended base oils (usually synthetic or group III base oil) and specialised polar additives which are composed of a polar functional group (i.e. “head”) and long nonpolar hydrocarbon “tail” and often exist in the form of inverse micelles in oils¹⁰. Fully formulated lubricants are mainly used in internal combustion engines and are graded according to their viscosity characteristics by The Society of Automotive Engineers (SAE).

2.2.3 Oil additives

Lubricating oils contain a large proportion of base oil (up to 95%) and an additive package varying between 5-25% depending on the application. For instance in a number of hydraulic and compressor oils only 1% additives are used, whereas certain metalworking fluids contain up to 30% additive⁹. The main reason for mixing additives is that the base oils generally cannot satisfy the requirements of high performance lubricants. Apart from a small portion of polymers including Viscosity index improvers (VII) and pour point depressants that are often added to oils to increase the range of temperatures that oils work, a number of additives are also added to improve the functions of the oils, which may include:

- Anti-wear additives
- Extreme pressure additives
- Friction modifiers

- Rust/corrosion inhibitors
- Anti-oxidants
- Detergents
- Ashless dispersants
- Anti-foam additives

Detergents and dispersants are discussed in detail below as they are associated to the experiments in this study. More details about other additives can be found elsewhere¹⁶.

2.2.3.1 Detergents

Detergents are metal salt nanoparticles comprising a carbonate core and surfactants outer layer which provide cleanliness, deposit prevention, reduced friction (i.e. fuel efficiency), good extreme pressure properties and are corrosion/wear inhibitors. Detergents typically comprise of large amounts of base (core), referred to as overbased, which are quantified by base number (BN) in oils. BN is a measure of reserve alkalinity of lubricants and measures the amount of potassium hydroxide (in milligrams) contained in per gram oil (mgKOH/g). In a model¹¹ for an overbased calcium carbonate detergent, three layers are defined as elucidated in Figure 2-2. The surfactant polar-head (hydroxide) binds to the mineral salt (carbonate) and stabilises the calcium carbonate (CaCO_3) particles which are typically long chain carboxylic acid, glycol or alcohol¹².

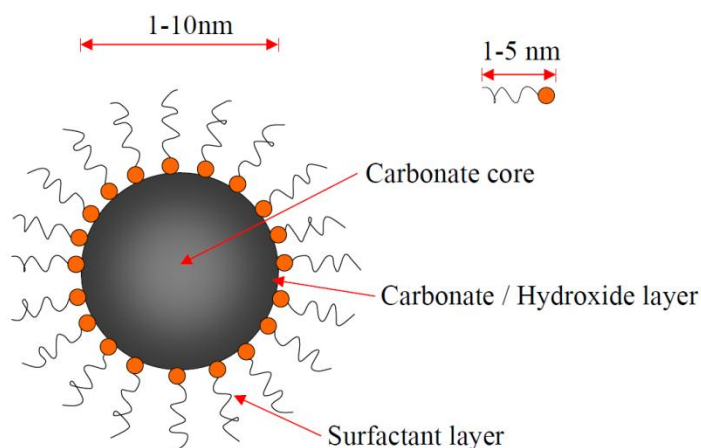


Figure 2-2: A mode of an overbased detergent^{13,14}

The main functions of detergents include: acid neutralisation, high temperature detergency, oxidation inhibition and rust prevention¹². The overbased property of the detergents neutralises acidic combustion and oxidation products such as sulphur, nitric and carboxylic

acids. During an effective collision, the base from detergents transfers into the acid-containing droplet which enables solubilisation of the salts and hence keeps the naturalised products suspended in the lubricant (Figure 2-3). This process takes only a few seconds and the droplets can be detached from the particles after the reaction due to the difference in sedimentation coefficients between the two product species.

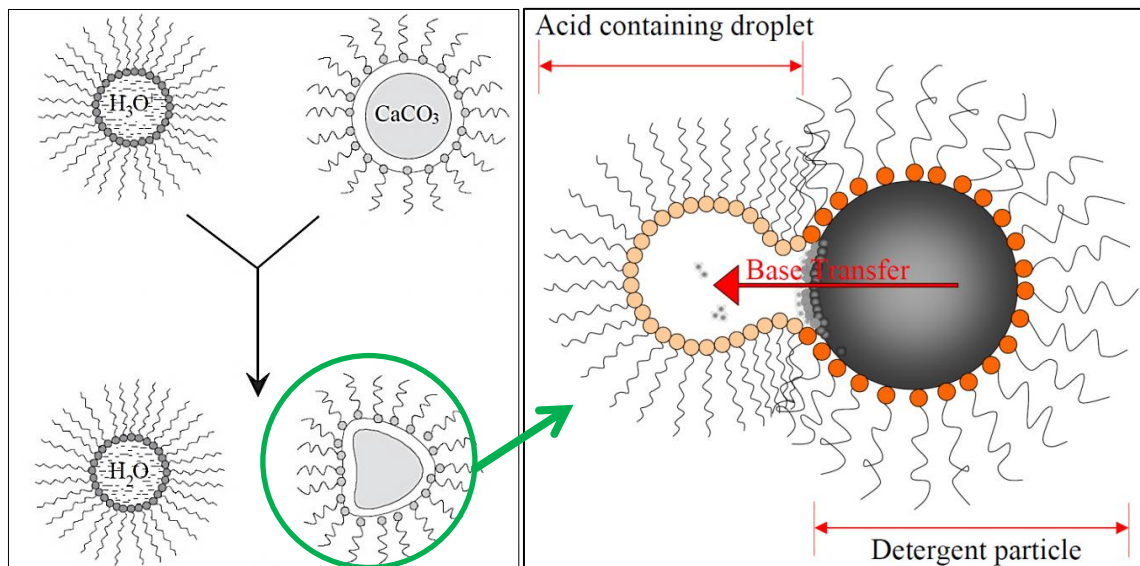


Figure 2-3: Acid neutralisation of overbased detergent¹⁴

The reaction between an organic acid (RH) and a base (B) gives two types of products, either a hydrogen-bonded complex (RH–B) or a hydrogen-bonded ion pair (R–HB⁺), as shown in Figure 2-4¹³. The strong attraction between positive and negative charged ions holds these products together in the oil (low-dielectric medium) and these products mainly depend on the relative acid–base strength of the reacting partners¹³.

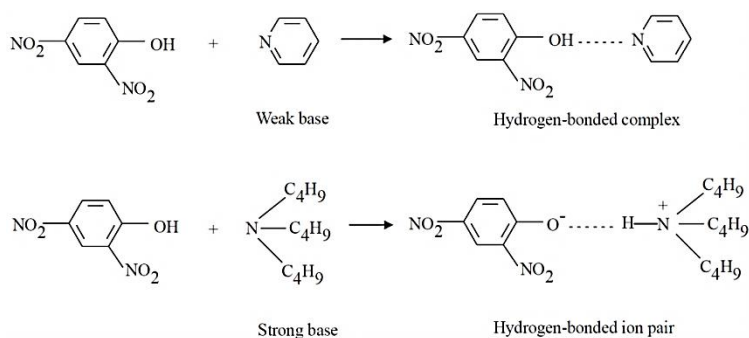


Figure 2-4: Acid and base reactions suggested by Hone et al.¹³

2.2.3.2 Dispersants

Dispersants are added to lubricating oil in order to stabilise contaminants and prevent filter plugging effects. They also control wear and lubricants viscosity by reducing formation of large soot particles, as shown in Figure 2-5. This process initiates by dispersant molecule attaching to an acid molecule on the soot surface (Figure 2-5a) followed by charge formation of the transferred protons from the acid group to the succinimide group (Figure 2-5b). Charged soot cannot mix due to steric or electrostatic factors (Figure 2-5c) and even if the dispersant molecule detach, a charge is left on the soot surface, leading to mutual electrostatic repulsion of modified soot particles¹⁴.

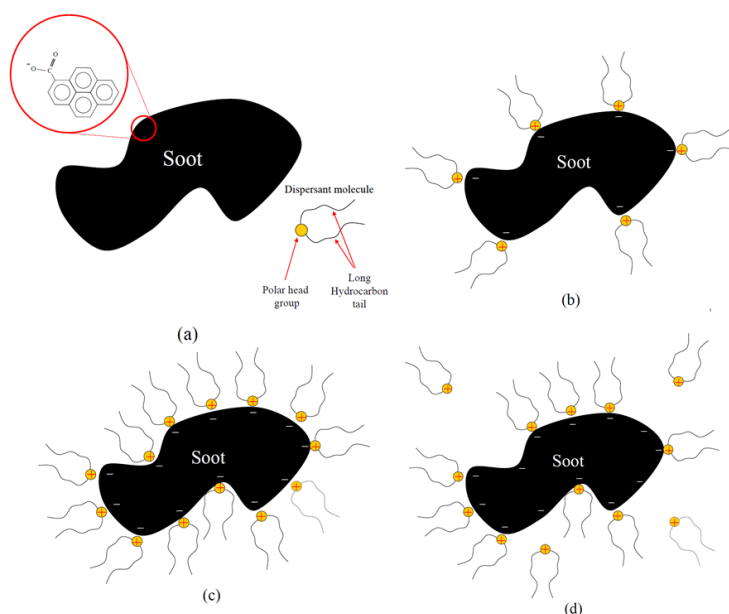


Figure 2-5: A schematic showing the mechanism of dispersant molecule preventing soot formation¹⁴

2.2.3.3 Antioxidants

Oxidation is probably one of the most detrimental causes of oil degradation. In the presence of oxygen, oil oxidises and the rate of oxidation process increases exponentially at higher temperatures. Oil oxidation process is discussed in details in Section 2.2.5.2. This section reviews antioxidants which are the molecules added to oil in order to inhibit oxidation of oil hydrocarbon stock.

The most noteworthy role of antioxidants is to protect different types of base oils under various operation conditions such as high temperature combustion engines. Antioxidants are

the sacrificial additives which interrupt oxidation and are divided into two categories of primary and secondary antioxidants. Primary antioxidants react with free radicals and remove them via chain terminating reactions. Most common primary antioxidants are phenolic, phenates, salicylates and amine. Secondary antioxidants decompose peroxide radicals to form non-reactive, non-radical, and thermally stable products. These products are harmless and do not contribute to further oxidation of the oil. Common secondary antioxidants are sulphur or metal-containing additives¹⁵.

Oxidation is generally controlled in lubricants provided the anti-oxidant additive is still present. Once the anti-oxidant additive is completely used up, oxidation will increase very rapidly, hence the amount of anti-oxidant in the oil is a very useful parameter to measure.

Type and amount of antioxidants differ depending on the application. Often, one additive acts as different additives, for instance Zinc dithiophosphates (ZnDTPs) are widely used as antioxidants, anti-wear and anti-corrosion additives in a number of applications such as engine oils. Oil oxidation accelerates once the antioxidants are depleted increasing oil acidity and viscosity.

Even with the most effective additive packages, the additives will be consumed and the oil will gradually lose its protective properties. The life of oils not only varies with the formulation of the lubricant (base stocks plus additive packages) but also closely relates to the machine operating conditions and the environment. Oil ageing implies that the quality of the oil has changed due to base oil oxidation and/or the oil is contaminated due to increases in moisture content, wear debris, natural dust/particles, etc. (discussed in Section 2.2.5). To optimise oil change intervals and provide the best protection for machines, oil quality needs to be monitored accurately and in a timely fashion. Over the years, a great deal of efforts has been spent to develop methods and technologies for oil quality monitoring. Before reviewing the development of oil monitoring technologies, key oil properties that affect the quality of oils and the main oil degradation processes are introduced below.

2.2.4 Oil properties

Lubricating oils have a large number of properties and they are classified into physical, chemical and electrical properties. The key properties that closely relate to oil quality and oil ageing processes are discussed here.

2.2.4.1 Physical properties

The main oil physical properties are viscosity, pressure, colour, odour, etc.

- **Viscosity**

Viscosity is one the most important physical properties of a lubricating oil. Oil viscosity changes significantly with temperature, shear rate and stress. It also changes with oil ageing due to oil degradation and contamination. For example, oil oxidation can cause oil thickening and increase the viscosity, similar to soot contents.

Viscosity can be defined as kinematic viscosity (ν , in *stokes* or m^2/s) and dynamic viscosity (η , in *Poise* or *Pa.s*). The two types of viscosities are related as follows:

$$\nu = \frac{\eta}{\rho} \quad (\text{Equation 2-1})$$

Where ' ρ ' is the density of the oil. Both oil density and viscosities vary with temperature and the dynamic viscosity of an oil changes with temperature based on the Vogel equation below⁹:

$$\eta = ae^{b/(T-c)} \quad (\text{Equation 2-2})$$

Where ' T ' is the absolute temperature in Kelvin, ' a ', ' b ' and ' c ' are constants varying for different oils. Typical viscosity-temperature plots for a number of oils are shown in Figure 2-6. As can be seen, the oil viscosity reduces noticeably over a relatively small temperature increase. For example, the temperature increase from 0 to 20 °C causes the viscosity of the Mineral Oil 160 VI (Viscosity Index) and SAE 30W 100VI to decrease by 35 cS and 4000 cS respectively.

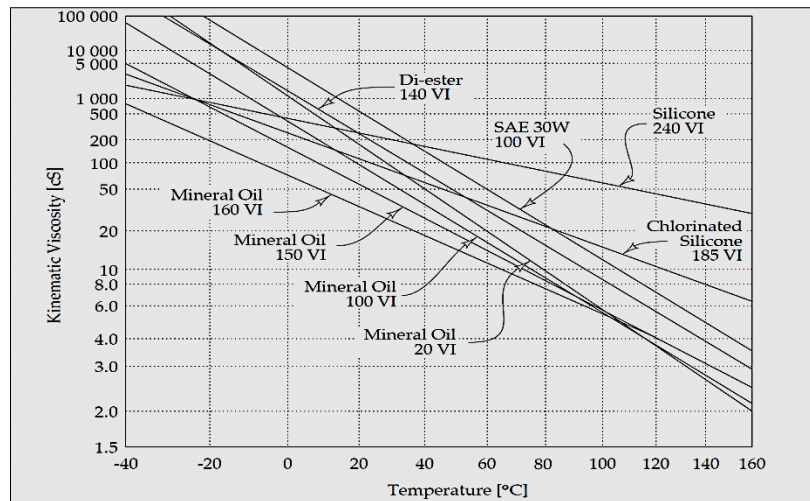


Figure 2-6: Viscosity-temperature plots of a number of particular oils⁷

- **Colour**

Oil generally darkens during ageing which is often used to assess oil condition. The ASTM D1500 defines the colour standards for oil analysis and colour index corresponds to changes in oil colour⁸.

- **Odour**

The smell of oil also changes over the course of oil degradation which can be used to assess oil condition. Aged oil normally exhibits a burnt odour¹⁶.

2.2.4.2 Chemical properties

The main chemical properties of lubricants include oil chemical compositions and its acidity/alkalinity which is expressed as oil acid/base number (AN/BN). Fresh oils with full package of additives tend to be slightly basic (or alkali) due to the presence of detergents and dispersants which are generally bases. During oil degradation, acidic by-products are formed as its additives are depleted increasing oil acidity. Thus, oil AN could be a useful indicator for oil ageing and/or oxidation process.

Acidity of aqueous solutions is measured and quantified using pH values. In non-aqueous solutions (e.g. oil), this term can be referred to as acidity or basicity. The process of acidity or basicity measurement in non-aqueous solutions is far more complex than in aqueous solutions due to, for instance, low ion concentration¹⁷.

- **pH theory & Measurements**

pH stands for ‘pondus hydrogenii’ and is a measure of the acidity or basicity of an aqueous solution. pH of a solution was defined by the Danish scientist Sorenson in 1909 as the negative logarithm (base 10) of the hydrogen ‘H⁺’ ion activity ‘a_{H⁺}’ and is calculated by:

$$pH = -\log_{10} a_{H^+} \quad (\text{Equation 2-3})$$

If the hydrogen activity fluctuates by a factor of ten, the pH value changes by one unit. The concentration of hydrogen ‘H⁺’ and its activity ‘a_{H⁺}’ are related by:

$$a_{H^+} = \gamma[H^+] \quad (\text{Equation 2-4})$$

Where ‘γ’ is the activity coefficient and the closer the value of ‘γ’ of hydrogen to 1, means a solution of higher acidity is present. pH of Pure water is said to be neutral, with a pH of about 7.0 at 25 °C (pH is measured at room temperature). Acidic solutions are defined as pH less than seven and basic or alkaline solutions greater than seven¹⁷.

pH can be measured using two electrodes: indicator/working electrode and reference electrode which can be combined into one. A galvanic cell (or a voltaic cell) is realised when two electrodes are immersed in a solution developing a voltage dependent on both reference and working electrodes. This voltage is developed from the reactions taking place between the electrodes and the species in the solution and the equilibrium between oxidised (O) and reduced (R) species. Electrons (ne⁻) are transferred in the redox (reduction-oxidation) reactions between species at the electrodes surface in the cell:



Ideally, the potential of the reference electrode should remain constant and only the variations in potential of the working electrode to varying pH should be measured. This is carried out by measuring the potential of working electrode against the constant potential of the reference electrode. Nernst equation¹⁸ is used to express the aforementioned potential between working and reference electrodes as:

$$E = E_w - E_{ref} = E^0 - \frac{R.T}{n.F} \cdot \ln a_{H^+} \quad (\text{Equation 2-6})$$

where:

E = Measured potential (mV)

E_w = Potential of working electrode (mV)

E_{ref} = Potential of reference electrode (mV)

E^0 = Electrode standard potential, constant (mV)

R = Gas Constant (8.3144 J/ K.mol)

T = Absolute Temperature (K)

F = Faraday's constant (96485 C)

n = Number of electrons transferred (ion charge)

The occurring reduction and oxidation processes release energy proportional to the cell potential (E). According to this equation, there is a dynamic equilibrium and if this equilibrium is moved by an irreversible reaction, for example by adding a reagent, the measured potential of the working electrode (WE) will change. This variation of WE is an indication of the relative concentration of 'O' and 'R'¹⁹. Equation 2-6 can be re-written using the base 10 logarithms as:

$$E = E^0 + 2.303 \cdot \frac{RT}{n.F} \cdot \log_{10} a_{H^+} \quad (\text{Equation 2-7})$$

At room temperature (i.e. $T = 25^\circ\text{C}$ or 298.15 Kelvin) for $R = 8.3144$ and $F = 96485$, $\frac{RT}{F}$ is a constant and for one electron exchange equilibrium ($n=1$) the above equation becomes:

$$E = E^0 + 0.05915 \cdot \log_{10} a_{H^+} \quad (\text{Equation 2-8})$$

This means, the electrode's potential changes by 59.15 mV for each pH unit change at room temperature. It should be noted that instead of a_{H^+} , H^+ can be used in the equations. Equation 2.8 can be illustrated graphically (*Figure 2-7*), where electrode response versus pH value is the slope (59mV per pH for Nernstian response) and is referred to in mV per pH. Two different sensitivity graphs are illustrated and as can be seen the electrode's potential decreases as the pH value increases.

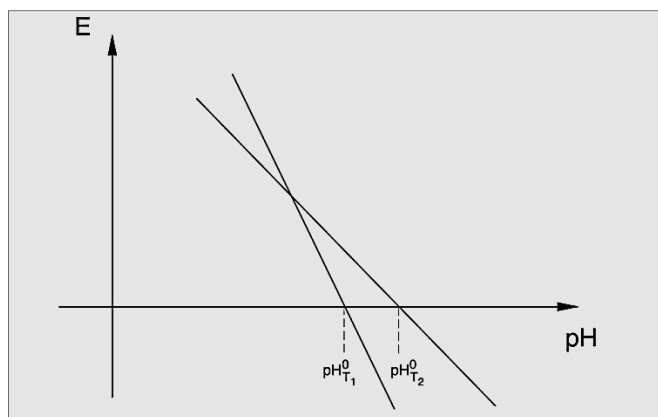


Figure 2-7: Electrode response versus pH value (pH-Voltage plot)²⁰

- **Acid and Base Number (AN & BN)**

The acidity of oils is typically quantified by the acid number (AN) and the alkalinity of oils is measured by the base number (BN). AN is measured as the amount of potassium hydroxide (in milligrams) required for neutralisation of one gram of acid in one gram of oil (mgKOH/g). AN value increases as oil ages due to accumulation of acids from combustion, contamination or oxidation. Likewise, BN is a measure of reserve alkalinity of lubricants and measures the amount of potassium hydroxide (in milligrams) contained in per gram oil (mgKOH/g)).

Acid level of lubricants is influenced by a number of factors such as oxidation level, chemical breakdown products, amount of water, type and amount of additives. Oxoacids are common types of acids produced in oils comprising of 1 oxygen atom bonded to 1 hydrogen atom and at least 1 other element such as carbon. Carboxylic, nitric or sulphuric acids are the main three groups of oxoacids^{21,22}. The corrosiveness of oils depends on the amount of weak acid e.g. carboxylic acid and strong acids such as nitric or sulphuric acid. The level of strong acids significantly affects the corrosiveness of the oil and the level of weak acids mainly affects the viscosity of the oil. It is important to assess both types of acids in oil to obtain a better understanding of the quality of the oil. For acidity monitoring, typically a series of AN and BN values is measured and the trends of the 2 are plotted on a graph. The increase in oil AN value has the opposite effect on oil BN trend (increasing AN reduces BN) over the time of oil usage as shown in Figure 2-8. It is recommended, by a number of engine and lubricant manufacturers, that the oil should be changed at the intersecting point of AN and BN plots on the graph or when the BN drops below that of the AN. The increase in iron content is due to the diluted sulphuric acid (explained in Section 2.2.5.1) which corrodes steel and cast iron very rapidly¹³.

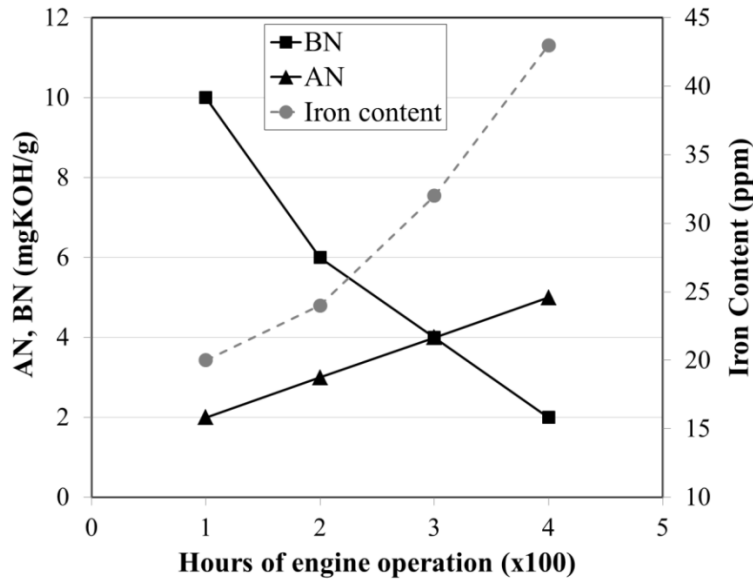
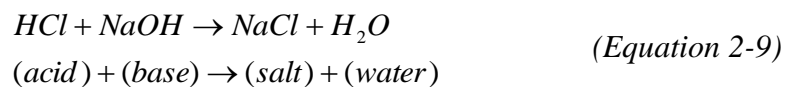


Figure 2-8: AN, BN and iron content trend in a used lubricant (adopted from²³)

• pH vs. AN/BN

Acids and bases are mixtures of positive and negative charge ionic compounds which break apart to form hydrogen ion (H⁺) and hydroxide ion (OH⁻) respectively in water. The concentration of H⁺ and OH⁻ determines the strength of the acid and bases which is measured on the pH scale. Acids are defined as electron pair acceptors and bases as electron pair donors. In case of equal number of hydrogen and hydroxide ions, the reaction between acids and bases neutralises each other producing salt and water:



Conventionally acid and base numbers (AN & BN) have been used to measure the concentration of acidic and alkaline elements in oil (instead of pH value). It is important to note, as opposed to pH concept, both acidic and alkaline elements can co-exist in oil. In reality, a number of oil additives such as dithiophosphates are amphoteric which means they can behave either as acid or base²⁴. Furthermore, a constant increase in oil acidity (i.e. AN) is expected as it is being used e.g. in an engine, but as dithiophosphates activate after certain usage, the AN value can initially decrease. The AN value starts to rise once these types of neutralising additives are used up. This fact clarifies the reason for monitoring both AN and BN in order to measure the true reactions and acid level in oil samples^{24,25}.

2.2.4.3 Electrical properties

Fresh lubricants are poor electrical conductors. However, as oil degrades, its electrical conductivity increases due to the increase in concentration of ‘conductive species’, such as carboxylic acid. Therefore, electrical properties are often used to assess the quality of oils.

- **Electrical resistivity, impedance and conductivity**

Resistance is a measure of how much a material opposes the flow of electric current. From Ohm’s law, the electrical resistance ‘ R ’ (ohm Ω) is defined as:

$$R = \frac{V}{I} \quad (\text{Equation 2-10})$$

Where ‘ I ’ (amps) is the current and ‘ V ’ (volts) is the potential difference applied.

In an alternating current (AC) circuit, resistance becomes a complex quantity, which also represents the ratio of the voltage to current. Impedance extends the concept of resistance to AC circuits with both magnitude and phase unlike resistance which only has magnitude. Impedance is represented as a complex quantity and can be calculated by complex division of the voltage and current. The phase and magnitude of impedance can be measured by sweeping the frequencies of an applied signal.

Conductance (‘ G ’ measured in Siemens) is the inverse of electrical resistance:

$$G = \frac{1}{R} \quad (\text{Equation 2-11})$$

Electrical conductivity (k) is the quantity of electricity per unit area transferred through a body at a given voltage gradient, i.e.:

$$k = \frac{1}{R} \times \frac{l}{A} \quad (\text{Equation 2-12})$$

Where ‘ l ’ (meters) and ‘ A ’ (square meters) are the length and cross section area of the resistor.

Therefore, the unit of electrical conductivity is Siemens m^{-1} (Sm^{-1}). Clean, dry, well refined and additive-free hydrocarbon oils are mostly poor conductors and in general their conductivity, at equilibrium, is in the region of 10^{-12} to 10^{-14} while a used oil could have a conductivity of 10^{-6} Sm^{-1} and act as an electrolyte²⁶. The electrical conductivity of mineral oils increases with temperature due to the greater mobility of electron carrying species such as acids. This value can be compared with the conductivity of an aqueous solution of Sodium Chloride (NaCl) which is about 1 Sm^{-1} .

If a constant potential difference is applied, conductivity decreases with time as the ions are accumulated at the electrodes, discharged and stabilised at a constant value. This leads to equilibrium by the formation and discharge of ions. As well as contaminants (such as water) and polar additives, oil oxidation also increases the conductivity of the oils due to the increase of acids in oils during the process of oil oxidation²⁶.

Conductivity can be measured by instruments which measure the current between 2 electrodes immersed in the oil with an applied voltage.

- **Electrical Strength**

This property expresses the maximum voltage that oil can withstand as an insulator before a discharge occurs. Electrical Strength is defined as kV per unit distance. This property is more significant for oils used as insulators in applications such as transformers and cables.

- **Dielectric Loss**

When a potential difference of ΔV is applied to a capacitor filled with a medium, the capacitor will store charge even after the source of potential difference is disconnected. The amount of charge stored is proportional to the magnitude of the applied potential across the conductors. In other words, the capacitance ‘ C ’ of a capacitor is the ratio of the charge on the capacitor to the magnitude of the potential difference across the capacitor in Coulombs per Volt or Farad (F):

$$C = \frac{Q}{\Delta V} = \varepsilon \cdot \varepsilon_0 \cdot \frac{A}{d} \quad (\text{Equation 2-13})$$

If the capacitor is filled with a dielectric, the capacitance increases by a factor of ε (*relative permittivity* or *dielectric constant*), that is:

$$C = \varepsilon \cdot C_0 \quad (\text{Equation 2-14})$$

Where ‘ C_0 ’ is the capacitance in the absence of the dielectric and ‘ ε_0 ’ is the electric constant of air (or permittivity of free space: $\varepsilon_0 \approx 8.854 \times 10^{-12} \text{ Fm}^{-1}$), ‘ A ’ is the area and ‘ d ’ is the distance between the two conductor plates²⁷. In order to measure electrical properties of oils, conventionally capacitor type electrodes are used. With this method, the oil is placed in between the conductors (electrodes) and assessed for dielectric constant.

- **Permittivity**

Permittivity is a measure of the resistance of an electric field being affected by a dielectric medium. It relates to the ability of a material to transmit or permit an electric field. Permittivity is a complex quantity in which the real part measures the changes in the capacitance of the electrodes and the complex part is related to dielectric losses explained in the previous section.

2.2.5 Oil degradation processes

The properties of lubricants, including their additives, will not remain unchanged throughout their life time. Oil degradation will cause loss in engine performance, reduced fuel efficiency, shortened useful oil life and initiation of component failure. An important factor in oil formulation is to sustain the required composition of oil for a specific period of time. Lubricant ageing is the changes in the properties and composition of the oil which leads to undesirable friction and wear. Oil degradation is a complex process which includes depletion or vaporization of components (additives), chemical changes and by-products (e.g. soot), accumulation of contamination from the ambient environment (e.g. water) and mechanical contaminants (e.g. wear particles). The ageing process also darkens the oil, changes its odour and increases the viscosity^{8,28}.

Oil contaminants and oxidation process are two important factors contributing to oil degradation. In internal combustion engines, oil contaminants are mainly sourced from incomplete combustion where for example residual exhausted gases (Exhaust Gas Recirculation (EGR)) blow through the piston rings and cylinder into the sump. These combustion gases contain products of air-fuel mixture, e.g. carbon monoxide, unburned hydrocarbons (soot) and water. Equation 2-15 shows these by-products and the reactive radicals which can also mix with each other in the lubricant:¹⁴



(Equation 2-15)

2.2.5.1 Oil contamination

Contaminants can generally be divided into solids, liquids and gases where the solid contaminants can damage the mechanical components and catalyse lubricant breakdown. Liquids change the oil viscosity hindering the lubricant functionality and gases (e.g. acidic combustion products) can corrode the surfaces in engines^{8,28}. A list of the main oil contaminants can be found in *Table 2-2*.

Type	Primary Source	Major Problems	Affected oil property
Acids	Oxidation, combustion blow-by, lubricant breakdown,	Metal corrosion, autocatalysis of lubricant breakdown	AN/BN, viscosity, conductivity
Soot	Combustion blow-by	Interfere with additives, abrasive wear, heavy deposits, oil thickening	Viscosity, conductivity
Water	Combustion blow-by, coolant leakage	Metal corrosion, promotes lubricant breakdown	Viscosity
Metallic particles	Component wear	Abrasion, adhesion, catalysis of lubricant breakdown	Conductivity
Metal oxides	Component wear, oxidation of metallic particles	Abrasion, surface roughening (adhesion)	TAN, viscosity
Minerals (silica sand) and dirt	Induction air	Abrasion, surface roughing (adhesion)	Conductivity
Exhaust gases	Combustion blow-by	Acids promoting lubricant breakdown	AN/BN
Glycol	Coolant leakage	Lubricant breakdown	Viscosity, Conductivity
Fuel	Blow-by gases	Lubricant breakdown	Viscosity, Conductivity

*Table 2-2: Lubricant contaminants type and sources*²⁸

The main oil contaminants are summarised below (adopted from^{9,16}):

Water: water from the environment or condensation can contaminate the oil. Water does not mix with oils chemically but forms an emulsion. Water contamination decreases the kinematic viscosity of the oil. Accumulated water causes further oil oxidation, additive consumption, corrosion of machinery surfaces and parts as well as extraction of acids and additives from the oil and formation of emulsions. The emulsions cause oil flow blockage and wear on abandon parts such as cylinder, ring, and piston due to insufficient lubricant.

However, water evaporates at high temperatures in engines thus it cannot be used as a reliable factor for oil quality monitoring.

Fuel: Fuel dilution in lubricants primarily causes film thickness reduction and wear of engine components. Fuel dilution influences lubricant electrical properties such as dielectric constant.

Dirt and dust: dust can enter lubricants, especially during the operation of moving parts in a dusty environment. Dust and particles such as silicon can be abrasive and significantly increase the wear of the components. Dirt from environment and residue from previous oil changes can also cause oil contamination and affect oil life. Silicon content of oil samples is monitored using spectrograph and total insoluble solid methods to monitor dust and dirt contamination monitoring.

Metallic and other wear particles: As the machine components wear, wear debris can get into the lubricant and contaminate the oil. Wear debris content within oil can also be an indication of machine components condition. Chemical elemental analysis is utilised to analyse oil debris contamination.

Glycol: The leakage from the coolant system is one of the most common and serious issues for engine oils. Coolant level can be measured by detecting the glycol, boron or sodium contents in the oil. Glycol, also found in antifreeze, decomposes at high temperatures and forms sludge and deposits.

Soot and combustion by-products: Soot is the main combustion by-product formed from carbon in diesel engines, which produces colloidal suspension in oil. The structure of soot attracts other species, forming larger soot particles which then increase oil viscosity. Soot production in engines is a complex process which depends on factors such as combustion characteristics, fuel composition and engine design (e.g. exhaust gas recirculation (EGR) system). For instance, different EGRs produce different circulating gases back into the engine. This reduces oxide or nitrogen (NO_x) emissions but also decreases the temperature and causes the development of particulate formation (e.g. unburned carbon) leading to the increase of soot contamination. In order to avoid soot particle agglomerating, dispersant additives are used to provide the formation of a colloidal suspension. Soot also has a significant influence on oil dielectric constant.

Thermal and oxidative degradation by-products: The oxidation process is explained in Section 2.2.5.2. This process produces insoluble by-products and weak carbon-based acids (e.g. RCOOH/carboxylic acids) that increase oil acidity and viscosity. Oxidation products can deposit on the piston rings and grooves, causing ring-sticking and increased blow-by. This will subsequently decrease the engine power and increase the fuel consumption. High-temperature operation increases oxidation and causes premature degradation of the lubricant base-stock. Moreover, the gases from combustion process or Exhaust Gas Recirculation (EGR), react with water producing acidic species, e.g. Sulfuric (H_2SO_4), hydrochloric (HCl) and nitric (HNO_3) acids. These acids ought to be neutralised by the additives (e.g. overbased detergents, as explained previously), otherwise they can potentially attack engine metal surfaces resulting in corrosion and polymerisation of organic species which results in resin formation and the build-up of deposits¹³.

It is generally thought that weak acids are formed in passenger car gasoline engines, whilst in heavy duty diesel engines, stronger acids are formed. In heavy duty diesel engines, large amounts of soot are generated in the oil which is why the oil formulations for gasoline engines are different compared to the formulation of a heavy duty diesel engine oil.

2.2.5.2 Oil oxidation process

Apart from oil contamination, oils are degraded mostly through oil oxidation processes. Oxidation is usually the most important life-limiting factor. Most chemical substances in oils have the tendency to react with oxygen which causes chemical changes in lubricating oils. Most of oxidative processes have the same or similar reaction patterns to the bi-radical status of oxygen. Lubricants, especially those used in combustion engines, usually operate in contact with air and therefore the chemical compounds react slowly but continuously with oxygen in air. The rate of this reaction depends on the compounds in the oil. For instance, paraffins, naphthenes and aromatics are more resistive to oxidation than asphaltenes and unsaturates. Oxidation produces undesirable by-products such as aldehydes and acidic compounds that may cause corrosion and increase viscosity and lacquering due to the generation of tarry deposits and insoluble products. In order to reduce these effects, the aromatics, asphaltenes and unsaturates are removed from the refining of mineral oils as much as possible¹⁶.

Oxidation can have the following effects on oil:

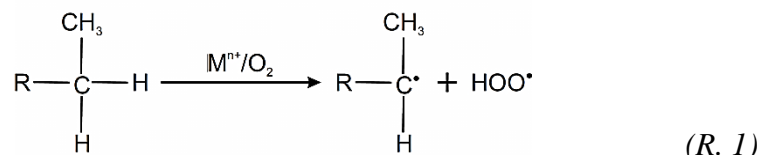
- Increase oil acidity due to formation of weak acids such as carboxylic acids. This will cause corrosive damages to metal parts such as lead (Pb) in bearings.
- Increase oil viscosity and eventually produce sludge and deposits due to condensation and polymerisation. This will cause blocking of filters and sticking of piston rings etc.

The oxidation mechanism can be separated for the reactions taking place at low (<120°C) and high temperatures (>120°C).

A) At low Temperature (<120°C)

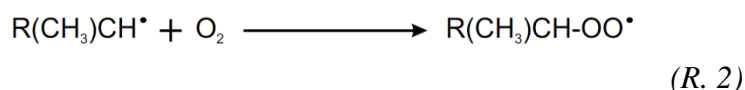
The first temperature phase is subdivided into 4 main stages: 1) initiation of the radical chain reaction, 2) propagation of the radical chain reaction, 3) chain branching and 4) termination of the radical chain reaction.

1) *Initiation:* In the first stage and under normal conditions, i.e. moderate temperature and oxygen partial pressure greater than 50 torr, radical chain reactions take place and the oxidation is catalysed in the presence of oxygen and traces of transition metal ions (Reaction 1).



R is a long-chain hydrocarbon substituent and the catalyst M^{n+} can be any of the metals: Cobalt (Co), Iron (Fe), Vanadium (V), Chromium (Cr), Copper (Cu) or Manganese (Mn). The rate of the initiation stage is very slow. In the above reaction an alkyl radical (-C•RH) is created as the result of initiation stage of oxidation.

2) *Propagation:* In the second stage, the alkyl radical formed in the initiation stage, reacts irreversibly with oxygen to form an alkyl peroxy radical (R.2).



This reaction has very low activation energy and is extremely fast. It is followed by the removal of a hydrogen atom from another hydrocarbon chain by the proxy radical:

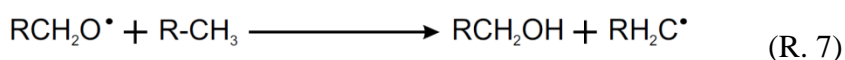
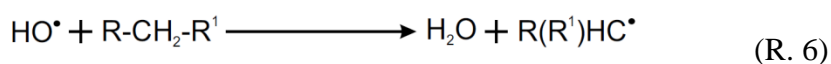
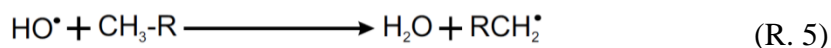


Products of this reaction are a hydroperoxide and a new alkyl radical, which can again react with oxygen as shown in Reaction 2. The rate of Reaction 3 is slow in comparison with Reaction 2 and this low reactivity causes high concentration of peroxy radical in the system relative to other radicals. Therefore at the end of this phase, various hydroperoxides are formed and the main hydrocarbon chains are consumed.

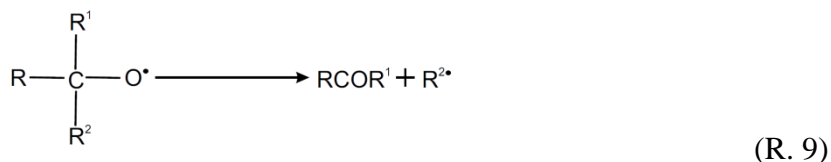
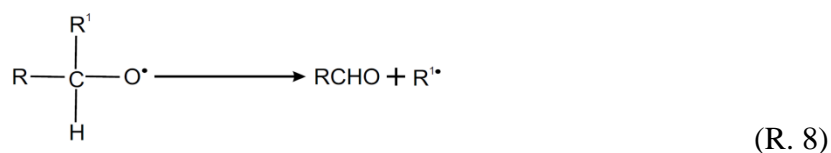
3) *Chain branching*: Several hydroperoxides (ROOH) are generated during the first and second stage of the oxidation. However, if the concentration of hydroperoxides (ROOH) is low, at high temperatures and in the presence of catalysts, alkoxy (RO•) and hydroxy radicals (HO•) are formed, as follows in reaction (4):



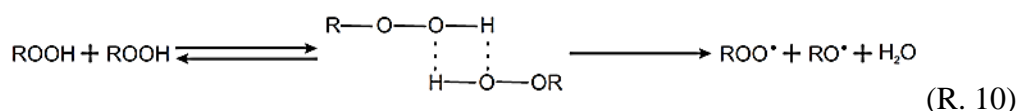
From Reaction 4, hydroxy and primary alkoxy radicals are formed, and as they are very chemically active, they extract hydrogen atoms from hydrocarbon molecules, as shown in Reactions 5, 6 and 7:



Secondary and tertiary alkoxy radicals form aldehydes (RCHO) and ketones (RCOR'), as can be seen in Reactions 8 and 9:



At high hydroperoxides concentration, hydroperoxides tend to react via a bimolecular mechanism as illustrated in Reaction 10:





In the secondary phase, the combination of aldehydes and ketones produces unsaturated aldehydes and ketones as a result of polycondensation process which also increases the viscosity of the bulk medium. These formed products are still oil-soluble. Polymerisation of the outputs of the polycondensation also takes place at this stage which produces insoluble sludge in the hydrocarbon. Further details on oil oxidation processes can be found in¹⁶.

2.3 Sensing technologies for oil condition monitoring

Sensors are used to produce an output signal as a function of input signals in reference to certain sensitivity parameters, converting information from one domain to another. Generally an operation model can be designed for a device which gives input information to the operator while the output is being measured based on calibration or complete determination of the model. Sensors can be divided into 2 groups. First group is the self-generating transducers which the only energy applied is the energy of the input signal so that the output signal will be zero when no input is present, examples include dynamos and thermocouples. In the second group sensors (also called modulating transducers) an independent device (source) is additionally used to apply energy. The applied energy is then modulated by a physical or chemical parameter, examples include the Pt-100 thermoresistive temperature sensor and pH sensing ISFET (Ion-Sensitive Field-Effect Transistor)²⁹.

Oil quality can be assessed based on the analysis of a number of oil properties, which can be conducted either off-line in a laboratory by taking oil samples from a system or on-line by incorporating appropriate sensors in the lubricant system in a machine. Over the years, laboratory based oil analysis has become an essential means to monitor oil ageing process providing guidance on oil changing for machine protection. For example, oil samples are regularly taken from heavy duty trucks for laboratory analysis to monitor truck engine health for maintenance purposes. However, it is every industry's desire to be able to monitor oil degradation in real-time to optimise oil changing and machinery maintenance.

2.3.1 Techniques for oil viscosity analysis

This section analyses the state-of-the-art development of oil quality sensing techniques for viscosity, acidity and electrical properties in detail including both off-line and on-line methods. Other property measurements and algorithm based techniques as well as integrated sensors are also reviewed.

Among the physical properties of oil, viscosity is the most important one to be monitored, thus techniques for viscosity monitoring are reviewed in the following section.

2.3.1.1 Off-line methods

American Society for Testing and Materials (ASTM) standards offers different methods for off-line oil viscosity measurements. One of the most common off-line methods is the kinematic viscosity measurement using capillary instrument (ASTM D445)³⁰. Lab-based viscosity analysis uses viscometers, such as capillary, rotational, cone on plate, falling ball viscometers (e.g. Gerin V-3 viscometer). Figure 2-9 illustrates a number of common viscometers⁷.

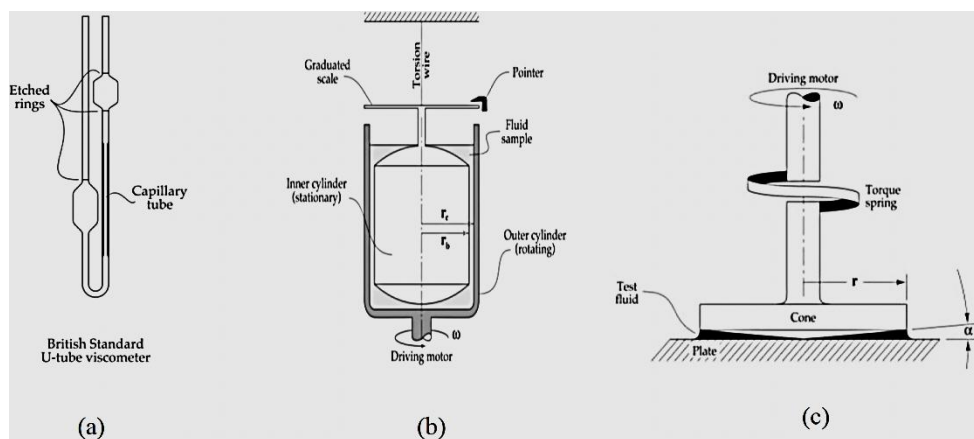


Figure 2-9: Viscometer examples: a) Capillary, b) Rotational, and c) Cone on Plate⁷

Kinematic viscosity is normally measured using a capillary viscometer, where a fix volume of oil flows under gravity through the capillary of a calibrated viscometer. Kinematic viscosity is the product of the measured flow time and the calibration constant of the viscometer. Since temperature can affect oil viscosity significantly, it should be closely controlled and reported. Other lubricant viscometers and their characteristics are summarised in Table 2-3.

Apart from laboratory viscosity measurement, viscosity can often be measured on-site using portable viscometers. There are also a number of portable viscometers commercially available in the market. Figure 2-11a shows a Visgage pocket viscometer by Eitzen Inc.ⁱ and Figure 2-11b is the Viscolite 700 by Hydramotion Ltd.ⁱⁱ Portable viscometers provide quick and convenient on-site viscosity measurements without thermometers and stopwatches and are being widely used in a wide range of industries.

ⁱ [http://www.visgage.com/m38 & m76 operation.htm](http://www.visgage.com/m38_&_m76_operation.htm)

ⁱⁱ <http://www.hydrmotion.com/contact.html>

Method	Measurement	Shear Stress
Saybolt and Redwood	Time for fix volume of oil flow through standard sized jet.	Low
Engler	Flow time for fixed volume of oil at specified temperature compared (as a ratio) with water at 20 °C.	Low
Cold cranking simulator	Speed at constant torque.	High
Brookfield	Torque at fixed speeds.	Low to moderate
Ravenfield	Torque at fixed speeds.	Very high
Mini rotating	Speed at constant torque.	Moderate

Table 2-3: *Viscometers and their characteristics*

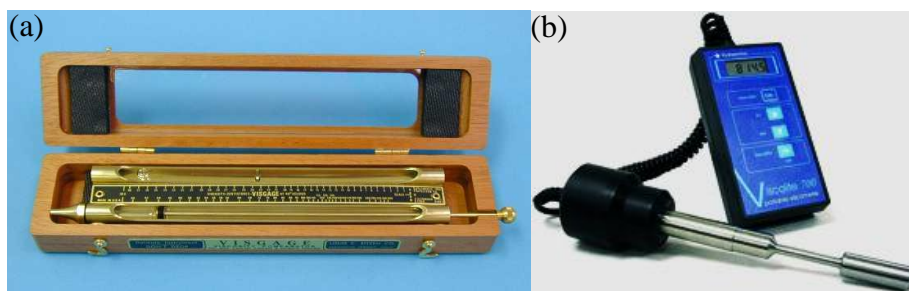


Figure 2-10: (a) *Eitzen Visgage viscometer*, (b) *Viscolite 700 by Hydramotion Ltd.*

2.3.1.2 On-line methods

Due to the importance of oil viscosity, there has been a large number of attempts on developing on-line viscosity sensors which can be divided into 3 categories: Macro-displacement of a body within the liquid, vibration and acoustic methods³¹.

Techniques based on macro-displacement are realised through modification of the laboratory measuring procedures such as the capillary and rotational viscometers. For instance, falling ball technique (fast-recovery viscometer), developed by Kasameyer et al.³², takes advantage

of electromagnetic concept and is currently produced by Paclpⁱⁱⁱ. This sensor is based on two coils which move a piston back and forth magnetically at a constant force. An electronic circuitry measures this two-way travel time to give absolute viscosity. These viscosity sensors, mounted into oil circulation lines, are remarkable for their small size. However, the presence of moving parts affects the reliability of these sensors due to possible presence of wear particles.

On-line vibration and acoustic sensors do not contain any moving parts. Vibration techniques determine oil viscosity by measuring the variations in the parameters of the forced oscillation of a submerged body, i.e. a probe. Tuning forks and micro-cantilevers are examples of vibration sensors. Hella³³ developed on-line tuning fork devices for oil viscosity and permittivity measurement. The main disadvantage of tuning fork sensors is that they do not relate directly to primary measurements and hence require calibration which can be time consuming.

Acoustic viscometers utilise shear waves to determine oil viscosity. William et al.³⁴ patented an acoustic oil viscometer which included a pulse generator, transmitting and receiving piezoelectric transducers, and a detector of the phase shift, all mounted in the walls of the oil line. The phase-shift detector which is connected to both transmitting and receiving piezoelectric transducers, determines the velocity of the received shear wave in terms of liquid density. The velocity is then used to calculate the kinematic and dynamic viscosities of the oil. This type of sensor seems to be the most promising on-line viscosity sensor among devices mounted directly into oil circulation lines and, mainly, into the lubrication systems of vehicles³¹. The main drawback of acoustic viscometers is that the acoustic wave velocity also depends on the level of oil contamination (such as wear particles) and air bubbles as well as the oil viscosity.

Although viscosity is often monitored, its interpretation is slightly complicated for engine oils. Often, a drop in viscosity of the oil is observed initially due to fuel dilution and permanent shear thinning of the viscosity modifier. Thereafter, a rise in viscosity occurs due to oxidation. However, by the time the viscosity increases rapidly, it is probably slightly too late to change the oil. On the other hand, AN and BN change more gradually with time and are more suitable for oil condition monitoring.

ⁱⁱⁱ <http://www.paclp.com/>

2.3.2 Techniques for chemical analysis

2.3.2.1 Off-line methods

- **Titration methods**

Conventionally, oil chemical properties (e.g. acid and base Number measurement) have been quantified using colorimetric (e.g. ASTM D974-12³⁵) and potentiometer titration methods (e.g. ASTM D664-09³⁶, D2896-07³⁷ and D4739-08e1³⁸) that have been widely accepted by industry. A number of manufacturers offer off-line titration based devices. *Figure 2-11* shows the acidity measuring device from Kittiwake^{iv}. The main advantages of the titration methods are the high accuracy, repeatability and reproducibility (< 5% error)²⁵. However, these methods are time consuming, costly and laborious.



Figure 2-11: Kittiwake (FG-K25197-KW) AN measurement device^{iv}

- **pH measurements**

Oil acidity can be assessed using pH measurements despite the fact that the pH value was originally developed for aqueous solutions (see Section 2.2.4.2). Ion Selective Electrodes (ISEs) or Specific Ion Electrodes (SIEs) are a group of sensors which directly measure and convert the activity or concentration of ions dissolved in a solution into an electrical potential. pH measurement is an electrochemical method which utilises devices, such as Ion-Selective Electrodes, to convert the chemical activity of hydrogen ions into an electronic signal, e.g. an electrical potential difference³⁹. Traditional glass membrane pH electrode, as part of ion-selective electrodes, utilises potentiometric method to continuously measure the pH of a solution. During the analysis, a potential is developed between a glass membrane indicator

^{iv} <http://www.kittiwake.com/oil-test-centre>

electrode (or working electrode WE) and a Reference Electrode (RE) immersed in a solution. The 2 electrodes are normally combined into a single equivalent probe (i.e. combination electrode). The WE is pH dependent and develops a potential related to the pH variation. The voltage developed between WE and RE depends on the ion exchange between univalent cations in the glass membrane and hydrogen ions in the solution. *Figure 2-12* elucidates the working principle of pH glass membrane electrodes in aqueous solutions. The WE is in contact with the solution via the glass membrane's outer surface and at the same time with the filling solution inside the membrane. Electrode filling is an electrolyte of a known composition and pH value. Also, the reference material inside the WE (Silver/ Silver Chloride in this case) is immersed in the filling solution to make a stable electrical contact between the potential measuring pH meter and the electrolyte in contact with the inner side of the glass membrane⁴⁰.

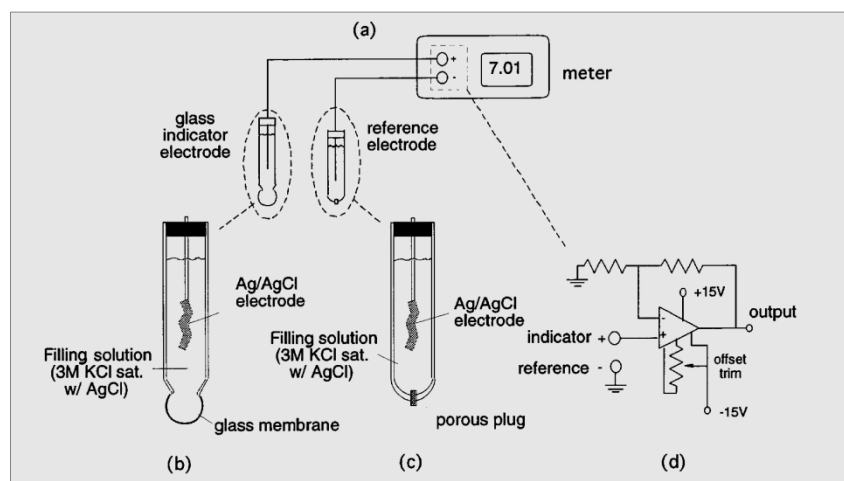


Figure 2-12: Glass membrane electrode (a) pH meter (b) WE structure (c) RE structure (d) pH meter amplifier circuit⁴⁰

The RE connects the meter and the solution under the test which is also in contact with the pH-sensitive glass membrane of the WE. The RE is similar to the WE in the sense that they both have reference elements immersed inside and both are filled with an electrolyte. However, the RE has a porous ceramic frit to facilitate the physical and electrical interaction between its filling solution and the solution under test. This ceramic frit creates a liquid junction which is significant as it can be a source of sample contamination (from RE), causing reliability problems as well as measurement errors. When the active component in the WE, i.e. the pH sensitive glass, is immersed in the solution, a thin hydrated layer ($\approx 100\text{nm}$) is created at the surface of the glass. At this layer, the hydrogen ions cause an exchange of glass ions for hydrogen ions which consequently develops a potential

difference¹⁷. Therefore, the value of measured pH is determined from the electrical potential difference between the WE and the RE. The pH meter senses and amplifies this potential difference, ideally with precision of 0.1 mV. The pH meter also must have high input impedance as the electrical resistance of the WE is relatively large. pH electrodes are calibrated using buffer solutions of known pH and the calibration graph of voltage-pH can be plotted and used for pH determination¹⁷.

Although glass pH electrodes are reliable and well characterised in aqueous solutions, due to their limitations, such as being fragile, they are not appropriate for oil acidity measurement. Ion selective electrodes based on solid state materials (utilising e.g. thick-film printing technique) have been developed for on-line oil acidity measurements, which will be reviewed in the next Chapter.

2.3.2.2 On-line methods

- **Metal oxide pH sensors**

Metal electrodes coated with an oxide are used as pH sensors at high temperatures and pressures. They can be in the form of a wire, polished disk or sputtered thin film, on an oxide formed through electrochemical or thermal oxidation, chemical vapour deposition, etc. These types of sensors have advantages such as chemical resistance, high temperature and pressure performance, non-glass construction as well as miniaturisation which make them popular in different applications.

Examples of this method include iridium oxide (IrO₂), ruthenium oxide (RuO₂) and lead oxide (PbO₂). Reduction reactions between a metal oxide sensor and the solution are shown in a general form below⁴¹:



where 'M' represents the metal of the metal oxide pair, such as iridium (Ir):



Smiechowski and Lvovich developed iridium oxide sensors for industrial lubricants manufacturing both Macro and Micro (MEMS) configuration versions⁴¹. They tested these sensors in diesel oils and observed a correlation between the outputs of their sensors against acid number values of the oil samples, as shown in Figure 2-13. However, the long term stability tests proved the electrodes instability over 24 hours in diesel oil. In Figure 2-13, A,

B and C represent different fabricated sensors in which A and B are the macro size sensors ('melt' and 'sputter' iridium oxide sensors) and C is the MEMS version.

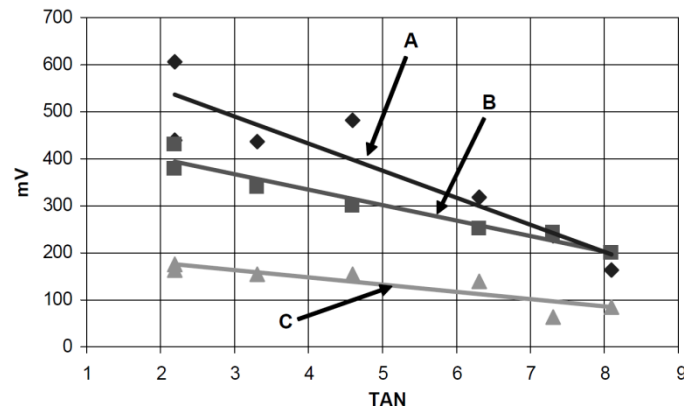


Figure 2-13: Output of iridium oxide sensors vs. acid number values in diesel oil samples⁴¹

Ion Selective Field Effect Transistors (ISFETs) are developed from metal-oxide-semiconductor FET (MOSFET) technology for measurements of ion concentration (such as hydrogen) in a solution. This method is similar to ISE and glass electrode discussed earlier that uses a pH-responsive membrane. The main difference is that the silicon chips in MOSFET performs the amplification of a field-effect transistor. The integral amplification miniaturises the size of the sensors and makes them relatively inexpensive, pocket-sized, battery-powered pH measurement systems^{40,42}.

Katafuchi and Kanamori tested pH-ISFET in different fresh and deteriorated engine oils to monitor oil acidity⁴³. Fresh oils were aged by carrying out actual engine tests according to the Japanese Automobile Standard Organisation (JASO) high-temperature detergency test method. Their results show that the pH-ISFET responded to the increase in oil acidity and decrease in base number as a result of oil deterioration in a so claimed linear fashion ($R^2 = 0.56$). However, their electrodes suffer from temperature influences as the tests were carried out at constant low temperature, i.e. 30 °C, to eliminate temperature effects. No further work based on this technique has been reported.

• Infrared (IR) Spectroscopy

IR analysis has become a very popular and powerful practice in monitoring aged engine oils and can progressively provide an extensive amount of information on degradation process of the oil. IR can detect contaminants (e.g. soot and water), oxidation index, sulphate index, etc. Nonetheless, due to the complexity of the oil samples (as oil is a mixture of a large number of different compounds, base oil and additives), the resultant spectrum derived from IR is also

complex. This necessitates greater detail of analysis and the spectrum of aged oil needs to be compared with the fresh sample of the same oil to draw a conclusion on the quality of the oil⁴⁴.

Although IR is a well-established and recognised sensing technique, its application is restricted to precisely controlled laboratory conditions and static measurements⁴⁵. To enable on-line monitoring, the bulky and expensive spectrometers in conventional IR systems must be replaced⁴⁶. Attempts in miniaturising the IR concept into an in-situ sensor have been made specifically to build it on industrial systems/engines to progressively monitor the condition of oil.

Andreas et al.⁴⁵ developed an ATR (Attenuated Total Reflection) sensor comprising a broad-band IR light source, 2 collimating mirrors, an ATR crystal, a filter-chopper and a pyroelectric detector. They employed a small and low cost infrared light source to keep the total cost of the sensor down. This sensor is claimed to be used for on-line monitoring of lubricant ageing but they only tested fresh and aged lubricants and compared the results. The results from the ATR sensor was compared with standard ATR measurements and it was shown that the results and accuracy of the developed on-line ATR are similar to the standard laboratory-based FTIR-ATR investigations of aged lubricants.

Agoston et al.⁴⁶ proposed an IR sensor using a thermal IR-emitter as the source and a narrow-band IR filter (interference filter) as the spectral line. On the detector end, they employed a thermopile sensor to sense the intensity of the IR light which has travelled through the filter and the sample (i.e. oil). Figure 2-14 shows the working principle and an image of the prototype sensor. The developed sensor was able to provide correlations between the measured values and the oxidation indices of aged lubricants, but is still in prototype stage and has not been miniaturised and tested real-time.

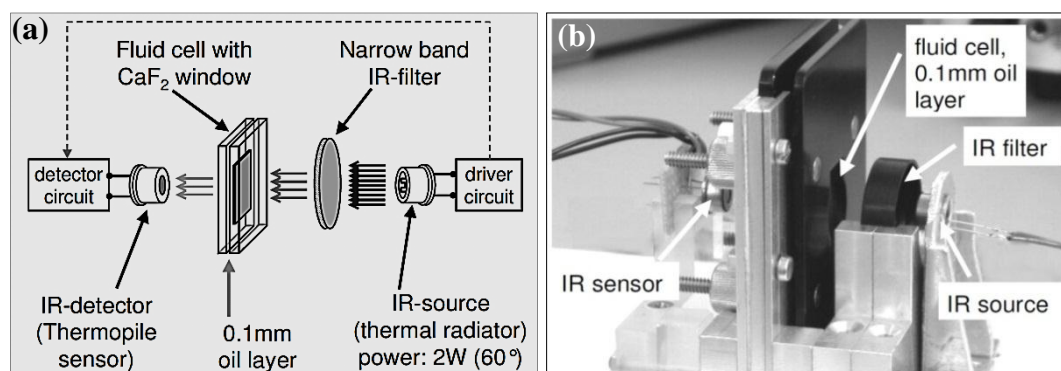


Figure 2-14: IR sensor a) sensor design, and b) the sensor prototype⁴⁶

2.3.3 Electrical property measurement

Oil electrical properties such as permittivity, impedance and conductivity change as it degrades. Fresh lubricants are poor electrical conductors. However, as oil degrades, its electrical conductivity increases due to the increase of concentration of conductive species, such as nitric acid (oxidation by-products) and contaminants (e.g. metallic wear particles, water). Therefore, electrical properties provide a potentially powerful means of assessing the quality of oils. The electrical properties of oil are often assessed by its AC impedance or DC conductivity measurements. This section reviews different techniques for measurement of oil electrical properties.

2.3.3.1 Impedance Spectroscopy (IS) and Electrochemical IS (EIS)

IS and EIS have been applied to a number of applications such as fuel cells systems, batteries, corrosion studies, biological analysis and biomedical sensors, polymer and coatings properties monitoring. EIS includes the investigation of materials in which ionic conduction is the key factor such as solid and liquid electrolytes. The main difference between EIS and aforementioned potentiometric pH measurement is that in the latter, there is no applied external potential difference (p.d.) whereas in the former, internal fields and p.d.s are present which produce the space-charge layers at interfaces. Features of EIS such as equivalent circuits (EC) and different transformation (e.g. Kramers–Kronig for data quality checking) are used to make the experiments efficient and reliable⁴⁷.

Industrial lubricants have components with a dipolar nature that allows examination of their properties using electrochemical impedance spectroscopy (EIS)⁴⁸. EIS can offer simple, relatively quick, inexpensive and temperature independent measurements and has been directly used to analyse lubricant condition in the industrial/automotive engines. EIS experiments, both on-line and off-line, comprise of 2 or more electrodes (depending on the application: 1 or 2 working, reference and counter electrodes), hardware and circuitry to apply DC or AC potential difference (p.d.) at a fix or variable p.d. and frequency, and to measure the resultant voltage, current and phase angle. In off-line systems, such as Solarton 1260, these components are all included in 1 device to apply voltage to a cell and measure the resultant signals.

When a two-electrode sensor is immersed into the engine oil, 3 regions are formed: electrode-oil interface, bulk oil layer and the second electrode-oil interface, illustrated in Figure 2-15⁴⁹.

Each of the equivalent circuits has a resistor and a capacitor in parallel. Therefore, the current flow reflects the bulk oil layer resistance and the electrochemical reactivity of the electrode-oil interfacial region. The bulk-layer resistor ' R_0 ' reproduces the resistance of lubricant and the interfacial resistors ' R_i ' and ' R_j ' are inversely proportional to the electrochemical reactivity of the relevant electrode-oil interfacial regions⁴⁹.

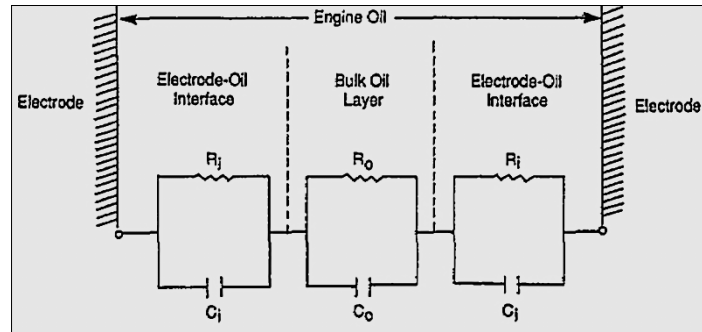


Figure 2-15: A schematic of a two-electrode EIS sensor showing the equivalent circuits⁴⁹

Lee et al.⁴⁹ found that increasing the concentration of glycol, which is a major component in antifreeze, in engine oil by 100ppm can reduce the bulk-layer resistance from 2 to nearly 0.3 Mega Ohms. During the measurement, a wide range of frequencies (1 mHz to 1 kHz) was applied using a frequency response analyser to derive an AC impedance spectrum which is capable of characterising the electrochemical properties of the system by utilising a precise equivalent circuit. A bode plot is produced from the measured impedance and phase angle versus the logarithm of AC frequencies. Based on the AC impedance plot, the plateau at the high-frequency represents the bulk resistance (R_0) and the plateau at the low-frequency is the total resistance (R_0+2R_i)⁴⁹.

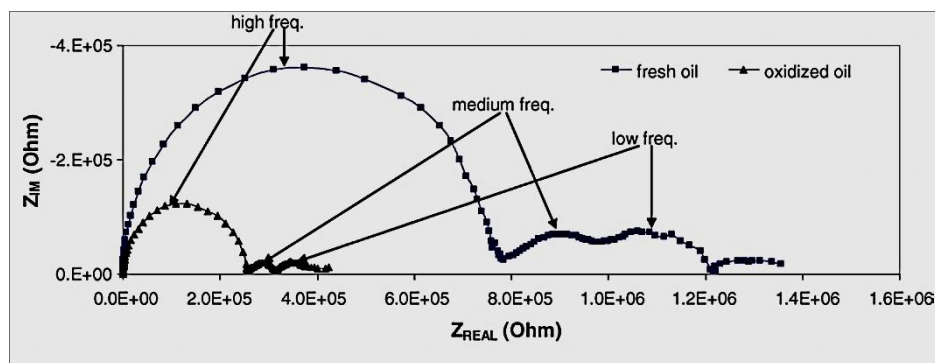


Figure 2-16: An impedance spectrum for fresh and oxidised oils⁴⁹

Ulrich et al.⁵⁰ used EIS alongside multivariate data analysis to estimate the level of soot and diesel contamination in engine lubricant. They used multi-frequency impedance measurements and found that soot affects the impedance during the entire frequency range

whereas diesel contaminant only influences the impedance at low frequency. Their experiments were carried out mostly at room temperature and temperature effect on their results was not investigated. This can be an important issue as the engine temperature is much higher than room temperature (typically up to 120 °C at the engine sump⁵¹).

Lvovich and Smiechowski⁵² used EIS and Cyclic Voltammetry (CV) to detect water leaks in lubricants. This was carried out by injecting water into lubricants and investigating the time dependent dynamics of water-oil interactions. Also, an empirical model including rate equations for defining the mass transport and charge transfer processes was developed. The measured bulk resistivity of oil dramatically decreased as the water was injected into the oil due to the high water conductivity. However, water quantification in lubricants remains a complex challenge as water-oil balance can be influenced by formation of inverse micelles, micro-emulsions and free non-bound water. For instance, lubricant detergents form inverse micelles with water in a continuous hydrocarbon oil phase with detergent surrounding the water in micro-droplets due to their strong surfactant nature.

Lee and Wang⁵³ developed a macro and a silicon-wafer micro size on-line sensor where 2 electrodes were combined with a dielectric material, i.e. engine oil, to form a capacitor. As an external AC voltage is applied, a current is induced which is either: (a) the displacement current of the capacitor, or (b) the leakage current. The electrochemical reactions occurring on the electrode surfaces cause the leakage current. However, the displacement current does not vary with the variation of oil samples. Therefore the induced current is related only to the amount of electrochemical reactivity occurring in the oil. The results showed that the output of the micro-sensor correlated with the AN values of the engine oil.

2.3.3.2 Conductivity measurements

The conductivity of the oil is calculated from the real-part of the complex impedance (i.e. resistance) and the cell constant (area and distance between 2 electrodes) using the equations below⁵⁴:

$$R = \rho \frac{d}{A} \Rightarrow \sigma = \frac{1}{\rho} \quad (\text{Equation 2-18})$$

Where R is oil resistance in ohm, ρ is the oil resistivity in ohm cm, σ is the oil conductivity in 1/ (ohm cm) or Siemens/ cm, A is the electrodes area in cm^2 and d is the distance between the electrodes in cm.

Wang⁵⁵ developed a platinum screen-printed conductivity sensor with a temperature sensor (RTD: resistance temperature device) on the back, illustrated in Figure 2-17. The sensor was installed on an oil drain plug of an engine and tested in real driving conditions. Oil samples were also collected periodically from the vehicle to measure other parameters such as AN, BN, viscosity and oxidation induction time. Figure 2-18 shows that oil conductivity initially drops as the detergents and antioxidants are depleted. If the 2 oil top-ups are ignored it is noted that there is a gradual increase in the oil conductivity toward point A, which was presumed to be associated with rapid oxidation once the anti-oxidant additives had been consumed. This curve and the acid number then decline after point A as a result of viscosity increase in the oil sample.

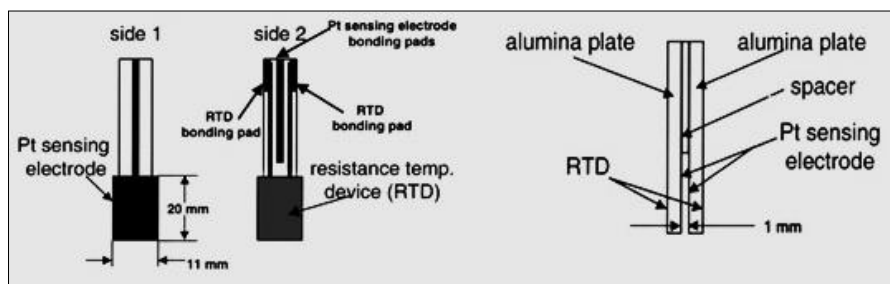


Figure 2-17: A schematic diagram of the platinum and RTD sensor⁵⁵

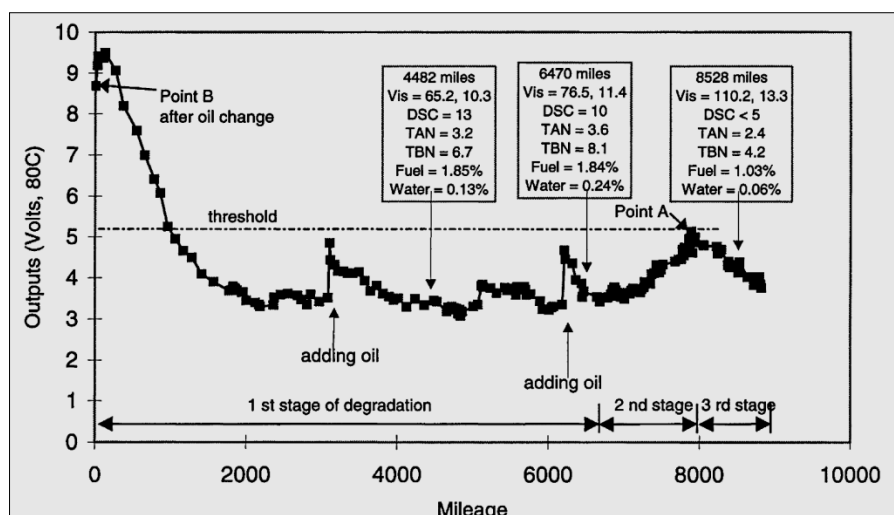


Figure 2-18: The plot of sensor outputs versus the mileage driven after the oil change⁵⁵

Potentiostat conductivity measurements have been carried out using polymeric bead matrix electrodes where changes in the resistance of a polymer depend on its oxidation products and free water⁵⁶. Latif and Dickert⁵⁷ imprinted polymer synthesised with Titania and Silica layers which act as recognition materials for acidic components of an aged oil. Thin film gold electrodes were employed as transducers to measure the conductance of polymer coatings and detect changes in oxidised products as lubricating oil ages⁵⁷. Figure 2-19 illustrates the interdigital electrodes structure printed on a glass substrate with gold and other sensitive layers. The sensor operates in AC mode at an optimum frequency. The conductivity of the oil is measured from the resistance between the electrodes to examine the condition of the oil under test. They used capric acid as a model compound and prepared different concentrations of it in fresh oil to observe the sensor responses. The results showed that the their sensors are highly sensitive to the added acid and output of the sensors increased approximately 3 micro Siemens for 50 mg/mL of added capric acid. However, oil contaminants such as fuel and water seem to influence the output signal considerably which in case of contaminants ingress would make the results defective.

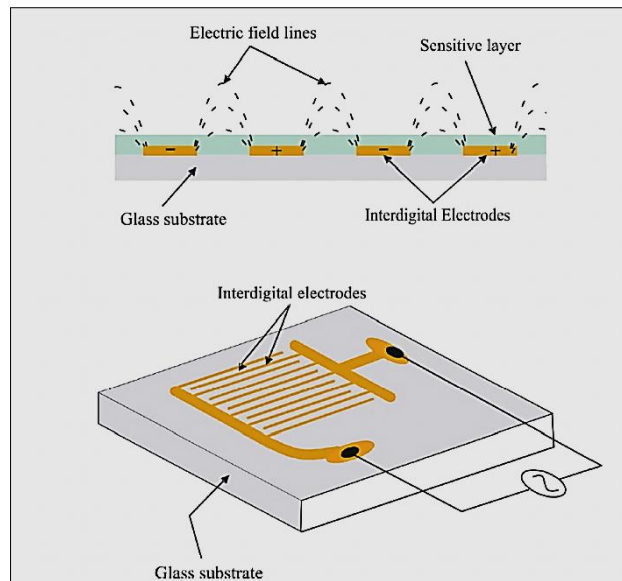


Figure 2-19: The conductometric sensor: polymer covering the inter-digital electrodes⁵⁷

2.3.3.3 Permittivity measurements

Complex permittivity can be measured by 2 or more electrodes, where the capacitance of the electrodes is related to the real part and the imaginary part represents the dielectric losses, which are related by dissipation factor (D or $\tan\delta$). Permittivity sensors are thus divided into 2 main groups: the ones that detect changes in the real part of the permittivity and those based on the complex permittivity measurements.

Noria developed a Predict Navigator as a portable screening device which can measure oil conductivity and permittivity at low and high frequencies⁵⁸. At low frequencies, changes in conductivity caused by water contamination can be measured (lower sensitivity detection limit= 100 ppm of water) and at higher frequencies, the permittivity of the oil can be measured which can be an indication of wear metals existence (lower sensitivity detection limit= 120 ppm of wear metal particles).

In an attempt to develop on-line inexpensive permittivity sensor, Raadnui and Kleesuwan⁵⁹ developed grid capacitance sensors in circular and rectangular shapes. The sensors can detect oil contamination as the dielectric constant of oils changes with contaminants such as water, fuel dilution, water, wear debris, etc. The working principle of their sensor is based on the calculation of oil capacitance between 2 series of parallel poles which is filled with oil sample. This sensor has not been tested in real engine environment.

Tan-delta dielectric sensor⁶⁰ is based on the permittivity of the oil and includes capacitive electrodes and an oscillator circuit which provides an output signal proportional to the oil Tan-delta. The dielectric sensor was tested in Mercedes-Benz cars but this is no longer the case⁶¹.



Figure 2-20 Tan-delta dielectric sensor^v

2.3.4 Indirect Methods

Apart from direct measurements of oil physical and chemical properties, indirect techniques such as algorithm and quantitative methods have also been employed to monitor oil condition. An example of indirect condition monitoring is the use of pressure transducer combined with temperature and engine parameter data, such as RPM, velocity, mileage, to output the condition of the oil⁶². Honda Motor Company⁶³ attempted to detect oil degradation by estimating oil temperature based on engine parameters and compare the results with the actual oil temperature from the thermostat.

Engine Management System (EMS) and Engine Control Unit (ECU) are also utilised within cars to constantly control and sense different parameters such as fuel level, engine and oil temperature, load, RPM and mileage. Complex algorithms have been designed to use and combine these collected data to pre-determine oil change interval time.

Ideally, a combination of direct and indirect methods, i.e. property measurement sensors and algorithm implementation would be a suitable approach for oil condition monitoring.

^v <http://www.tandeltasystems.com>

2.3.5 Integrated sensors

The above review has focused on sensing techniques based on single measurement, e.g. viscosity, acidity or conductivity. However, in order to accurately assess oil quality, a number of oil properties have to be measured due to both the large variety of oil formulations and the complexity in oil degradation and contamination processes.

There have been a number of attempts to integrate sensors for lubricant monitoring. Hella Limited developed a low cost microsensor which could provide oil level, conductance, density, permittivity, temperature and viscosity measurements³³. The system employs a tuning fork quartz resonator that measures electrical impedance and provides information related to the oil viscosity and permittivity (Figure 2-21). Further development and commercialisation of this system is not reported.

Duchowski & Mannebach developed a sensor that could simultaneously measure temperature, relative humidity, relative viscosity, and relative permittivity of the oil. Quartz Crystal Microbalance (QCM) was used for viscosity measurements and 4 sensors were built on a single chip⁶⁴. Again, no further development and commercialisation have been reported.

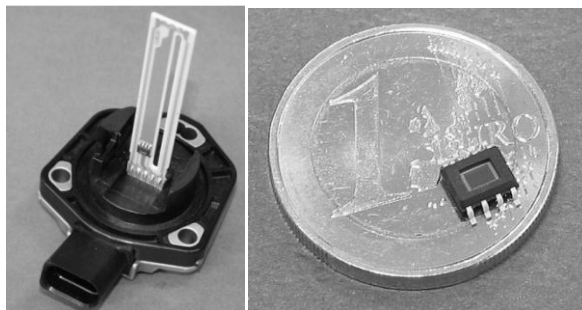


Figure 2-21: Integrated oil sensor developed by Hella limited³³

Car manufacturers have also attempted to develop various oil condition monitoring sensors. General Motors⁶⁵ used a 2-electrode conductivity measurement for in-situ oil type and contaminant determination. Nissan Motor⁶⁶ developed capacitor electrodes for dielectric measurements in order to identify soot content and oil deterioration stage. Ford Motor⁶⁷ used copper sensor to detect corrosion properties of oil. The concept was that as the oil ages the copper starts corroding which is a measurable scale. Volvo Trucks⁶⁸ built an oil maintenance indicator by measuring the oil pressure and counting the number of filter changes. This was accompanied by the engine parameters data such as RPM (revolutions per minute) to output a

status of the oil condition. Up to now, no established products are commercially available for car engines lubricant monitoring.

2.4 Summary

Formulated lubricating oils consist of a base oil with additives to reduce oxidation rates, however once these additives are consumed the performance of the oil will rapidly decrease threatening the life of the machine. Oil degradation was discussed in detail and it was mentioned that the oil quality decreases mainly due to oxidation and contamination, such as debris, fuel and coolant dilution etc. Oxidation produces undesirable by-products such as aldehydes and acidic compounds (weak acids e.g. carboxylic acids) that may cause corrosion and can lead to varnish and sludge formation.

Oil quality monitoring can be carried out off-line or on-line in which off-line methods involve taking oil samples regularly and analysing them in a laboratory, measurements can include viscosity, wear debris detection, elemental/chemical analysis etc. These methods can provide accurate analysis however they are time consuming and may not be very timely. On-line oil monitoring provides timely information on oil condition that enables condition-based lubricant maintenance and saves the cost of unplanned failure as well as preventing unnecessary oil changes. Single oil property sensors, such as Quantitative Debris Monitor (QDM) sensor, Cambridge viscosity sensors, PAJ water-in-oil sensor and the Tan-delta dielectric sensor are available. However, to date only 2 types of sensors have been employed in the automotive market⁶⁹: dielectric measurement sensors, such as the TEMIC QLT-Sensor⁷⁰ and solid state oscillating crystal devices including flexural⁷¹ and acoustic wave⁷² sensors for viscosity measurement. The TEMIC QLT-sensor measures the dielectric constant of lubricant and inputs the results into software which predicts oil state based on the engine parameters. Viscosity of oil is an important property to monitor but the viscosity of oil does not change significantly under normal ageing conditions and increases marginally due to oxidation. However, viscosity changes significantly as a result of water/fuel ingress in oil. Therefore, viscosity monitoring alone cannot provide a complete picture of oil degradation process and needs to be combined with other sensors (e.g. dielectric) in order to serve as an oil monitoring system. Single sensor approaches only provide a limited view on oil degradation which is highly complex in nature; a multi-sensor approach offers a more complete monitoring solution.

Due to the complexity of oil chemistry during degradation processes, there have not been any reliable on-line sensors for oil chemical property monitoring. IR sensors are bulky and adversely susceptible to the engine's harsh environment and iridium oxide sensors⁴¹ had

significant stability and sensitivity issues. The work presented in this thesis focuses on developing on-line chemical sensors using solid state metal oxide electrodes which detect the acidity increase of oil due to oxidation and other degradation processes. Thick film technology, as an inexpensive and viable technique, was selected for fabrication of the electrodes as it has proven sensing capabilities in pH measurements of aqueous solutions, which will be discussed in the next chapter.

Chapter 3 provides a link between the studied literature and the theory behind the actual work carried out for this project in which the thick film technology and theory will be presented as a mean to develop chemical sensors to measure oil acidity. Thick film technology, introduced over 50 years ago, has been used to produce a wide range of sensor electrodes. Thick film sensors allow flexible design, offering a wide range of materials with closely controlled parameters and provide low cost infrastructure and mass production opportunity. They are small, robust with a good reproducibility and required minimal treatment. Also, there has been a competent and equipped research group at the University of Southampton with an expertise in producing and testing thick film physical and chemical sensors. This offered a great opportunity and established the platform to study their applications in oil acidity measurements which have not been investigated in the past. The rest of this thesis reports the design of the thick film acidity sensors and investigates the feasibility of detecting oil acidity using these sensors.

Chapter 3. Thick Film Technology

3.1 Introduction

In the previous Chapter, it was discussed that thus far, no reliable on-line sensor has been reported for oil chemical condition monitoring. It was shown that there have been attempts on developing ion selective electrodes for oil acidity/pH detection in the past but were flawed for various reasons such as being expensive, not being suitable in extreme engine conditions (e.g. being fragile), limited temperature ranges and not paying attention to designing and testing an on-line reference electrode.

Microelectronics sensor development is expanding considerably due to the requirement of industry for compact and reliable sensing solutions. Solid-state sensor technology and specifically, the silicon-based devices have been commonly used in the fabrication of novel sensors. Although this technique has many advantages such as high degree of integrability, it suffers from the major drawback of being an expensive solution⁷³. Thick film (TF) technology for sensor development was introduced 50 years ago for producing hybrid circuits. For thick film circuit production, the main factor is the scheme of film deposition, called screen printing, which is perhaps one of the oldest forms of graphic art reproduction. Screen printing makes this type of sensors robust, inexpensive, compact and applicable to many applications such as automotive electronics. Thick film generally can be applied to different categories of sensor development such as physical, chemical, gas and commercial sensors. The key factor in popularity of thick film technology is its integrability with other enabling technologies (e.g. silicon) to provide solid-state sensors in an economical manner^{73,74}.

One of the main advantages of thick film technology is its ability to produce hybrid integrated circuits (ICs) in a miniaturised package. Figure 5-3 shows an example of conventional silicon pressure sensor combined with thick film integrated circuits on alumina substrate⁷⁴. This technology also provides support structure to other sensors⁷⁵. Nevertheless, the main area of interest for thick film technology is where it contributes to sensor development by employing the film itself as a principal sensing element. There are many examples for this, such as thick film resistors as strain gauges. Thick film strain gauges can be used as pressure sensors⁷⁶, load cells⁷⁷, accelerometers⁷⁸, temperature sensors⁷⁹, and so on. Other thick film sensor examples include: magnetoresistive sensors⁸⁰, thermopiles, chemical and gas sensors⁷⁵. Thick film sensors can be categorised into different sensing groups such as mechanical (e.g. piezoresistive and piezoelectric), magnetic (e.g. magnetoresistive linear displacement sensing⁸¹) and chemical groups (e.g. acidity (pH), and humidity sensors)⁷⁴.

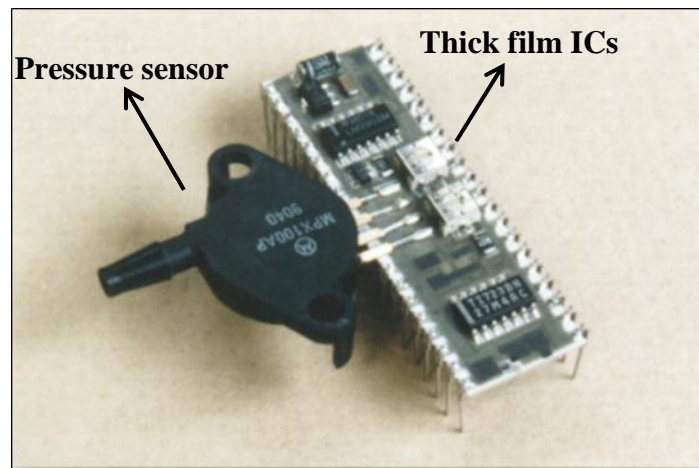


Figure 3-1: A Silicon pressure sensor integrated with thick film integrated circuits⁷⁴

3.2 Screen printing technology (sensor fabrication)

In the fabrication process of thick film technology (also called ‘printed-and-fired’), conductive, resistive and insulating pastes containing glass frits are used (Figure 3-2). They are deposited in patterns defined by screen printing and fused at high temperature onto a ceramic substrate. Film thicknesses are normally in the range of 5–20 micrometres (μm) and multi-layer structures can be built.

Ceramics materials, mainly alumina (particle sizes in the range 3–5 μm , and 94-98% alumina content), are most frequently utilised as the substrate. In thick film fabrication, various components (such as conductors and dielectrics, as shown in Figure 3-2) are produced by applying and adding inks or pastes on the substrate sequentially to produce the required conductor patterns and resistor values. Inks used may contain:

- a binder: glassy frit for the encapsulation and mounting of components which melts and binds metal particles together on the substrate
- the carrier: organic solvent systems and plasticisers which are additives used to control the ink viscosity/fluidity in the printing process
- Pure metals, alloys, and metal oxides used as deposited materials

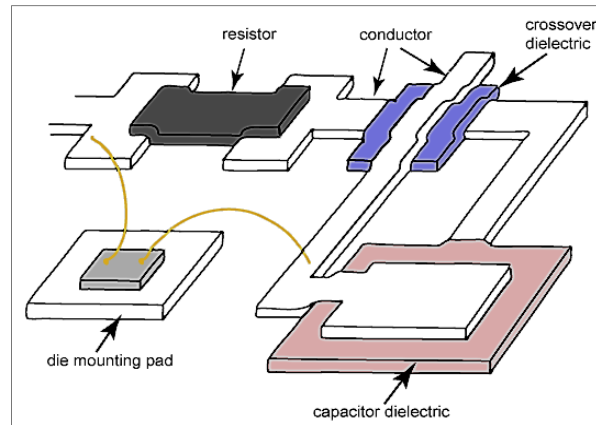


Figure 3-2: Schematic of different materials (inks and pastes) used, to produce conductors and other components of a thick film circuit⁷³

The pastes used as conductors include gold, silver, palladium, platinum and more recently copper and nickel (not mature pastes yet). Gold is a good conductor but expensive and has solderability issues. Silver is less expensive and solderable but its atoms migrate under the influence of DC electric fields causing short-circuits and reactions with many of the resistor paste formulations. Palladium and platinum are normally employed as alloys of gold and silver to form robust conductor pastes. They are solderable and have good adhesion to the substrate. For instance, silver-palladium paste is one of the popular materials used because of its low-price and robust performance⁸².

Dielectric and resistor pastes are the other two types of pastes. Latest resistor pastes use oxides of ruthenium, iridium and rhenium. These pastes are less sensitive to variations in the firing profile (i.e. heating process; rising/preheat zone, peak/hot zone and decrease/cooling zone).

The pastes are printed on the substrate by ‘screen printing’. Screens are manufactured from highly tensioned stainless steel or a polyester mesh with about 40% transparency or open area. They have open weave so that the printing paste can go through them, on the substrate (Figure 3-3). Figure 3-4 summarises the printing process, where the squeegee (on the top) pushes down on the screen and prints the ink on the substrate. After printing, as the squeegee’s force is released (not pushing any longer), the screen returns to its original position and the paste is printed on the substrate.

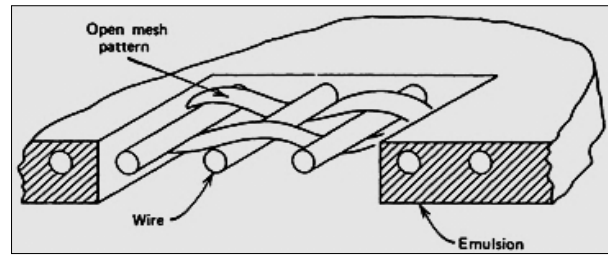


Figure 3-3: Cross-section of the open weave section of a thick film screen⁷³

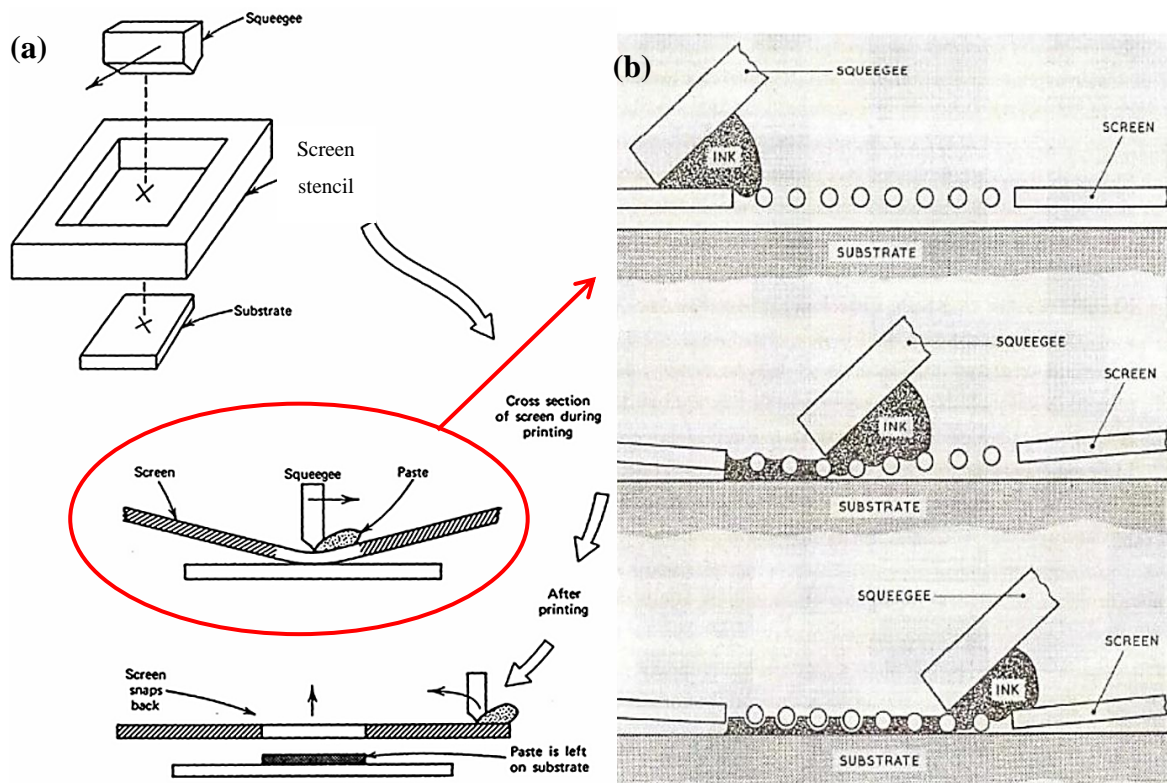


Figure 3-4: (a) Thick film printing process⁷³, (b) squeegee pushing the ink through the porous area of the screen⁸³

The final step is the firing/drying (annealing) of the printed film. This stage is carried out to soften or melt the glassy frits, sinter the fine powders and to make the complete film a solid composite material. This is to produce a cohesive and adhesive film on the substrate, carrying the conductor, resistor or dielectric materials. Paste manufacturer usually specify the firing profiles and the temperatures to be in the range of 100 °C to 1000 °C. Annealing is generally accomplished using a belt furnace (Figure 3-5). Continuous metal belt inside multi-zone furnace provides the required profiles for the substrates passing through them⁷³. After firing, metal particles bind together as glass frits melt which is not usually homogeneous (in micro

scale) and can potentially be problematic. An example of particle structure of a deposited layer is illustrated in Figure 3-6.

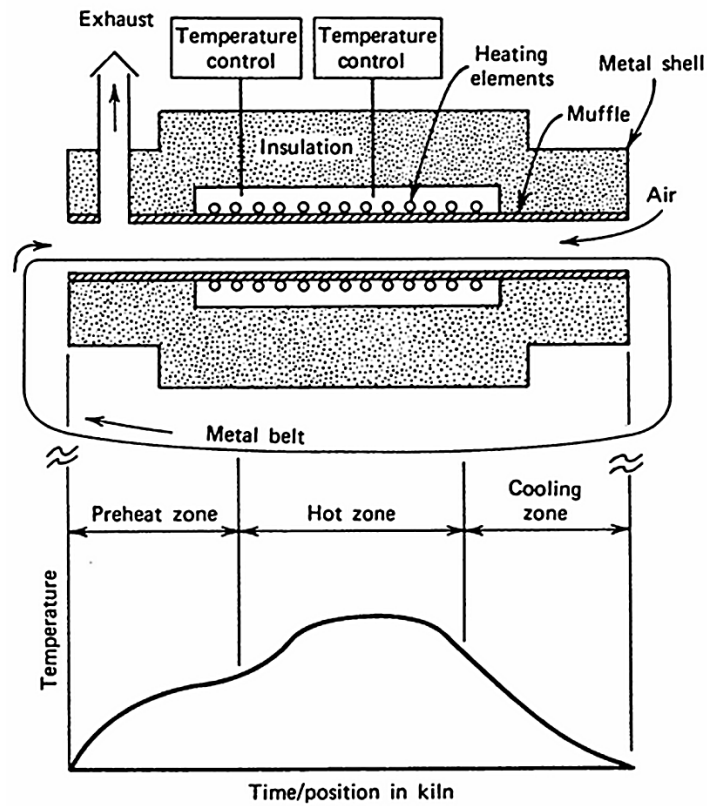


Figure 3-5: A thick-film furnace parts⁷³

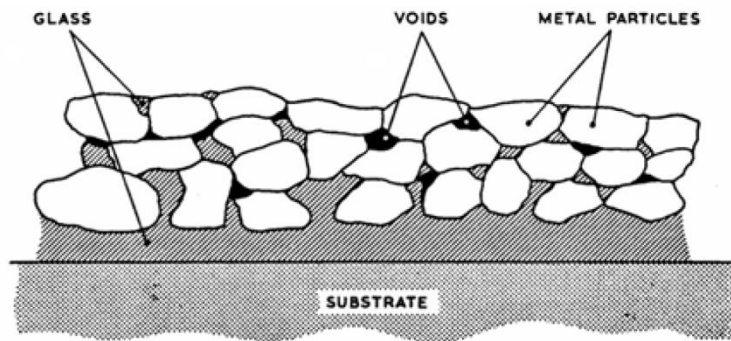


Figure 3-6: particle structure of a thick-film paste after firing⁷³

3.3 TF ion-selective electrodes for chemical sensing

The work reported in this Thesis explores the feasibility of detecting oil acidity using thick film (TF) sensors. TF technology has been used to produce a wide range of sensor electrodes. However their applications in oil acidity measurements have not been investigated before. TF working principle is based on electrochemical cell theory where one reference and one ion selective (e.g. hydrogen) electrode (ISE) are inserted in a solution under test. Properties of the latter electrode change according to the concentration or activity of the examined ion, i.e. hydrogen, in solution whereas the former electrode is used as a reference point. Measured property of ion selective electrode can be potentiometric, amperometric or cyclic voltammetry where the first 2 are easier to perform. A schematic of a potentiometric electrochemical cell is illustrated in Figure 3-7.

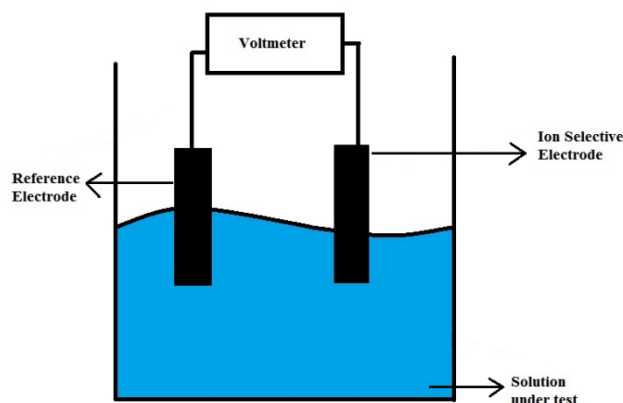


Figure 3-7: Two electrodes electrochemical cell configuration

The potential of the reference electrode should remain unchanged while the potential of the working electrode changes as its chemical constituents react with the desired specie or ion in the solution. Oxidation and reduction processes in dissimilar concentrations of specie in different solutions cause the measured potential (in voltmeter) to change if constant potential of reference electrode is achieved. The theory of potential difference calculation was discussed in Chapter 2 according to the Nernst equation.

Recently, there has been extensive research in the field of electrochemical ion-selective electrodes (ISE) for chemical sensor development. Large numbers of ISE developments have been reported as a response to the high demand for non-expensive, non-fragile and on-line chemical sensors. Fog and Buck⁸⁷ investigated the basis for metal oxide semiconductors to be used for pH sensing comparing performance of metal oxides such as platinum oxide (PtO₂),

iridium oxide (IrO₂), ruthenium oxide (RuO₂), osmium dioxide (OsO₂), tantalum oxide (Ta₂O₅) and titanium dioxide (TiO₂). They found that a reversible reaction is formed between the aforementioned insoluble metal oxides and the solution shifting the equilibrium of the reaction toward either direction depending on the pH of the solution. Their sensing electrodes were used against a standard calomel reference electrode.

Mihell and Atkinson⁸² designed thick-film pH electrodes based on ruthenium dioxide which produced near-Nernstian (~59.15 mV/pH) behaviour in the pH range 2–10 and displayed stable performance over 60 days of testing. For their experiments they used commercial silver/silver chloride reference electrode (BDH GelPlas).

Belford et al.⁸⁴ examined the performance of 4 thick film metal oxides (platinum/gold, platinum oxide, copper oxide and iron oxide) as pH sensitive materials in aqueous solutions against a standard calomel (Hg/Hg₂Cl₂) reference electrode. They found copper oxide had the highest sensitivity to pH but also had the utmost drift (20mV daily).

McMurray⁸⁵ and Koncki⁸⁶ reported new composite thick film electrodes based on RuO₂ and pH electrodes. They also produced near Nernstian sensitivity (~51mV/pH) for their RuO₂ electrodes versus commercial reference electrodes.

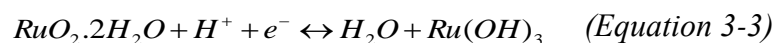
The ion selective electrode is required to respond to the change of the hydrogen ion (H⁺) concentration in the solution. Ruthenium oxide (RuO₂) working electrode has been demonstrated to have the highest sensitivity to pH changes compared to any other metal oxide tested⁸². Ion selective electrodes such as ruthenium oxide electrodes used here were explained by Fog and Buck⁸⁷ to undergo the following reaction:



Where MO_x is the higher oxidation state metal oxide and $MO_{x-\delta}$ is the lower oxidation state. The potential for this reaction is given by:

$$E = \left(\frac{RT}{F}\right) \ln a_{H^+}^l + \left(\frac{RT}{F}\right) \ln a_o^s + const. \quad (\text{Equation 3-2})$$

Another possible mechanism involved only 1 redox reaction between 2 insoluble ruthenium oxides:



Where $RuO_2 \cdot 2H_2O$ is the nominal composition of hydrated ruthenium dioxide and $Ru(OH)_3$ is the hydrated ruthenium sesquioxide which can also be written as $RuO_2 \cdot 3H_2O$. The potential of the reaction is given by:

$$E = E_0 - 0.0591pH \quad (\text{Equation 3-4})$$

Where, E_0 is the standard potential of the cell. Theory predicts a sensitivity of 59 mV/pH under room temperature. In practice, thick-film ruthenium oxide electrodes have shown an almost Nernstian response of 56mV/pH in aqueous solutions.

In this study, thick-film ruthenium oxide (RuO_2) working electrode against silver/silver-chloride (Ag/AgCl) reference electrodes have been selected to measure acidity levels in lubricating oils. Thick film RuO_2 working electrode has shown good sensing capabilities in pH measurements for aqueous solutions.

3.4 Reference Electrode

The pH sensors developed in this work, typically employ similar configuration as shown in Section 3.3, in which electrochemical cells (i.e. potentiometry, electric voltage (potential)) is used to measure the concentration of hydrogen ions. The pH sensor consists of 2 electrodes, a pH sensitive electrode (or H^+ ion selective electrode), and a silver/silver-chloride (Ag/AgCl) reference electrode.

Reference electrode is required to have a stable potential while the ion selective electrode (i.e. the working electrode) responds to the change of the H^+ concentration in the solution. The primary standard for reference electrodes is the standard hydrogen electrode (SHE) which has the highest degree of reproducibility. There are also “second kind” reference electrodes such as mercury and silver type with an excess of a sparingly soluble salt⁸⁸. Mercury reference electrodes have disadvantages such as being toxic at vapour phase and liquid at room temperature whereas silver is solid at its standard state making it applicable to thick film solid state electrode construction.

ISE sensors are impractical without a suitable reference electrode (RE) which is an essential form of electrochemical sensor. RE is an inevitable and vital part in a potentiometric measurement system⁸⁹. There are many types of conventional reference electrodes which have electrolyte solution in their construction, but it would be difficult to utilise such devices in on-line sensor implementation. Examples of ion selective electrodes (ISE) discussed in

Section 3.3, showed that most ISE sensors were used against conventional reference electrodes which in practice is not feasible for on-line pH measurement due to difficulties such as being brittle (in case of glass RE) and bulky. On the other hand, developing and manufacturing reference electrodes with electrolyte regions in their design have proven to be complicated and this could be the reason for the low degree of devotion to these sensors⁸⁹. There have been attempts reported in miniaturising reference electrodes such as the work carried out by Desmond et al.⁹⁰ in which 2 types (different number of layers) of silver/silver chloride RE (vs. a combination pH electrode connected to a Metrohm 654 pH meter) were fabricated using screen printing method on silicon substrates producing near Nernstian response (56mV/pH). However, these reference electrodes proved to be unstable when tested over seven days.

There are also similar reference electrodes reported such as those developed by Mroz⁹¹, Simmons et al.⁹², Kisiel⁹³, Martínez-Mañez⁹⁴ and Tymecki et al.⁹⁵. The main challenge with reference electrodes is the stability issue and their drifting after a certain amount of time depending on their construction. A novel solution to overcome this issue (i.e. extending electrodes stability) was the introduction of thick film electrodes and fabrication of printed reference electrodes (solid state) which has already shown a viable commercial application in areas such as blood glucose test strips⁹⁶. In this study, the developed reference electrodes attempt to mimic the operation of a conventional electrolyte-filled reference electrode which has already been successfully employed in a range of aqueous-based solutions, e.g. pH control of power station water feed lines⁹⁷.

Different types of fabricated thick film silver/silver chloride (Ag/AgCl) reference electrodes have been selected to investigate the feasibility in measuring acidity levels in lubricating oils. Different types of reference electrodes were tested in order to compare and select the most suitable for oil acidity measurements. Detailed design and fabrication process is explained in Chapter 4.

Silver/Silver Chloride (Ag/AgCl) as part of silver halide group is the most common reference electrode due to its availability and the use of potassium chloride as the electrolyte in the conventional RE. As shown in Figure 3-8, a chloride electroplated silver wire is immersed in a saturated solution of potassium chloride (usually 3.5 M) which is contained in a glass tube. The glass tube has a glass frit at the bottom in order to allow ion exchange between the liquid under test (electrolyte), silver wire and the electrical conductor.

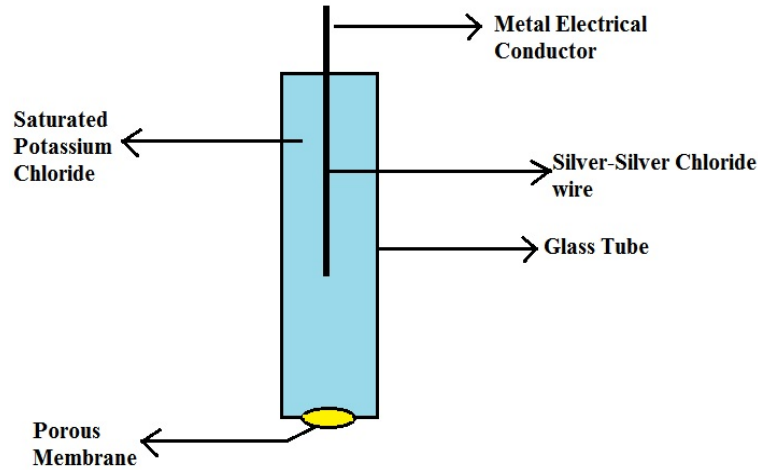
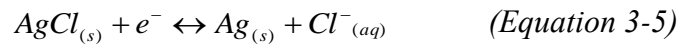


Figure 3-8: Schematic of a silver-silver chloride reference electrode

Similar to the conventional type (i.e. glass bulb RE), the following reversible reaction occurs on the TF Ag/AgCl electrode:



The potential of this electrode is determined by the Nernst equation in the form shown below:

$$E = E^\theta + \left(\frac{RT}{nF}\right) \ln \frac{[a^{\text{AgCl}}]}{[a^{\text{Ag}}][a^{\text{Cl}^-}]} \quad (\text{Equation 3-6})$$

Where E is the electrode's potential (V), E^θ is the electrode's standard potential (V), R is the universal gas constant ($8.31 \text{ J mol}^{-1} \text{ K}^{-1}$), T is the temperature (K), F is Faraday's constant (96485 C mol^{-1}), n is the number of electrons involved in the reaction and a^x is the activity of x in the solution (x is either Ag, Cl or AgCl). AgCl is a sparingly soluble salt and it immediately saturates the solution keeping its activity constant, while the activity of silver is controlled by the activity solubility product which is the product of the activities of silver and chloride and is invariant at a certain temperature. Therefore, the potential of the electrode depends only on external changes of the chloride activity. Activity is the product between the activity coefficient (i.e. the ratio of chemical activity to actual concentration) of the specific ion and its concentration. For moderate concentrations the activity coefficient is close to 1 and therefore it can be replaced by the ion's concentration. The equation can be written in a simpler form:

$$E = E^\theta - 0.0592 \log[\text{Cl}^-] + 0.0592(k) \quad (\text{Equation 3-7})$$

Where k is the ratio of solid Ag to AgCl, which is largely invariant due to the bulk quantities present in the electrode. Generally, the electrode is surrounded by a saturated solution of potassium chloride (KCl) which minimises the Cl^- concentration dependence of the electrode to maintain a constant potential.

Commercial Ag/AgCl reference electrodes (Figure 3-9) are conventionally used in the laboratory and in aqueous solutions but they have disadvantages such as robustness and ruggedness in non-aqueous solutions and are brittle and expensive. In lubricant acidity monitoring, oil can also potentially block the porous plug of the electrode. This necessitates the need for a solid state, inexpensive, rugged and accurate (range of millivolts) reference electrode for oil pH monitoring.



Figure 3-9: Commercial (Beckman Coulter) silver-silver chloride reference electrode

3.5 Summary

In this Chapter, thick film technology and measurement theory were reviewed in detail. Solid state ion selective electrodes using thick film technology have shown good sensing capabilities in pH measurements for aqueous solutions. However, their feasibility for detecting pH of non-aqueous solutions and lubricating oil acidity has never been explored before.

The advantages of TF sensor development, such as low-cost infrastructure, mass production opportunity, miniaturised dimensions and robustness with a good reproducibility, were discussed. TF sensors also suffer from disadvantages such as uneven surfaces as a result of errors in the manufacturing process. Printed and fired surfaces are typically not homogeneous in micro scale which can lead to issues such as dissimilar sensitivity of electrodes. However, this issue can be rectified by using more sophisticated and accurate printing equipment to ensure the electrode surfaces are uniform. This effect will be discussed further in Chapter 6 of this thesis.

Chapter 4. Experimental methodologies

4.1 Introduction

In Chapters 2, a detailed review of the theories and techniques of oil condition monitoring was presented. Chapter 3 introduced Thick Film technology and presented the theory of working and reference electrodes. In this chapter, experimental methodologies employed for accomplishing the aims and objectives set in Chapter 1 are discussed. These include off-line and on-line oil condition monitoring methods in which on-line acidity sensors (thick film electrodes) are developed and tested and the results are validated using laboratory-based devices/techniques such as viscometer, impedance spectrometer for conductivity and conventional titration method for acid number (AN) measurements. Three key properties, i.e. conductivity, viscosity and acidity of oils were selected to be monitored and experiments were performed to analyse their behaviour with the degradation process of oils. As previously discussed in Chapter 2, no publication has reported commercially available on-line oil acidity sensors due to the complexity of oil chemistry and the difficulties in simulating oil ageing in laboratories. Thick film technology has shown to be a good mean of chemical sensor development hence it was chosen for acidity sensor fabrication in this work.

Figure 4-1 illustrates the overall test approach for this project. Thick film sensor fabrication is shown on the left-hand side of the schematic including both working and different types of reference electrodes. Sensor fabrication is followed by sensor evaluation (displayed in the centre and right-hand side of the schematic) which is divided into two main parts. In the centre of the schematic, the calibration, different experiments carried out with degraded oil samples as well as the sensor performance studies are shown. Lastly, off-line methods such as AN measurement which are used to validate and support the experiments are shown on the right-hand side of the schematic.

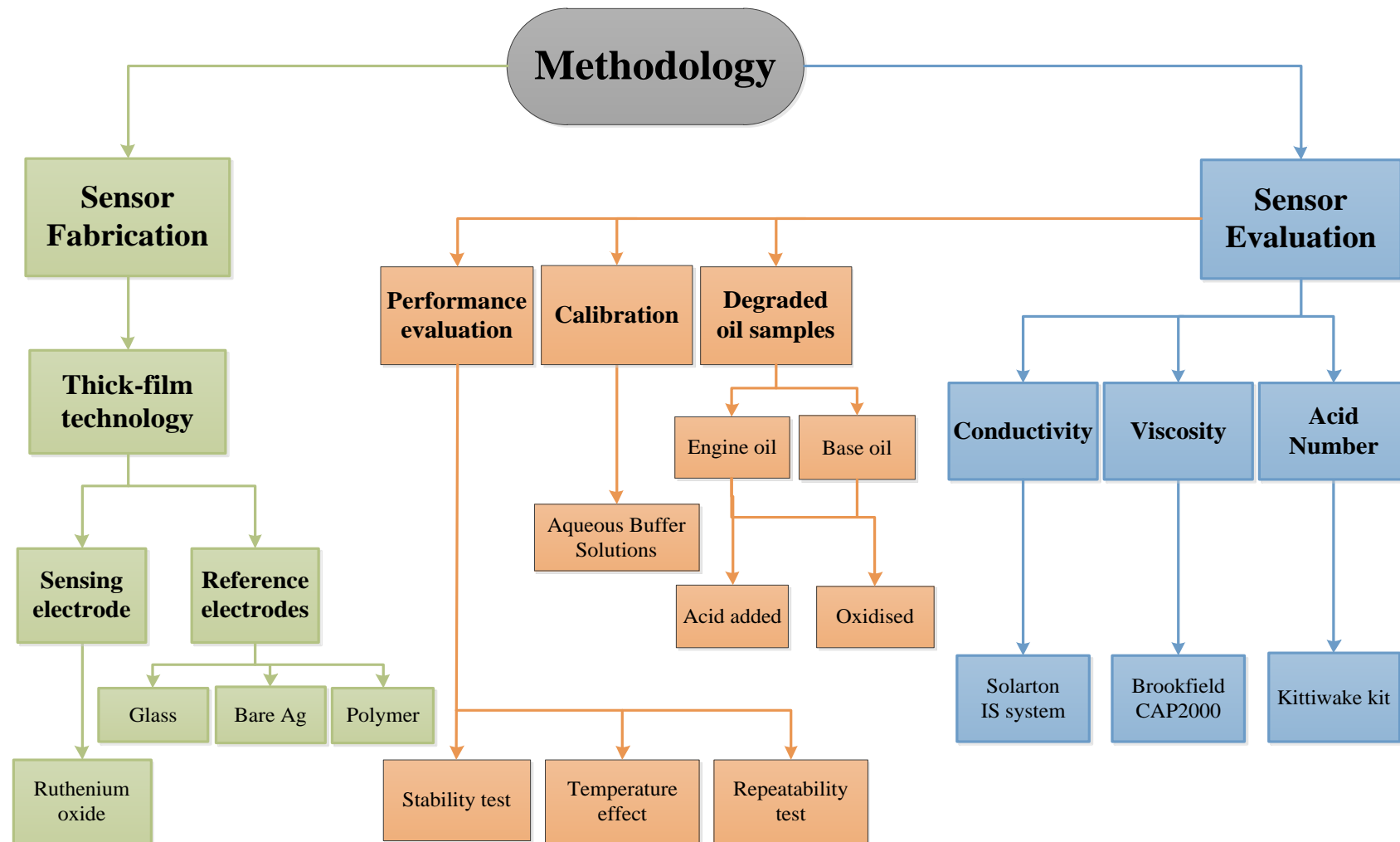


Figure 4-1: Schematic demonstrating the overall test methodology

4.2 Thick Film Electrodes for Oil Acidity Measurement

4.2.1 Electrode Design & Construction Process

In this study, ruthenium oxide (RuO_2) thick film electrode was used as the working electrode against 3 types of thick film reference electrodes. The first type was a bare silver conductor while the other two types had the extra layer of Ag/AgCl , one with polymer-based binder and one glass-based. Lastly a commercial glass gel-filled Ag/AgCl reference electrode (Beckman Coulter A57193) was also used. Different types of reference electrodes were tested in order to compare and select the most suitable for oil acidity measurements. Details of the TF reference electrodes are shown in Table 4-1. Figure 4-2 illustrates the schematic of the thick film electrode fabrication process divided into 7 main stages.

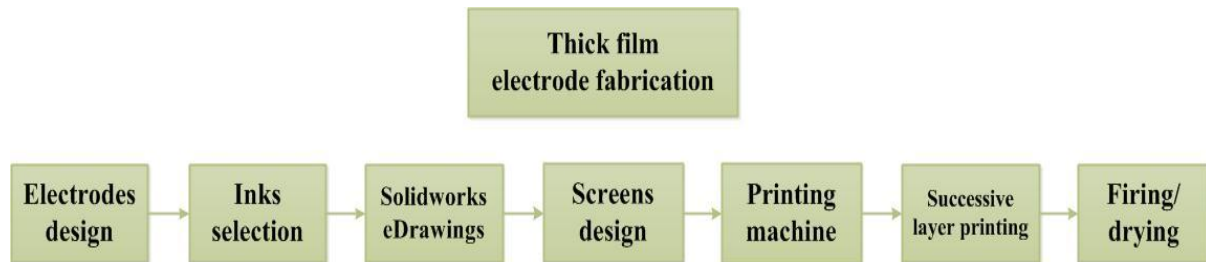


Figure 4-2: Schematic demonstrating the thick film electrode fabrication process

The thick-Film electrodes were screen-printed onto 50 mm x 50 mm, 96% alumina substrates (Coorstech) with thickness of 0.625 mm, where each substrate was divided into six equal sized electrodes and pre-scribed with laser lines so that each electrode could be easily snapped off along those lines. Therefore, 6 electrodes were fabricated simultaneously on a single substrate.

The electrodes were constructed by successive screen-printing of each layer. The screen designs for each layer were produced using a software called *Solidworks eDrawings* to give precise dimensions of the mesh openings. Each screen was designed to print a single layer of the electrode using Aurel printing machine (Aurel C880 printer).

4.2.1.1 Reference electrodes

For the fabrication of the thick film Ag/AgCl reference electrodes, 3 layers were printed using 3 screens. All the 3 screens were made from stainless steel and were manufactured for the Aurel C880 Printer by MCI, Cambridge. The first layer printed on the substrate was the silver conductor. The mesh opening on the screen was a rectangle with dimensions of 2.25 mm x 44.55 mm which are the sections through which the ink passes the screen and prints on the substrate. Secondly, a dielectric layer was deposited on top of the silver layer, leaving a small window opening exposing the underlying silver. The screen mesh opening had a rectangular shape of 6.5 mm x 43.8 mm. The window size was 3.4 mm x 3.4 mm square while a part of the underlying layer approximately 4.15 mm x 2.25 mm was exposed for soldering of connecting wires. The silver conductor layer was printed using ESL-9912 ink and on top of this, dielectric insulator ESL 4905-C was deposited to protect the conductor from the electrolyte. Next, the screen for the Ag/AgCl layer was a square window of 4 mm x 4 mm, slightly bigger than the exposed silver (3.6 mm x 3.6 mm) making sure all the silver was covered. Two types of Ag/AgCl were used, a polymer based ink provided by Gwent Electronic Materials (GEM C61003P7) and the other type was glass based ink provided by Universidad de Polit cnica de Valencia in Spain (PPCFB2).

The construction procedure mimics the construction of the single junction glass gel-filled Ag/AgCl commercial reference electrode. The schematics, including the layers and the inks used for the construction of the reference electrodes are shown in Figure 4-3 (glass Ag/AgCl), Figure 4-4 (polymer Ag/AgCl) and Figure 4-5 (bare silver).

4.2.1.2 RuO₂ working electrode

For the working electrode construction, three different inks were used. The first layer was the conductor which was Platinum Gold (ESL 5837) and was screen printed on the same type of substrates (alumina), with the same screen as the silver conductor layer for the reference electrodes, with exactly the same procedure. For the second layer a polymer dielectric insulating paste was used (GEM 2020823D2) with the same screen as the one used for the dielectric insulator for the reference electrodes. On top of that, over the window exposing the conductor, ruthenium oxide paste was printed (C505502D7) as the sensitive material for the detection of H⁺ ion concentration. The screen used for this layer was the same as the one used for the Ag/AgCl layer of the reference electrodes. Typical construction of a working and

reference electrode is shown in Figure 4-3. After the printing process for each layer the electrodes were held at room temperature for 10 minutes to allow relaxation of surface stresses and then dried in an infrared mini dryer (DEK 1209, Figure 4-7). The layers that required 850°C firing were fired in a 6 zone belt furnace (BTU VQ41) at a peak temperature of 850°C with an ascent and decent temperature of 50°C/min keeping it at peak for 10 minutes. Drying and curing temperatures for each paste are provided in Table 4-2.

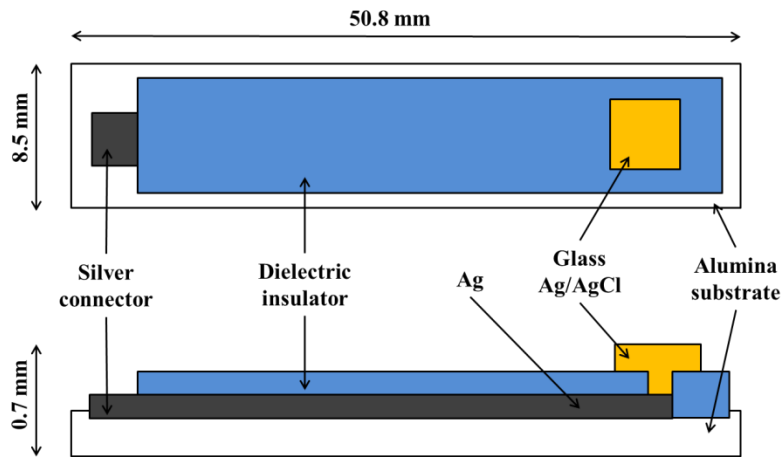


Figure 4-3: Top-view and cross section of glass Ag/AgCl thick film reference electrode

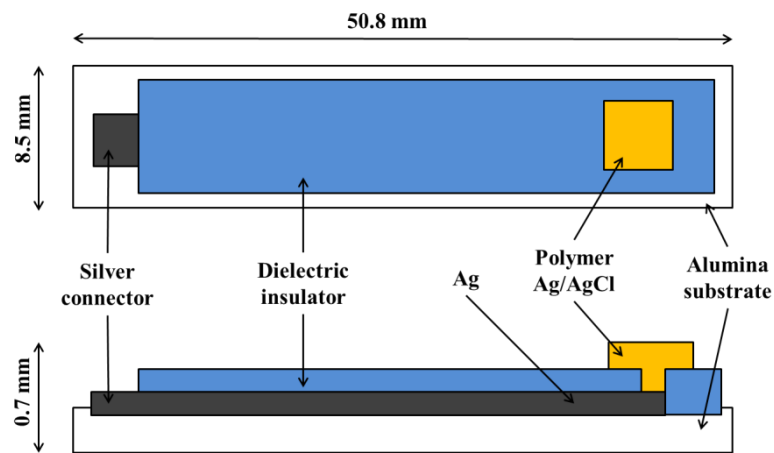


Figure 4-4: Top-view and cross section of polymer Ag/AgCl thick film reference electrode

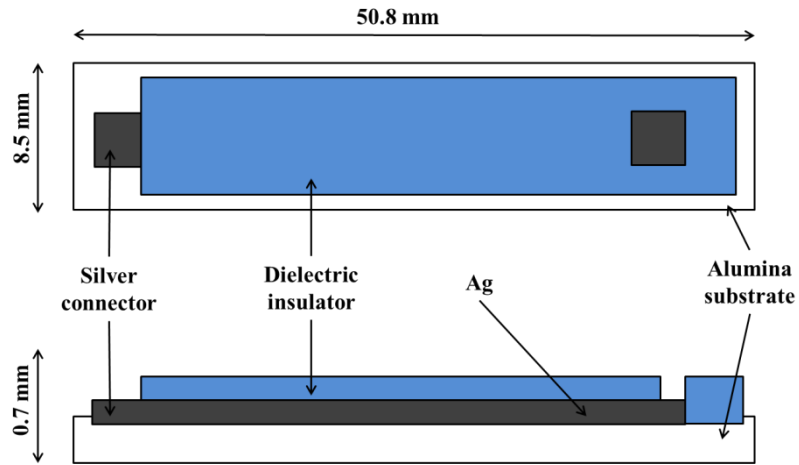


Figure 4-5: Top-view and cross section of bare silver thick film reference electrode

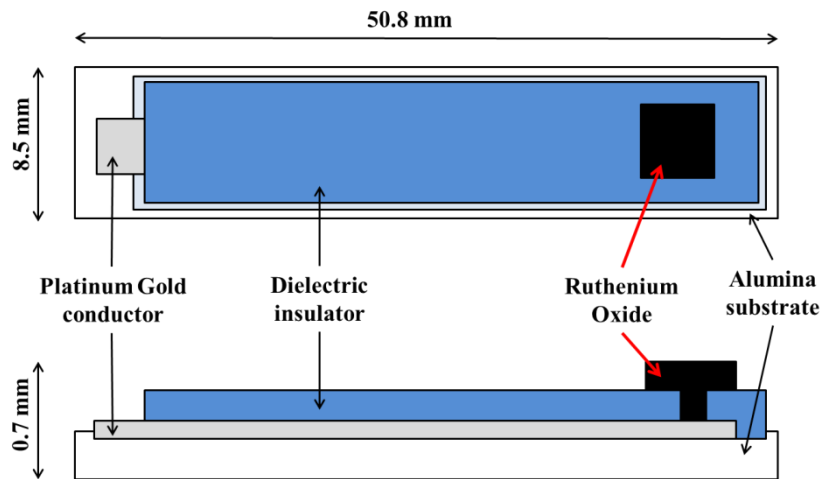


Figure 4-6: Top-view and cross section of ruthenium oxide thick film working electrode



Figure 4-7: DEK 1209 infrared mini dryer

Reference Electrodes	Name	Description
1	Commercial	Commercial Beckman Coulter
2	Glass	Silver (ESL9912-A), Dielectric layer (ESL4905-C), Glass Silver-Silver Chloride
3	Bare Ag	Silver (ESL9912-A), Dielectric layer (ESL4905-C)
4	Polymer	Silver (ESL9912-A), Dielectric layer (ESL4905-C), Polymer Silver-Silver Chloride

Table 4-1: List of reference electrodes used for the experiments

Layer	Paste	Drying temperature (° C)	Drying time (min)	Curing temperature (° C)	Curing time (min)
Platinum Gold Conductor	ESL 5837	125	10 – 15	850	~45
Dielectric polymer insulator	GEM 2020823D2	-	-	80	30
Ruthenium oxide	C50502D7	-	-	80	10 – 15
Silver conductor	ESL-9912-A	125	10 – 15	850	~45
Dielectric insulator	ESL-4905-C	125	10 – 15	850	~45
Polymer silver - silver chloride	GEM C61003P7	-	10	60	30
Glass silver - silver chloride	PPCFB2	150	10	390	~30

Table 4-2: Drying and curing temperatures for the pastes used for thick film electrodes fabrication

4.2.2 Electronics and circuitry

To detect the acidity of oil/aqueous solutions, a WE and a RE were connected to a voltmeter in order to record the potential difference between the 2 electrodes. Conventional voltmeters, such as Keithley 2000 Multimeter with 1 M Ω input impedance, can accurately measure the potential difference of thick film electrodes in aqueous solutions. Aqueous solutions have low impedance or high conductivities, for example the conductivity of sodium chloride (NaCl) is 1 Sm⁻¹, whereas oils are low conductive mediums, e.g. aged oils conductivity is approximately 10⁻⁶ Sm⁻¹ (depending on type of oil). Therefore, such voltmeters cannot detect the developed potential difference between the electrodes and oil sample due to low input impedance. A high input impedance voltmeter from Metrohm was selected for the experiments. Metrohm 827 pH lab has a high input impedance (~tera ohm) and resolution (0.1 mV & 0.1 pH). Additionally, in order to reduce the signal to noise ratio, the electrodes were soldered to a coaxial cable. Figure 4-8 shows the schematic of the experimental setup for oil acidity measurement.

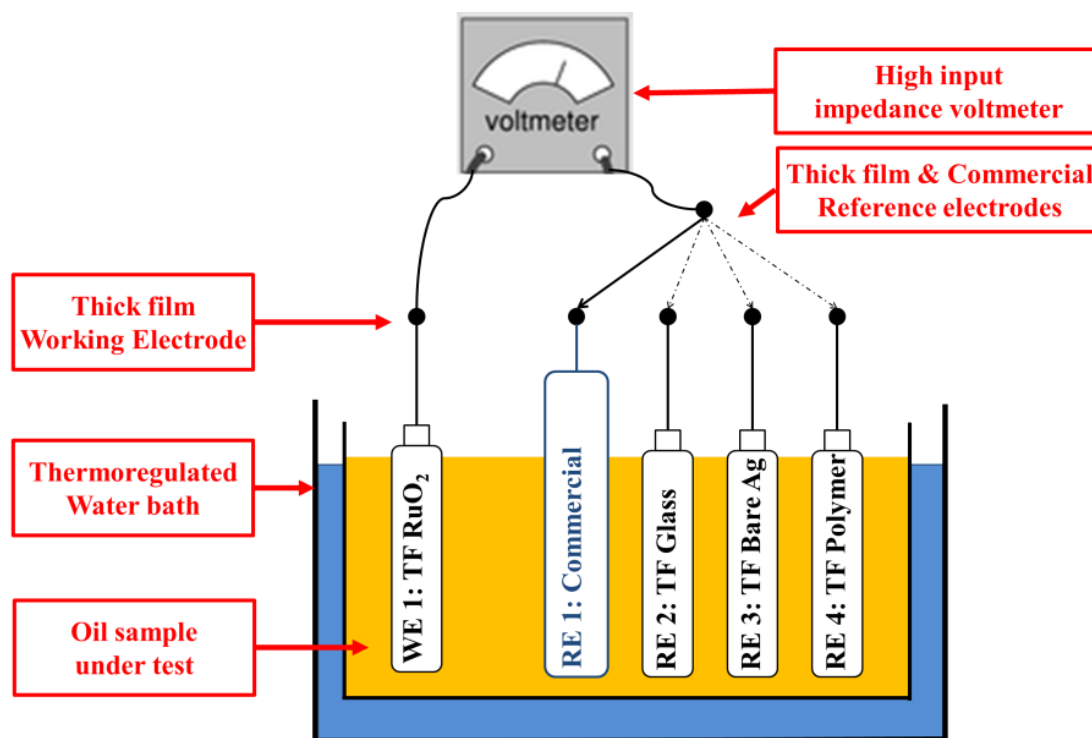


Figure 4-8: Schematic of the experimental setup for oil acidity measurement

4.2.3 Hydration and Calibration of the electrodes

All electrode pairs were hydrated and calibrated in aqueous buffer solutions at room temperature prior to being tested in oil samples to determine the baseline response of the TF sensors and confirm their functionality. Hydration time for the electrodes, i.e. the period after which the electrodes produce stable potentials, was determined by monitoring them in a pH 7 buffer solution. Then the sensors were cyclically calibrated in 3 buffer solutions (pH= 4, 7 and 10, Figure 4-9). For calibration purposes, the Beckman Coulter commercial reference electrode was used as a comparison. After the hydration and cyclic calibration processes, the electrodes were tested in oil samples.

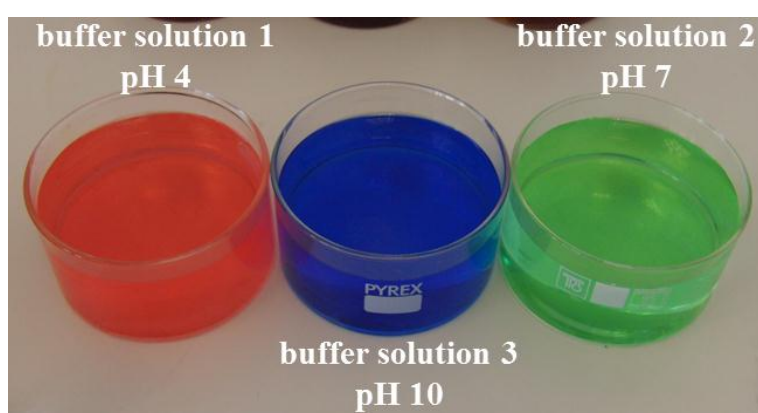


Figure 4-9: Three different pH buffer solutions (250 ml in glass container) used for calibration of the electrodes

4.3 Acid Number (AN) measurement

In order to validate the performance of the thick film electrodes, Acid Number (AN) of oil samples was measured using a Kittiwake test kit (Multi-parameter FG-K1-110-KW) at room temperature, following the 'ASTM D974-12' standard, using colour-indicator titration. Initially, 20 ml of titration Reagent D in red colour was poured into a jar. Then, 2 drops of Kittiwake AN Titrant were added (one at a time) to the jar, changing the colour of the Reagent D to light green. Thereafter, 1 ml of an oil sample was added to the jar. The colour of the liquid mixture in the jar turned back into red due to the acidic features of the oil sample added. Again, AN titrant was added one drop at a time to the jar, swirling it between each drop and counting the number of drops added. The number of drops required to turn the colour of the solution back to green was counted and the AN value calculated (AN

[mgKOH/g] = number of drops x 0.1). For instance if 14 drops are required, the AN value would be $14 \times 0.1 = 1.4$ mgKOH/g (0.1 is the sample size factor).

4.4 Conductivity measurement

Oil electrical properties such as permittivity, impedance and conductivity change as it degrades. Fresh lubricants are poor electrical conductors. However, as oil degrades, its electrical conductivity increases due to the increase of concentration of “conductive species” such as nitric acid (oxidation by-products) and contaminants (e.g. metallic wear particles, water). Therefore, electrical properties provide a potentially powerful means of assessing the quality of oils.

For this study, EIS tests were performed using a Solartron 1260 gain-phase frequency analyser model 1260A, connected to a Solartron dielectric interface model 1296A, controlled by a PC running Solartron “Smart” software permitting automated data collection. The test cell utilised a cup-plate geometry which has an electrode diameter of 42 mm and an electrode gap of 0.5 mm (spacer) requiring 3ml of oil, as illustrated in Figure 4-10. Measurements were carried out at 2 temperatures (50 and 80 °C). Before each EIS measurement, 15 minutes were allowed to achieve a stabilised temperature. An AC voltage (100 mV RMS amplitude) was applied at constant amplitude and the frequency was varied from 1 MHz to 1 Hz. 8 points per decade were collected and the data were averaged over 10 cycles. The conductivity of the oil is reciprocal of electrical resistivity which can be calculated from the resistance and the cell constant (area and distance between 2 electrodes) obtained using Equation 4-1⁵⁴:

$$R = \rho \frac{d}{A} \Rightarrow \sigma = \frac{1}{\rho} \quad (\text{Equation 4-1})$$

Where ‘ R ’ is oil resistance in ohm, ‘ ρ ’ is the oil resistivity in ohm cm, ‘ σ ’ is the oil conductivity in 1/ (ohm cm) or Siemens/ cm, ‘ A ’ is the electrodes area in cm² and ‘ d ’ is the distance between the electrodes in cm.

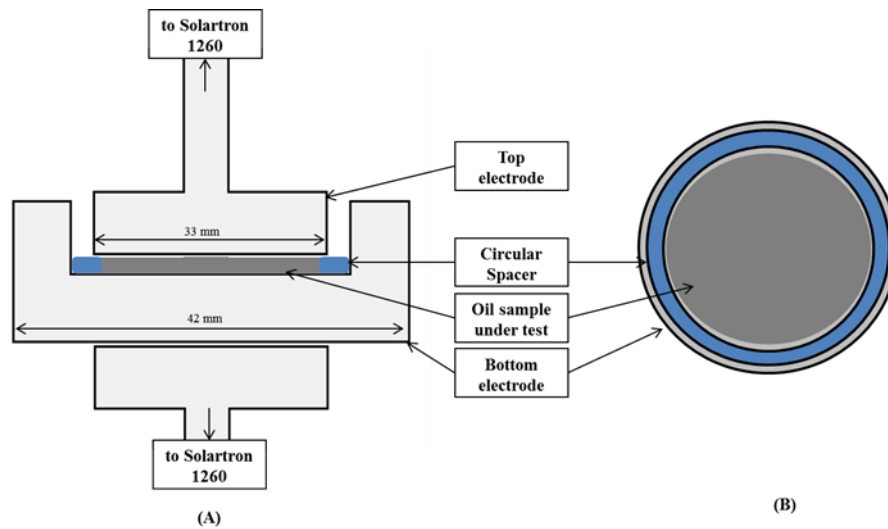


Figure 4-10: The EIS test cell configuration, (A) side view; (B) top view (excluding the top electrode)

4.5 Viscosity measurement

Brookfield CAP2000 viscometer (‘cone and plate’) was used to measure the viscosity of the oil samples. A ‘cone and plate’ viscometer is in principle a torque meter in which a cone is used to interact with the sample on a stationary flat plate and is rotated at discrete speeds. The torque measuring system senses the resistance to rotation of the sample under test which is proportional to the shear stress in the fluid. The shear stress is then converted to absolute centipoise units.

Brookfield CAP2000 viscometer, shown in Figure 4-11, can measure viscosities from 0.2 to 15,000 Poise, at shear rate ranging from 10 to 13,000 sec^{-1} (5-1000 RPM) at 5 to 75 °C. For viscosity measurements at higher temperatures, the standard ASTM D341⁹⁸ was used to convert viscosity at different temperatures. For viscosity measurements, 1 ml of oil sample was placed on the peltier plate and the cone spindle is lowered by the handle to interact with the sample rotating at desired speed. The viscosity is measured and displayed on the digital display.

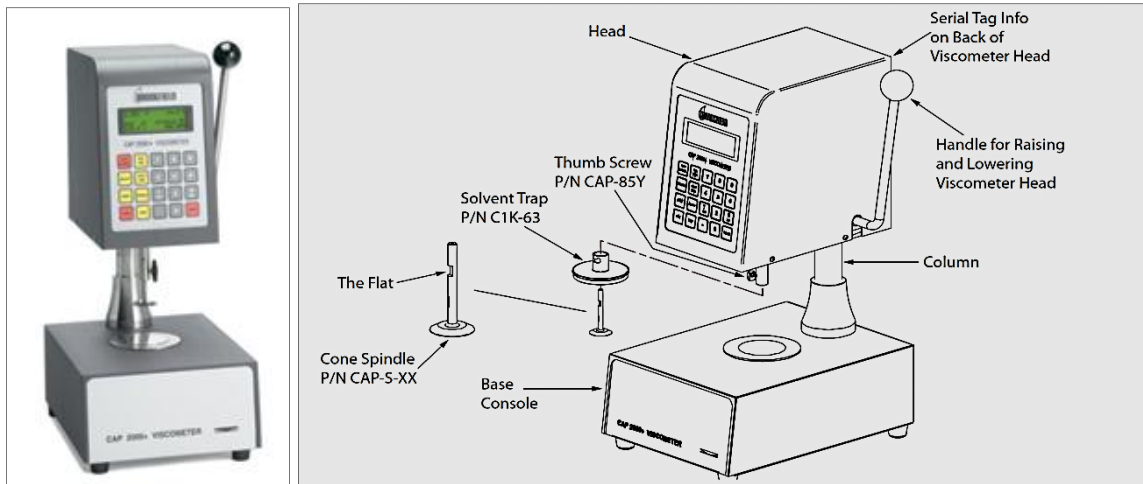


Figure 4-11: Brookfield CAP2000 viscometer^{vi}

4.6 Oil samples

To evaluate the performance of the acidity sensors, both a base and a fully formulated engine oil samples were artificially degraded by adding nitric acid or oxidation methods. Table 4-3 summarises the oil types and the degradation processes used.

	Oil type	Method of degradation	No. of samples
1	Base oil: Motiva Star 6 Group II	In-house oxidation (at Shell lab)	7
2	SAE 5W-30 engine oil (with additives)	In-house oxidation (at Shell lab)	7
3		Nitric acid added	13

Table 4-3: Detail of the case studies and oil samples

4.6.1 Oxidised base & fully formulated engine oil samples

Base oils are relatively simple solutions in comparison to fully formulated engine oils as they do not contain any additive packages, hence the TF sensors were initially tested in oxidised base oil samples. This was then followed by testing the TF sensors in oxidised fully formulated engine oils in order to evaluate the performance of the sensors and also compare the properties of the 2 types of oil samples which were oxidised in the same way.

Oil samples for this experiment came from a proprietary in-house Blown NO_x (BNOX) oxidation test carried out at Shell's Houston laboratories. During the oxidised process, 350 ml

^{vi} <http://www.brookfieldengineering.com/products/viscometers/laboratory-cap-2000.asp#specifications>

of fresh Motiva Star 6 base oil (a group II base oil containing no additives) and SAE 5W30 engine oil were oxidised at a temperature of 155 °C, whilst an air/NO₂ mixture (NO₂ concentration was 3000 ppm) was passed into the oils at 200 cc/min. For fully formulated oil, this test causes oxidation in approximately 60-80 hours. In base oil, however, since the oil sample contained no additives, oxidation occurred much sooner, and substantial viscosity increases were seen after only 24 hours. Oil samples were taken at 6 oxidised stages (durations), i.e. 2, 4, 8, 16, 20 and 24 hours for base oil and 24, 48, 72, 96, 120 and 144 hours for fully formulated engine oil (Table 4-4). The colour of the base oil samples became darker with the oxidation time (see the image of the oil samples in Figure 4-12).

Oil samples	BO oxidation (hours)	FFO oxidation (hours)
1	0	0
2	2	24
3	4	48
4	8	72
5	16	96
6	20	120
7	24	144

Table 4-4: Oxidised base and fully formulated oil samples

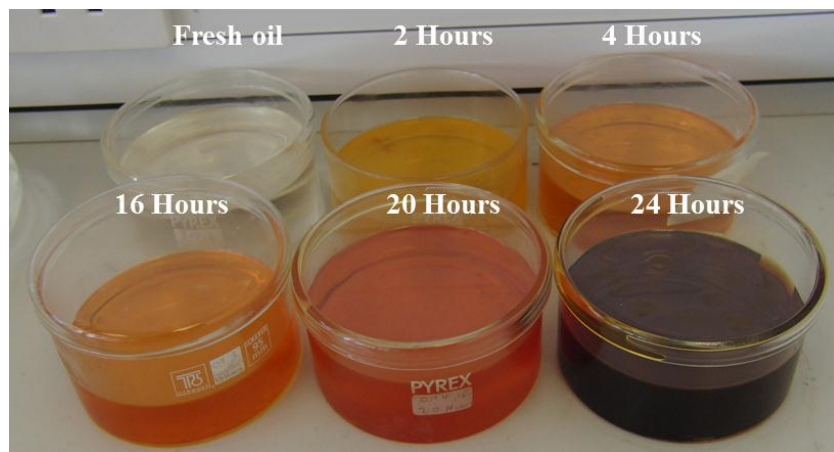


Figure 4-12: Shell oxidised base oil samples

4.6.2 Adding nitric acid into fresh fully formulated engine oil

Using a different degradation method, the acid concentration of fresh oil was artificially increased by adding nitric acid into fresh fully formulated engine oil. Oil samples were prepared by progressively adding nitric acid drops (70% concentration, Fisher Scientific) into 250 mL of off-the-shelf Magnatec Fully Synthetic SAE 5W30 fresh engine oil. Nitric acid was diluted with water in order to reduce its concentration to 30%. Nitric acid was used as it replicates the combustion engine by-product as discussed in Chapter 2. To ensure the acid mixes well in the oil, the oil samples were constantly stirred for 15 minutes while the acid drops were added using a pipette (Fisher Scientific) into the oil before the responses from the TF electrodes were recorded. However, the added water formed emulsions and did not mix well with the oil. This method was also tried with base oil but the water effects were more significant and did not produce useful results.

Details of the 13 oil samples with added acid concentrations are shown in Table 4-5.

Oil samples	Concentration of acid (ppm)		Oil samples	Concentration of Acid (ppm)
1	0		8	400
2	25		9	700
3	50		10	1000
4	75		11	1300
5	100		12	1600
6	150		13	2000
7	200			

Table 4-5 Details of the Oil samples

4.7 Sensor evaluation tests

During acidity testing, all electrodes (WE and RE) were initially hydrated and tested in aqueous buffer solutions to ensure that acceptable performance of the electrodes was achieved. The electrodes were then tested in the oil samples at 2 temperatures (50 and 80 °C). These temperatures were chosen to represent engine operating temperatures within the oil sump⁵¹. Measurements were performed after 15 minutes of heating the oil samples to allow temperature stabilisation. Each measurement for each electrode pair was repeated 5 times and mean and standard deviation values were calculated.

4.7.1 Temperature effects test

Temperature has a great effect on different oil properties such as viscosity and also on the performance of the TF sensors. Therefore, the performance of the TF electrodes in 3 buffer solutions (pH 4, 7 and 10) at different temperatures (25 °C, 40 °C, 60 °C, 80 °C) was investigated. Temperature effect tests on both oxidised base and fully formulated oils were carried out at room temperature (~20 °C), 30 °C, 50 °C, 70 °C and 90 °C. Two oil samples from each set (4 and 20 hours oxidised base oil samples alongside 48 and 120 hours oxidised fully formulated oil samples) were selected to investigate the temperature effects on the thick film electrodes. The selected oil samples are from lower (i.e. 4 hours base and 48 hours oxidised fully formulated oil samples) and higher oxidised oil samples (i.e. 20 hours base and 120 hours oxidised fully formulated oil samples). The conductivity and viscosity measurements of the same oil samples at these temperatures were also carried out.

4.7.2 Stability and repeatability test

In order to determine the long term stability (also called drift test) of the TF electrodes in oil samples, the TF electrodes were tested in 24 hours oxidised fully formulated engine oil for nearly one month. This test involved inserting the TF WE and REs alongside the commercial RE in the 24 hours oxidised oil sample at 50 °C and taking readings at regular intervals (daily). Relatively fresh fully formulated engine oil sample (i.e. 24 hours) was selected for this test as the degradation of the engine oil is much slower than the base oil due to additive packages and it can be assumed that the acidity would remain constant throughout the test.

Repeatability of the thick film electrodes were also investigated by repeating the same tests using different set of electrodes in the oxidised base oil samples at 50 and 80 °C following the same procedure.

Chapter 5. Results and Discussions

5.1 Introduction

In the following sections the results from acidity measurements of different oil samples using thick-film ion selective electrodes are presented and compared with the off-line measurements (i.e. viscosity, conductivity and AN). The TF acidity electrodes were tested in a number of oil samples categorised based on the type of the oil (fully formulated engine oil or base oil) and methods of degradation (i.e. oxidation or adding acid).

Before presenting the results of TF electrodes in oil samples, the hydration and calibration results for the electrodes in aqueous buffer solutions are discussed in Section 5.2. In Section 5.3, measurements from oxidised base oil samples are presented. This section also includes a detailed electrochemical impedance spectroscopy (EIS) analysis of the oxidised oil samples. As discussed in Chapters 2 and 4, EIS enables the measurement of electrical properties of oil samples, such as conductivity, which were used for supporting thick film sensors results and also to establish relationships between different oil properties (e.g. viscosity and AN). The performance of the acidity sensors in oxidised fully formulated engine oil samples are discussed in Section 5.4. Section 5.5 compares the performance of the TF electrodes in oxidised base and fully formulated oil samples and investigates the degradation effects (i.e. oxidation) on both types of oil samples by examining the conductivity, AN and viscosity. Section 5.6 examines the behaviour of the TF sensors in fresh engine oil and oil samples with added nitric acid to simulate a series of oil acidity levels. The results were also compared with oils AN, viscosity and conductivity.

5.2 Hydration and pH testing in buffer solutions

All electrode pairs were initially hydrated in a pH 7 buffer solution to determine the baseline response of the TF sensors (both working and reference electrodes) and confirm their functionality. The sensors were then cyclically tested in 3 aqueous buffer solutions (pH= 4, 7 and 10) prior to being tested in oil samples. The Beckman Coulter commercial reference electrode was also tested for comparison.

Typical hydration results for 2 different sets of TF electrodes are shown in Figure 5-1 and Figure 5-2. From the first hydration results (Figure 5-1), it can be seen that all electrodes stabilised within 2 hours of hydration. Hydration time of the thick film electrodes depends on the fabrication and printing variations. The commercial electrode stabilised very quickly while it took at least 60 minutes for the TF reference electrodes to be stabilised. Amongst the 3 types of TF reference electrodes, the glass electrode stabilised the quickest while the other 2 took nearly 100 minutes to stabilise. This is normal with most solid state electrodes and a reason why they generally have to be pre-hydrated hence the hydration process establishes the equilibrium required for the sensors to perform. Furthermore, different electrode types stabilised at different potentials due to the differences in the construction, structure and materials of the electrodes. It is also noted that the different electrodes stabilised at different potentials. This should be relatively consistent for each type of electrodes and the variations again come from the printing process. Figure 5-2 illustrates the hydration graph of a different set of TF electrodes, measured with a different data logger and sampling rate, in which similar performances for different electrode pairs are observed. Commercial reference electrode stabilised rapidly after only 10 minutes but it took about 60 minutes for the TF glass and polymer and almost 60 minutes for the TF bare silver to stabilise. The output potential levels of the electrodes are similar to the previous set (Figure 5-1) but the initial changes for the TF glass and polymer are different.

Figure 5-3 illustrates the pH testing results in aqueous buffer solutions. The results from the pH testing in buffer solutions (Figure 5-3) show that both the commercial and the TF reference electrodes responded extremely well to the pH changes in the buffer solutions and a linear relationship was found for all the electrode pairs, see the sensor response vs. pH plots in Figure 5-4. The slopes (or sensitivities) for the commercial, the TF Glass, TF Polymer and TF Bare Ag REs when paired with RuO₂ WE are 60.2, 51.3, 54.1 and 35.6 mV/pH

respectively. Thus the commercial RE exhibited near an ideal Nernstian behaviour while the TF Glass and Polymer REs also showed near Nernstian responses⁹⁹ and the Bare Ag RE slightly under-performed. The fact that the commercial RE provided consistent outputs during the hydration and close to ideal Nernstian behaviour in cyclic testing in pH buffer solutions, demonstrates that the TF RuO₂ WE also performed consistently.

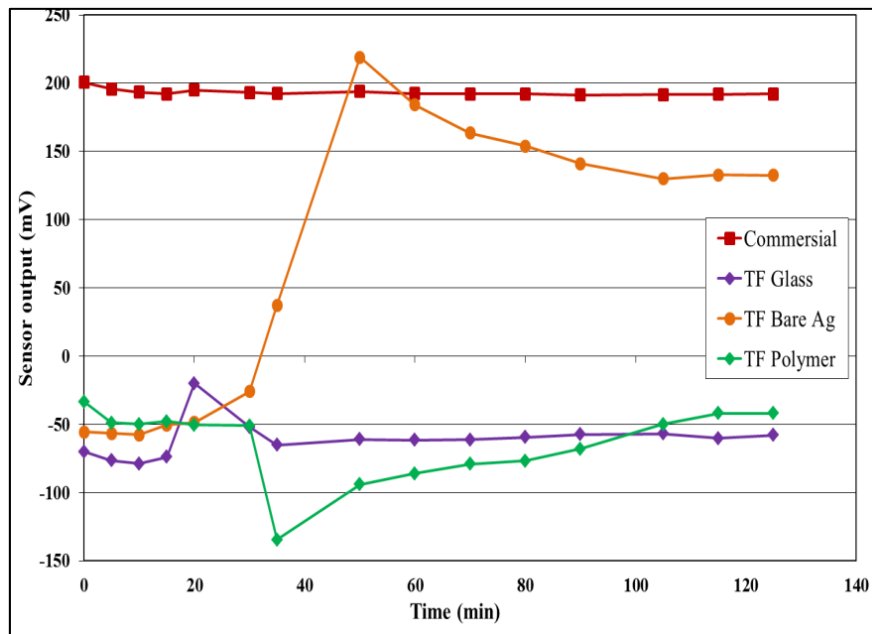


Figure 5-1: The hydration response of TF electrodes in aqueous buffer solution (pH 7)

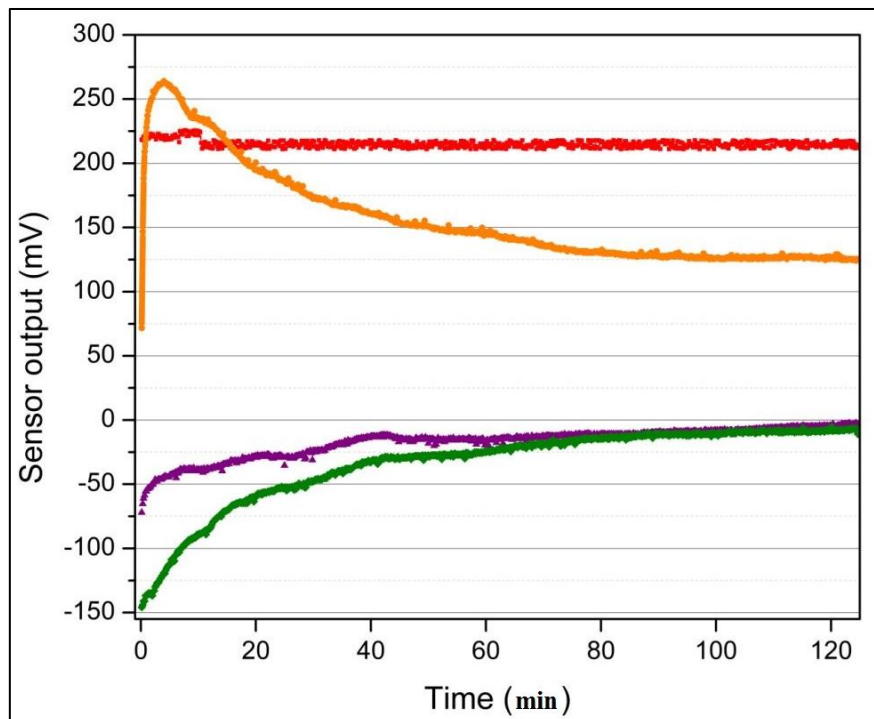


Figure 5-2: The hydration response of TF electrodes in aqueous buffer solution (pH 7)

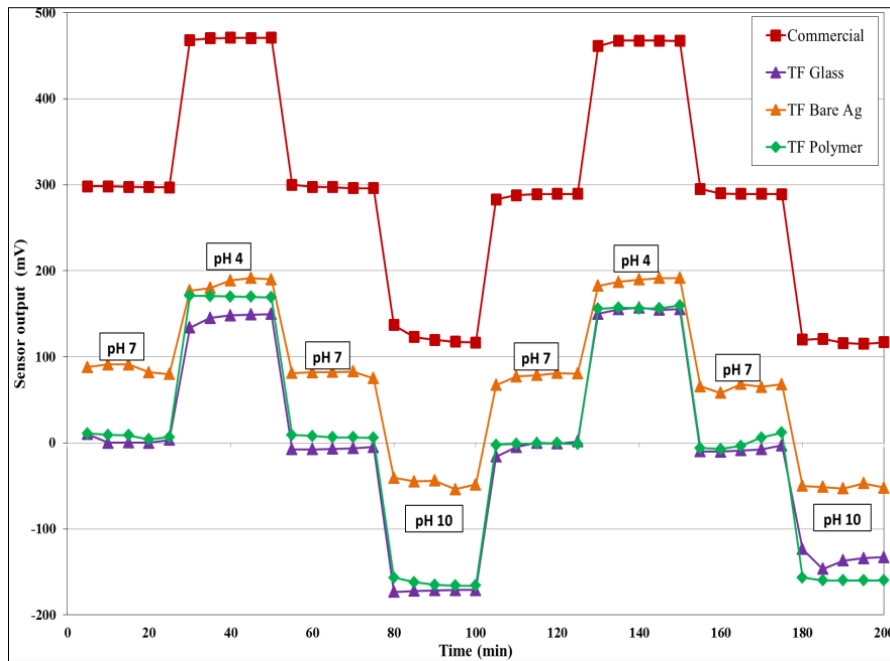


Figure 5-3: Graph of working electrode vs. different reference electrodes and a commercial reference electrode in different pH buffer solutions

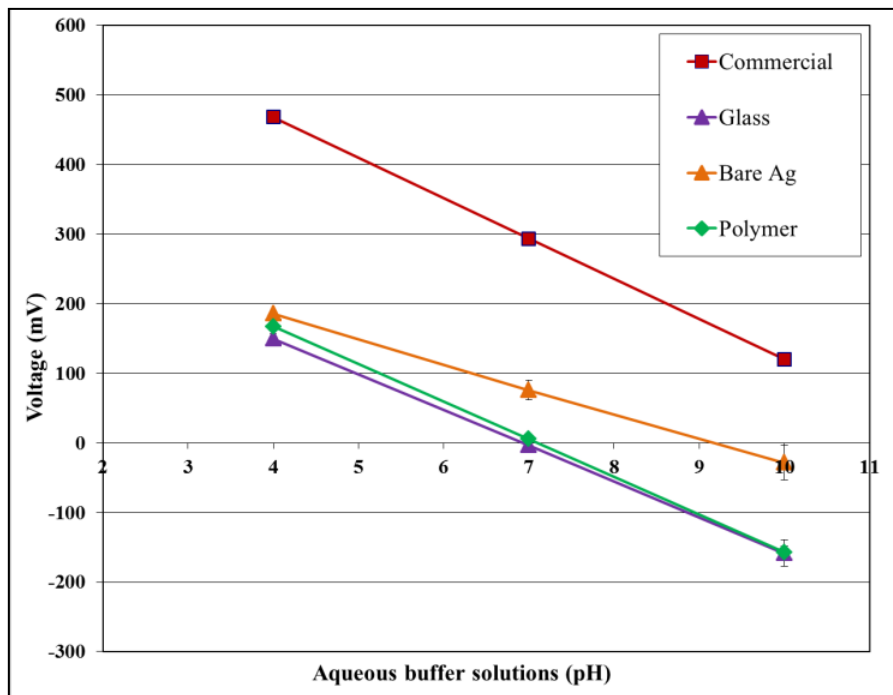


Figure 5-4: Calibration graph for each reference electrode

5.3 Oxidised base oil samples

5.3.1 AN, viscosity and EIS results

The details of the oxidised oil samples, AN, water content and viscosity measurements at two temperatures are shown in Table 5-1.

Oil samples	Oxidation (hours)	Acid number (mgKOH/g)	Viscosity at 50°C (mPa.s)	Viscosity at 80°C (mPa.s)	Water content (µg/ml)
1	Fresh oil	0	25	10	7.8
2	2	1.7	30.6	12.5	330.1
3	4	4.7	37.5	15	541.5
4	8	12.5	52.5	19	1819.1
5	16	28	80	27	2495.0
6	20	29	120	36.2	1736.8
7	24	32	166.8	49.3	1328.0

Table 5-1: Details of the oxidised oil samples

5.3.2 Electrochemical Impedance Spectroscopy (EIS):

The EIS results are presented in two forms, namely Bode and Nyquist plots. Figures 3 and 4 are the Bode plot representation of the oxidised oil samples impedance at 50 and 80 °C. Figures 3a and 4a show the impedance magnitude of each oil sample as a function of frequency (on logarithmic scales) and Figures 3b and 4b show the corresponding phase angle data. In each case, results obtained from different samples are presented using different colours (e.g. green for fresh oil and red for the oil aged for 24 hours). The impedance magnitude of the fresh oil displays an inverse dependence on frequency and the phase angle between the voltage and current is close to -90° , indicating that, as expected, the characteristics of the system are dominated by capacitive effects. The behaviour of 2 hours (dark grey line) oxidised oil sample is very similar to that of fresh oil, apart from the phase angle at lower frequencies (1 Hertz) which goes up to -65° at 80 °C. For more highly oxidised oil samples at lower frequencies down to 1 Hz (which for all practical purposes can be considered as DC) the impedance is constant with frequency and the phase angle is close to zero indicating predominantly resistive behaviour. For instance the resistive behaviour of the 8 hours oxidised oil sample starts are around 10 Hz in comparison to 100 Hz for the 20 and 24 hours oxidised oil samples. Therefore, the higher the oxidation of the oil samples, the lower is the impedance and their system behaves more like a resistor. The 80 °C graphs are quite similar to those for 50 °C; however, the overall level of impedance is lower. Figure 5-7

illustrates the capacitance magnitude of the oxidised oil samples as a function of frequency and, as can be seen, the capacitance increases at low frequencies for higher oxidised oil samples. Please note that the lines included in the figures to connect the data points together only serve to guide the eyes.

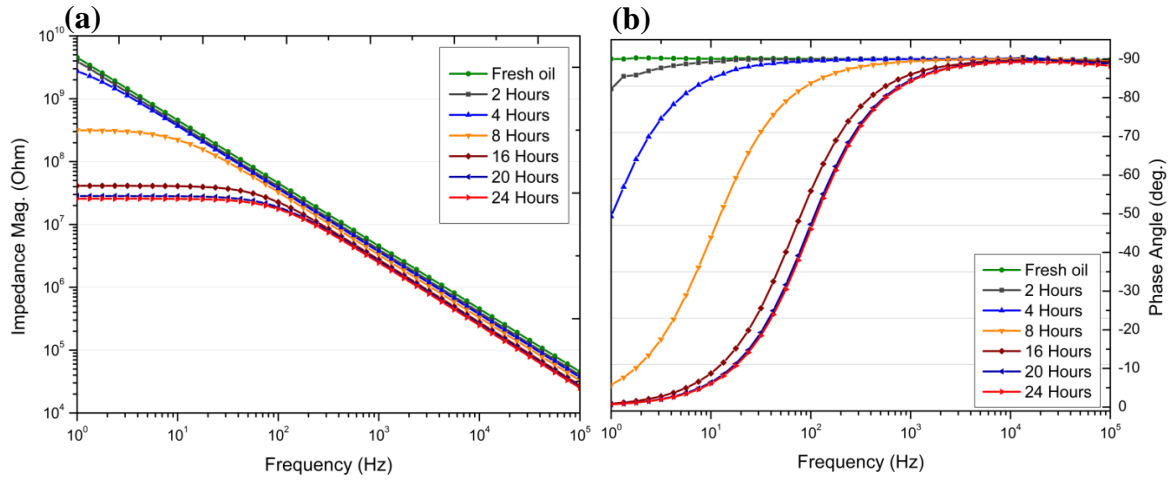


Figure 5-5: Bode plot of the oxidised oil samples at 50 °C

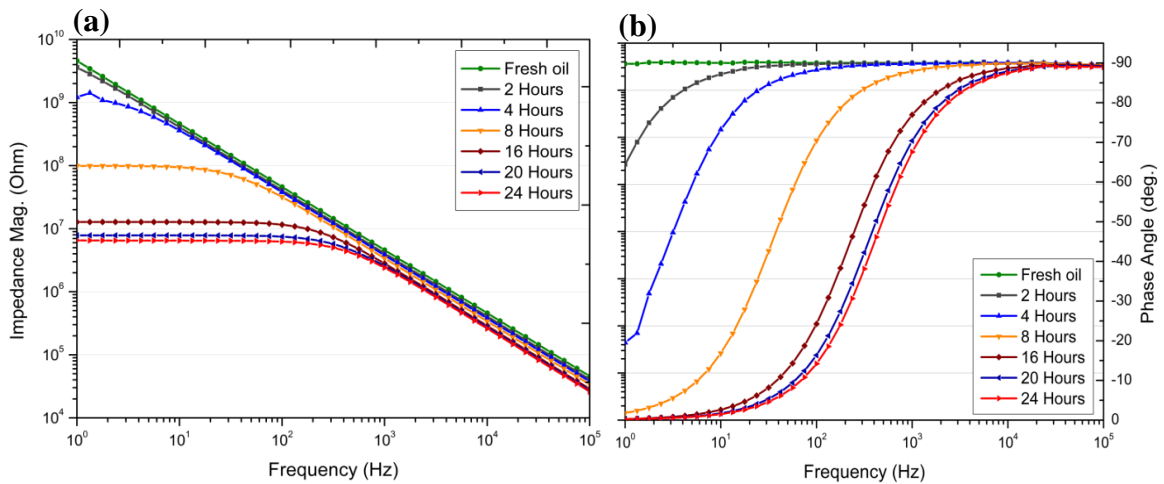


Figure 5-6: Bode plot of the oxidised oil samples at 80 °C

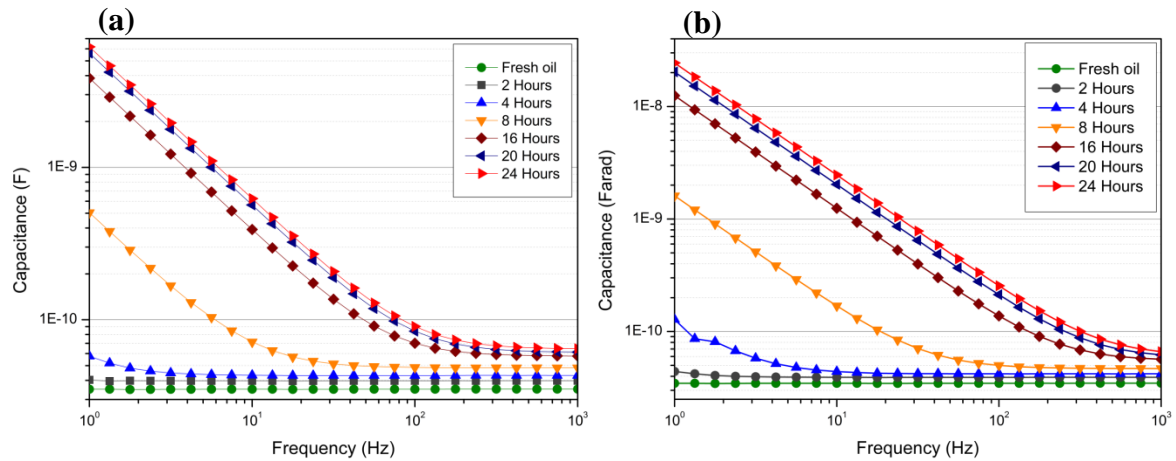


Figure 5-7: Capacitance magnitude of the oxidised oil samples (1-1000 Hz), at: a) 50 °C and b) 80 °C

The real (on the x-axis) and imaginary (on the y-axis) parts of the impedance of the oxidised oil samples are plotted in Figure 5-8 and Figure 5-9 as Nyquist plots or complex plane impedance diagrams at 50 and 80 °C respectively. Each point on the plot (i.e. impedance at different frequencies) is also representative of the impedance as a vector of length ($|Z|$) and phase angle (ϕ). As can be seen, semicircles are formed (except for fresh and 2 hours oxidised oil samples) and as the oxidation hours increase, the circles become smaller due to reduced impedance (the diameter of the semicircle corresponds to the resistance R). As seen in the more highly oxidised oil samples (i.e. 8, 16, 20 and 24 hours oxidised oil samples), perfect semicircles represent the impedance response corresponding to a single charge-transfer process and resistive behaviour of the oil samples. Fresh and 2 hours oxidised oils show significant capacitive impedance (very large semicircles) indicating a very high impedance to the passing current and capacitive behaviour. As expected, the radius of the semicircles reduces at higher temperatures due to decreased impedance. A minor glitch is observed in the impedance data of the 4 hours oxidised oil sample in Figure 5-9.

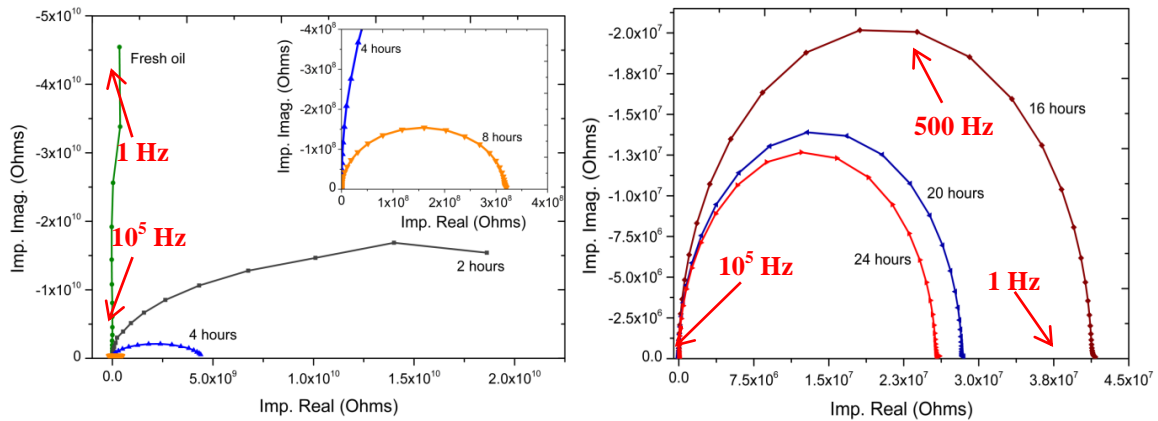


Figure 5-8: Nyquist plots of the oxidised oil samples at 50 °C

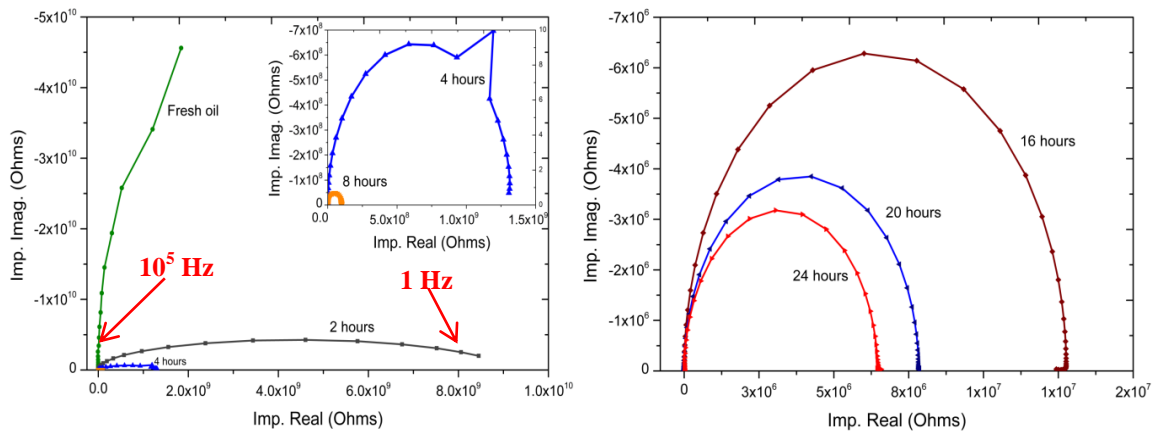


Figure 5-9: Nyquist plots of the oxidised oil samples at 80 °C

The effective conductivity was calculated from the impedance in the *DC regime* (or frequency independent Z), i.e. the impedance at low frequency (1 Hz) which represents the bulk resistance of the oil sample. Figure 5-10 depicts the effective conductivity plots of the oxidised oil samples at 50 and 80 °C and indicates that the oil conductivity increases with oil oxidation time. It is noteworthy that the rate of conductivity increase at lower oxidation times (i.e. over the first three oil samples) is much lower than that for the more highly oxidised oil samples (last four oil samples), probably as a consequence of fast radical chain propagation after 4 hours of oxidation. The slow increase in the conductivity of the oil samples between 0 to 4 hours can be an indication of the first phase of oil oxidation process, i.e. slow radical chain reaction at the oxidation initiation stage.

The conductivity of the oil samples at 80 °C is higher than that at 50 °C which may be a result of the lower oil viscosity and higher ion mobility at the higher temperature.

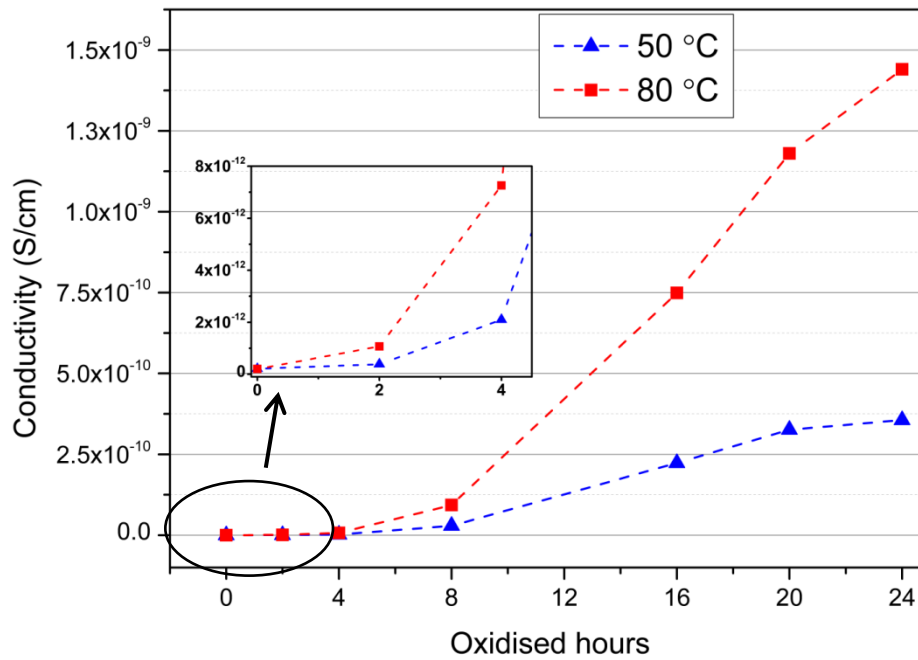


Figure 5-10: Effective conductivity of the oxidised oil samples at 50 and 80 °C

5.3.3 Measurements using TF sensors

Figure 5-11 illustrates the responses of the electrodes (4 WE-RE pairs) in the various oil samples at 50 °C and 80 °C. The performance of the 4 electrode pairs at 50 °C and 80 °C was, surprisingly, very similar, especially for the bare silver RE when compared to both of the solid state Ag/AgCl RE's and the commercial liquid electrolyte RE. This is probably due to the fact that any changes in the potential of the reference electrodes are insignificant compared to the change in potential of the working electrode. The consistency in the potential of the bare silver RE was unexpected in comparison to Ag/AgCl REs and the results suggest that the bare silver does not react with the chemical species in the oil. Therefore, it acts as a simple conductor with a stable voltage similar to the other REs. The negative polarity from the electrodes indicates that the working electrode had a lower potential than the reference electrodes. At 50 °C, the output voltage of the TF sensors increased with oxidation time up to 20 hours and plateaued up to the 24 hours oxidised oil at approximately 0 volts. This plateau is observed sooner at 80 °C from 16 hours onward at which point the output voltage also reached approximately 0 volts. Zero volt potential suggests the presence of a short circuit by sensor malfunction probably caused by the extremely high acidity of the oil samples. The AN of 29 and 32 mgKOH/g for 20 and 24 hours oxidised oil samples are extremely high compared to maximum AN value of 6 mgKOH/g in turbine, gear and hydraulic oils¹⁰⁰. The ruthenium oxide working electrode is probably being stripped/ reduced by the high acidity of

the solution, enhanced by the elevated temperature which could potentially leave ruthenium metal (no oxide) or even the bare metal of the back contact (platinum/gold) on the substrate. In any case, this could then leave just a purely conductive electrode pair with no H^+ response. When that happens, the sensor tends to short circuit as there are two conductors in the same oil having very similar electrode potentials. At this point, oil conductivity has increased significantly responding as an electrical component which results in an almost zero potential. This phenomenon was further investigated by comparing the SEM (scanning electron microscope) and EDX (energy-dispersive X-ray) analysis of the surface and cross section of the fresh (before testing in oxidised oil samples) and used (after testing) ruthenium oxide working electrode. Figure 5-12a illustrates the uniform surface of the fresh electrode and the SEM results of the used electrode (Figure 5-12b) shows the damage to the top layer of the TF working electrode. EDX analysis of the fresh electrode shows that there is a uniform layer of ruthenium oxide on the top layer of the WE. Alternatively, the EDX analysis of the used electrode (tables for the points A and B below the Figure 5-12b) shows the removal of the top layer, on certain parts of the electrode, as evidenced by the presence of substances from the bottom layer (platinum/gold). The small amount of palladium substance observed in the bottom layer, is used extensively in platinum/gold pastes by the manufacturer, to increase the solderability of the conductor. The carbon on the surface of the used electrode might be from the oxidised oil samples.

The maximum rate of change of acidity occurs between 2 and 16 hours at 50 °C, while at 80 °C it occurs between 0 and 16 hours. The rate of most reactions is highly dependent on temperature. As the temperature increases, the rate of the reaction increases. The reduction of ruthenium oxide to ruthenium metal, destroying the sensors, occurs earlier at 80 °C than at 50 °C for the same exact reasons.

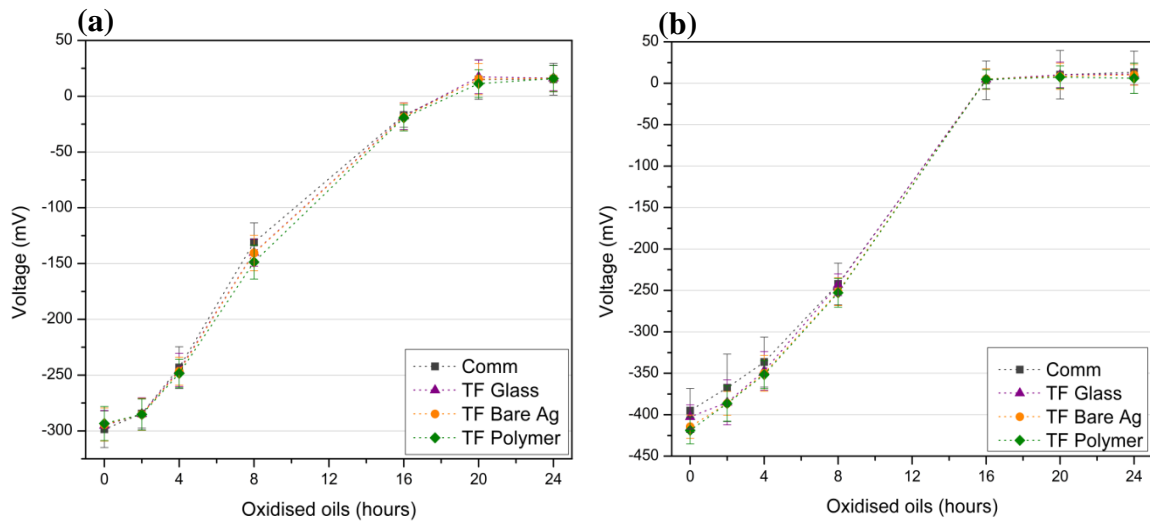


Figure 5-11: TF sensors output in oxidised oil samples, a) at 50 °C and b) at 80 °C

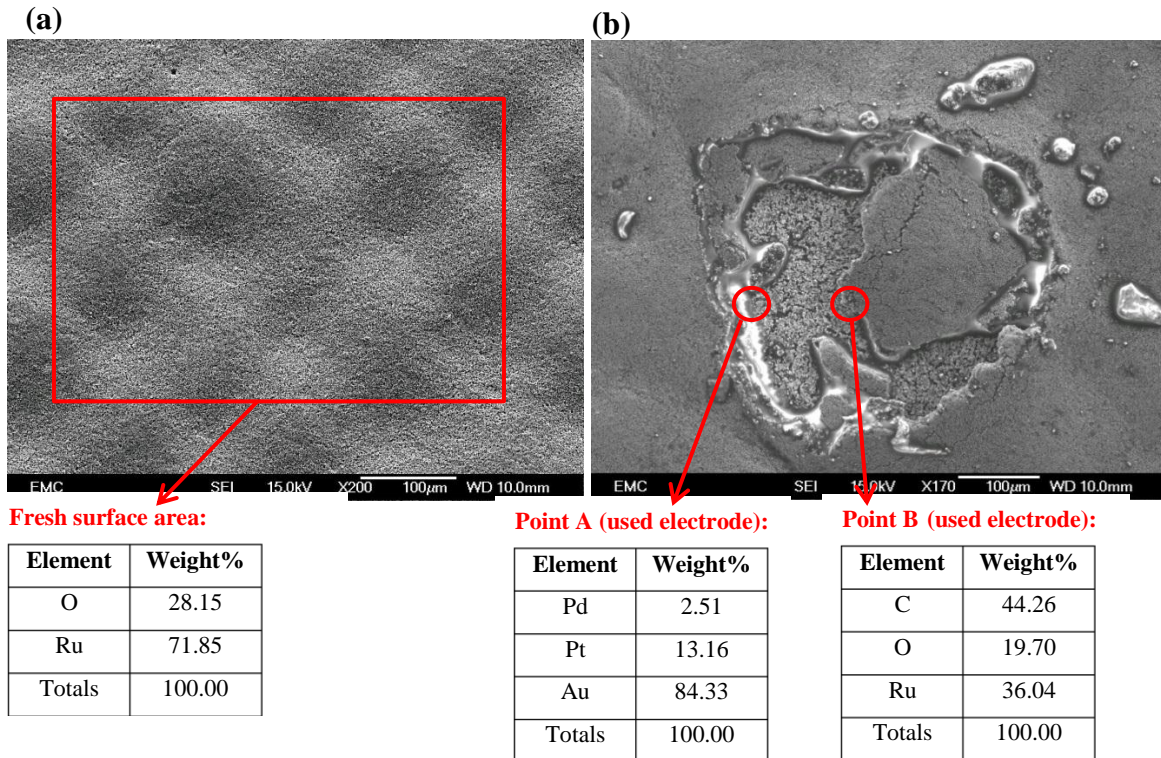


Figure 5-12: SEM results and the EDX analysis (shown in the tables below the figures) from fresh and used TF RuO₂ working electrodes: (a) surface of the fresh electrode (X200), (b) surface of the used electrode (X170)

5.3.4 TF sensors vs. AN, viscosity, conductivity & water content

The AN of the oil samples at room temperature increased with oxidation time as shown in Figure 5-13 and Figure 5-14. It can be seen that the oxidation process has produced significant amounts of acidic compounds, such as carboxylic acids, in the oil even at very low oxidation time i.e. 2 and 4 hours. This is because without additives, such as anti-oxidants, to prevent the acidity increase by neutralising the formed acidic compounds, the base oil can be oxidised easily. Different phases of the oxidation process can be observed in the AN graph, where the slow increase in oil acidity between 0 and 4 hours represents the oxidation *initiation* stage, followed by a rapid increase in oil acidity between 4 and 16 hours (*propagation, chain branching and auto-oxidation* period) leading to *termination* phase in which cross-linking considerably increases oil viscosity between 16 and 24 hours where a slow increase in AN is seen. This is also reflected in the viscosity changes.

The rate of increase in oil acidity is much higher at low oxidation hours (0 to 28 mgKOH/g for 0-16 hours of oxidation) compared to high oxidation times (28 to 32 mgKOH/g for 16-24 hours of oxidation). This is probably because the oxidation process has entered its final phase, i.e. termination phase in which the carbons are consumed/oxidised, i.e. hydrogen bonded to carbons are replaced by oxygen, producing CO₂ and H₂O and various other products such as carboxylic acid^{16,101}.

Figure 5-15 shows the output of the TF electrodes versus acid number at two temperatures. As can be seen, all of the TF electrodes responded to oil acidity changes in a linear fashion (R^2 value of >0.98 for all electrode pairs) with low errors (~2%). This demonstrated that the sensor can be used to detect the oil acidity and oxidation at the temperatures tested. This relationship does not occur for the output of the TF electrodes versus viscosity and conductivity (Figure 2-16 and Figure 5-17 respectively) although both viscosity and conductivity increase. This indicates that the sensors are highly sensitive to oil AN and not viscosity and conductivity.

The viscosity of the oxidised oil samples initially increased gradually from 25 to 80 mPa.s for the 0 to 16 hours oil samples but more significantly at higher oxidised times (from 80 to 166.8 mPa.s for 16 to 24 hours oxidised oils). This is probably due to the association of organic acids such as carboxylic acids in oil as carboxylic acid compounds being highly attractive causing them to behave as a larger molecule which increase the oil density of the

molecules resulting in considerable viscosity increase at higher oxidation hours^{16,101}. The output of TF electrodes versus viscosity at 50 °C and 80 °C is shown in Figure 5-16. There seems to be no relationship between the TF sensors output and oil viscosity and the performance of the sensors is independent of viscosity.

The conductivity of the oil samples increased with the level of oxidation, similar to that of the viscosity and AN. The output of TF electrodes versus conductivity at 50 °C and 80 °C is shown in Figure 5-17. Oil conductivity is dependent on many factors such as temperature. It can also be influenced by two parameters: directly proportional to ion concentration and inversely dependant on viscosity which itself affects the ionic mobility in the oil sample and depends on temperature. The increase in oil ion concentration as a result of oxidation is more dominant than the inverse viscosity effect, hence the conductivity continues to increase even at high viscosities at both temperatures.

As can be seen in Figure 5-16 and Figure 5-17, TF sensors output vs. viscosity and conductivity have similar shape as TF sensors output vs. oxidised oils (in hours) which suggests that the performance of the TF electrodes is independent of viscosity or conductivity. Conductivity only becomes a major factor when ruthenium oxide is reduced to ruthenium and acts as a simple metal conductor in the case of the most highly oxidised oil samples. In these oil samples, instead of oil acidity measurement, the potential difference between the two electrodes (two metal conductors due to extreme AN) in oil is measured. The oil has a very high conductivity at this point and, therefore, the potential difference recorded is extremely low (almost zero).

Figure 5-18 illustrates the response of TF electrodes (TF RuO₂ WE vs. Polymer RE, Polymer RE was selected randomly to represent the output of the TF electrodes) at two temperatures (i.e. 50 °C and 80 °C) together with the water content measurement of the oxidised oil samples at room temperature. As can be seen, the water content of the oxidised oil samples increase with the oxidation hours for the first five oil samples and decrease considerably for the last two oil samples. Water is a by-product of oil oxidation; hence, as expected, the water content rises as oxidation progresses. The decline in the water content of the last two oil samples may be caused by solubility issues as a result of excessive oil viscosity, i.e. the oil is not fully dissolving within the timescale allowed for the testing. As discussed, the TF electrodes demonstrated a linear correlation with oil acidity (AN) and water content increase may have accelerated the disassociation of acid in oil. This effect might have improved the

performance of the TF electrodes in detecting the H⁺ concentration in the oil samples. This phenomenon can be further explored to observe the exact effect of water on the TF electrodes. The water content test was not carried out for the other oil samples due to time constraints.

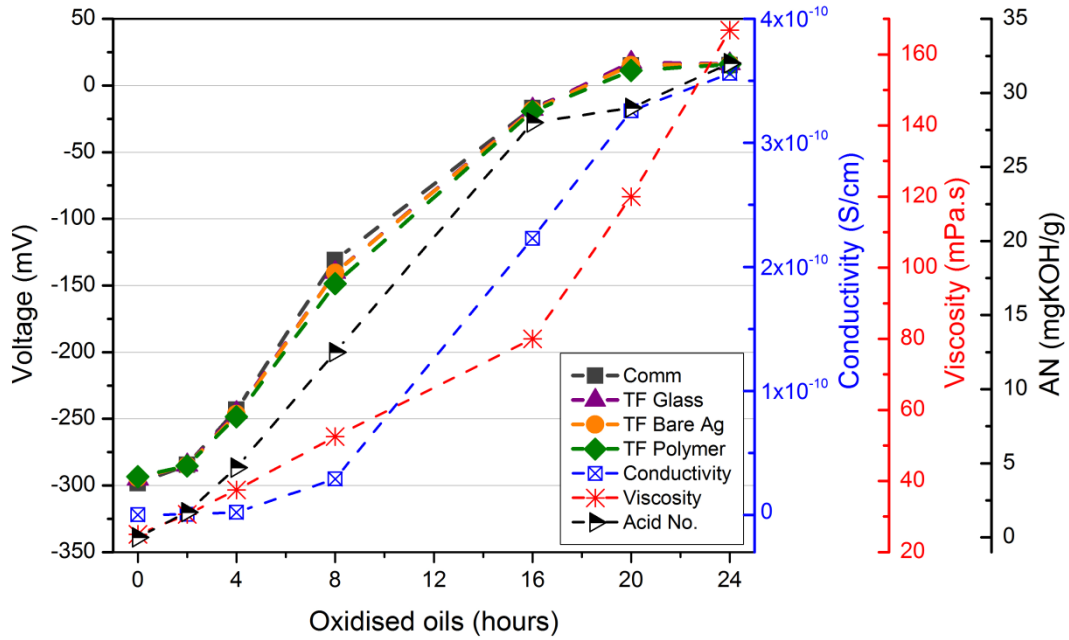


Figure 5-13: Thick-film electrodes output alongside AN, viscosity and conductivity graphs at 50 °C

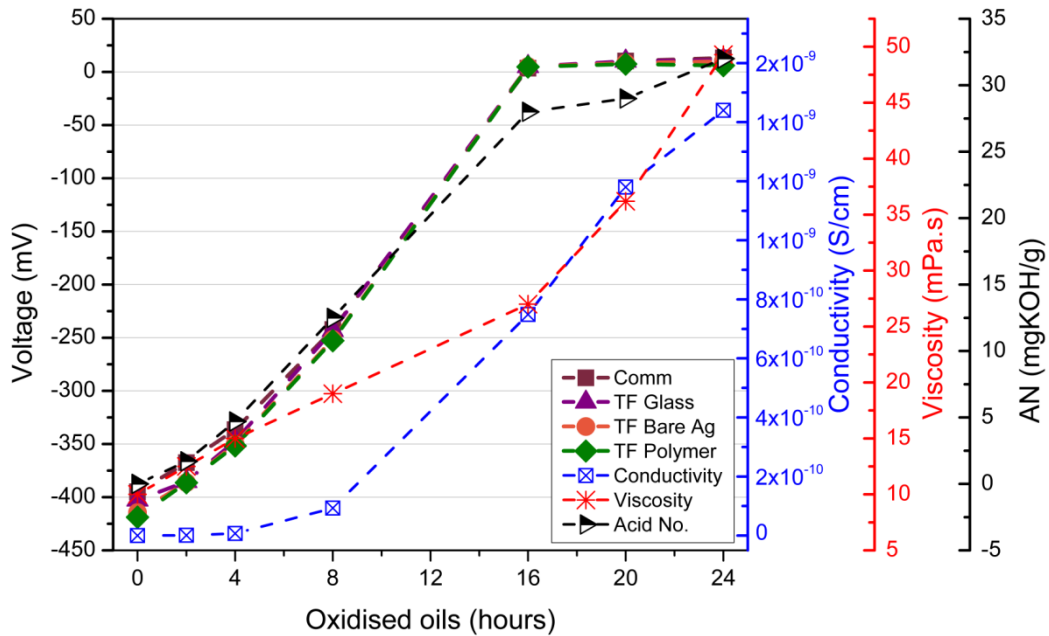


Figure 5-14: Thick-film electrodes output alongside AN, viscosity and conductivity graphs at 80 °C

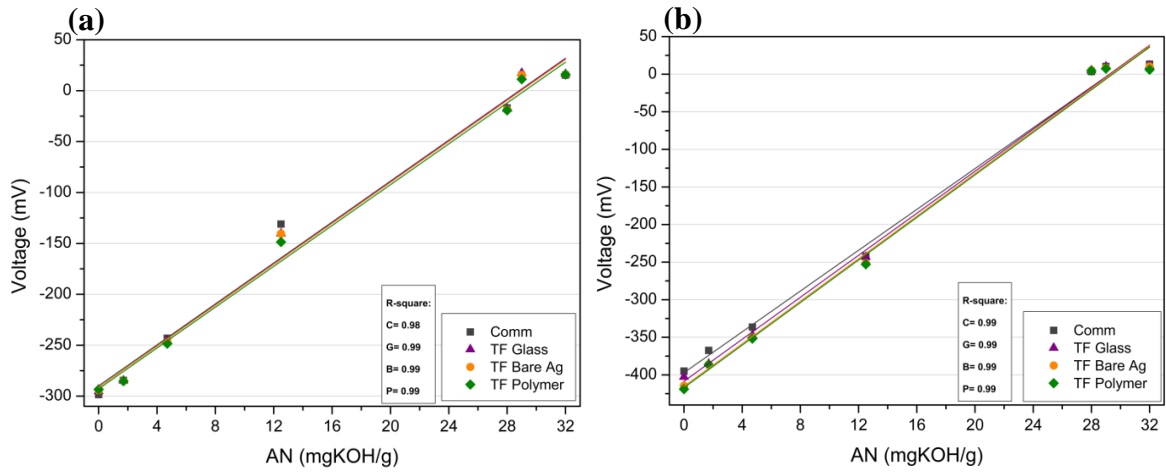


Figure 5-15: TF vs. AN of the oxidised oil samples, a) at 50 °C and b) at 80 °C

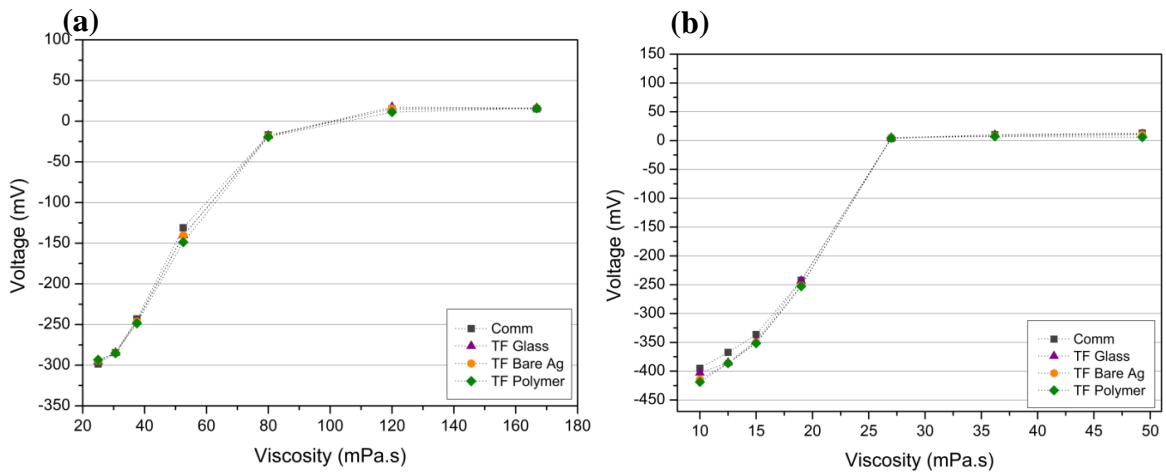


Figure 5-16: TF vs. viscosity of the oxidised oil samples, a) at 50 °C and b) at 80 °C

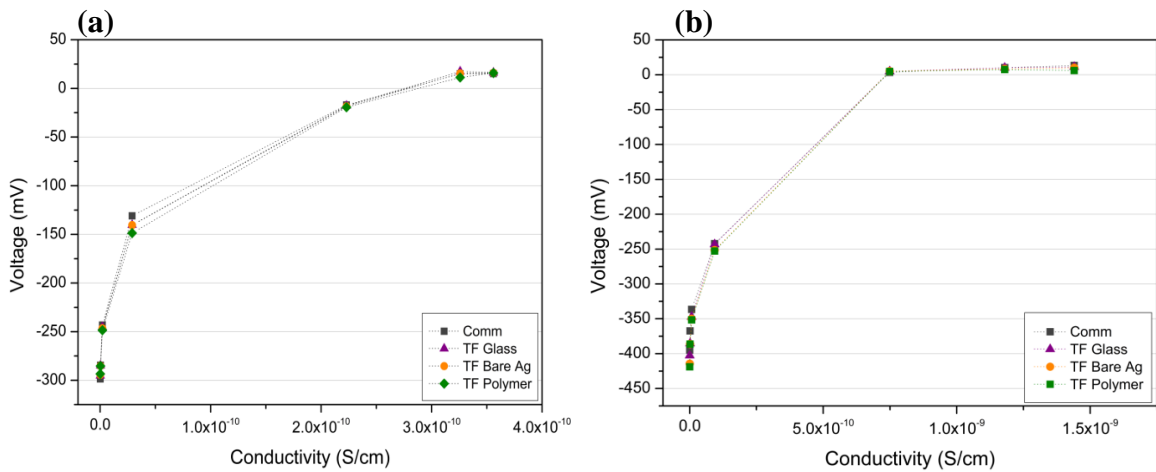


Figure 5-17: TF vs. conductivity of the oxidised oil samples, a) at 50 °C and b) at 80 °C

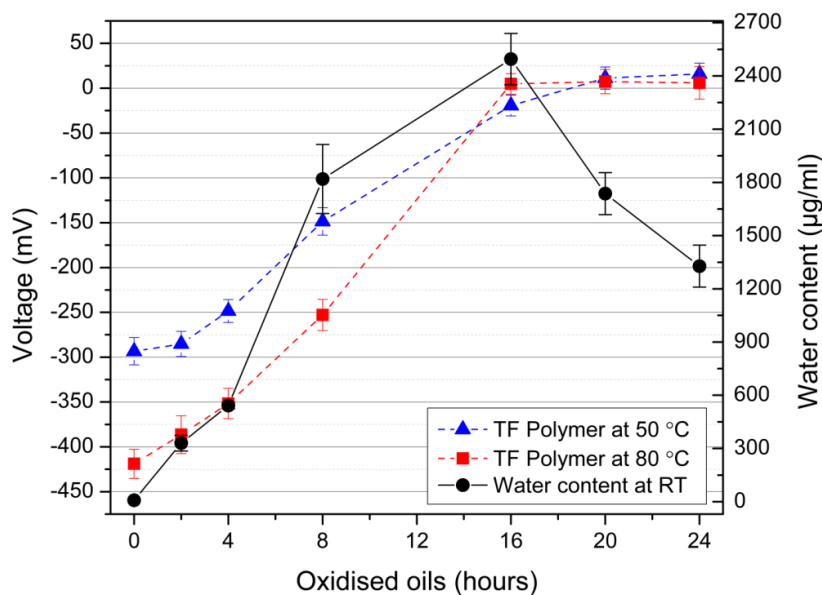


Figure 5-18: TF RuO₂ WE vs. Polymer RE at 50 °C and 80 °C (left hand-side Y-axis) alongside water content plot (right hand-side Y-axis) of the oxidised oil samples (measured at room temperature (RT))

5.3.5 Conclusions

Oxidised base oil samples, produced under controlled conditions, were used to evaluate the performance of the novel TF acidity sensors. Other properties including oil acid number (AN), viscosity and conductivity were measured for comparison. The main conclusions are:

- The EIS results have demonstrated that this is a viable technique to measure oil conductivity. As the oil oxidation time increases, the conductivity of oil samples also increased. The rate of increase of the oil conductivity could be a reflection of different oil oxidation stages.
- The novel TF sensors detected the oil oxidation and acidity increase. The TF sensors detect the acidity increase in base oil linearly at both 50 and 80 °C with low errors.
- Sensor working range: it was found that the sensors perform well in overly oxidised oil samples giving a linear response within the approximate AN range of zero to 25 mgKOH/g.
- Temperature has an influence on the lifetime and usable range of the sensors as the output was reduced at higher temperatures, most probably due to accelerated failure of the ruthenium oxide layer.

Table 5-2 summarises the TF sensors performance and other oil properties in oxidised base oil samples.

Parameters measured		Reason	Range
TF sensors	Increased up to 20 hours at 50 °C and 16 hours at 80 °C. Plateaus afterward for both temperatures.	Probably different oxidation phases are observed: plateau at the end can be due to high AN	300 mV increase at 50 °C 400 mV increase at 80 °C
AN	0-4 oxidised hours slow increase 4-16 oxidised hours sharp increase 16-24 oxidised hours slow increase	Probably different oxidation phases are observed	0 to 32 mgKOH/g at room temperature
Conductivity	Sharp increase until 16 hours oil sample. Slower increase for the last 3 oil samples at both temperatures	Polar oxidation by-products such as accumulated acids increase conductivity. High viscosity slows the ion mobility and therefore slower increase for the last 3 oil samples.	1.44e-9 (S/cm) increase at 50 °C 3.56e-10 (S/cm) increase at 80 °C
Viscosity	Slow increase 0-16 hours. Much faster increase for the last 3 oil samples	Oxidation branching and auto-oxidation accelerates the degradation and cause a significant viscosity increase at both temperatures	141.8 mPa.s increase at 50 °C 39.3 mPa.s increase at 80 °C
Interesting points:	<p>1. AN, Conductivity and viscosity all increased at different rates presenting different phases of oxidation process. TF sensors follow AN linearly. The plateau at the end is probably due to very high AN. Slow start rate in increase of the AN can also be explained by the oxidation 'initiation' phase.</p> <p>2. The point the viscosity of the oil starts increasing sharply, i.e. 16 hours can be the start of oxidation branching in which oxidation is at its peak reducing the conductivity and AN increase rate.</p>		

Table 5-2: Summary of the oxidised base oil samples test

5.4 Oxidised engine oil samples

In Section 5.3, the performance of the TF acidity electrodes in oxidised base oil samples alongside conventional off-line measurements was discussed. The changes in base oil properties as a result of systematic oxidation were also analysed. Base oils are relatively simple solutions in comparison to fully formulated engine oils and hence the TF sensors were initially tested in base oils. As discussed in Chapter 2, fully formulated engine oils consist of up to 95% base oils but the distinguishing factor between the two types of oils is the additives blended in fully formulated oil. Additives are complex formulations which improve the performance of engine oils. In this section, the protective role of additives, particularly anti-oxidants, within fully formulated oil samples will be perceived when the measured properties of these oil samples are compared to the additive-free (i.e. base oil) results shown in Section 5.3.

5.4.1 TF sensors responses

Figure 5-19 illustrates the responses of the electrodes (4 WE and RE pairs) in the oxidised engine oil samples at 50 °C. Responses from all electrode pairs initially increased sharply with oxidation for the 24 hours oxidised oil sample. RuO₂ WE vs. bare silver RE produced the highest change of 145 mV followed by Polymer (138 mV), Glass (87 mV) and Commercial RE (60 mV). After, the 24 hours oil sample, the output of all electrode pairs initially reduced and stayed constant before increasing at the oxidation hours of 96 and 120.

Figure 5-20 shows the output of the TF electrodes at 80 °C. The performance of the 4 electrode pairs was similar at 50 °C and 80 °C but the absolute voltage level of the electrodes were lower at higher temperature as expected according to Nernst equation. At 80 °C, the increase in the output of the electrodes in higher oxidised oil samples starts sooner, from 72 hours oil sample and the increase in the responses of the electrodes is more significant. This is probably due to the fact that higher temperatures increase the disassociation rate of acids in a solution and therefore the electrodes are responding to this. It is also noticed that the polarity of the output voltage of the electrodes was positive at both temperatures.

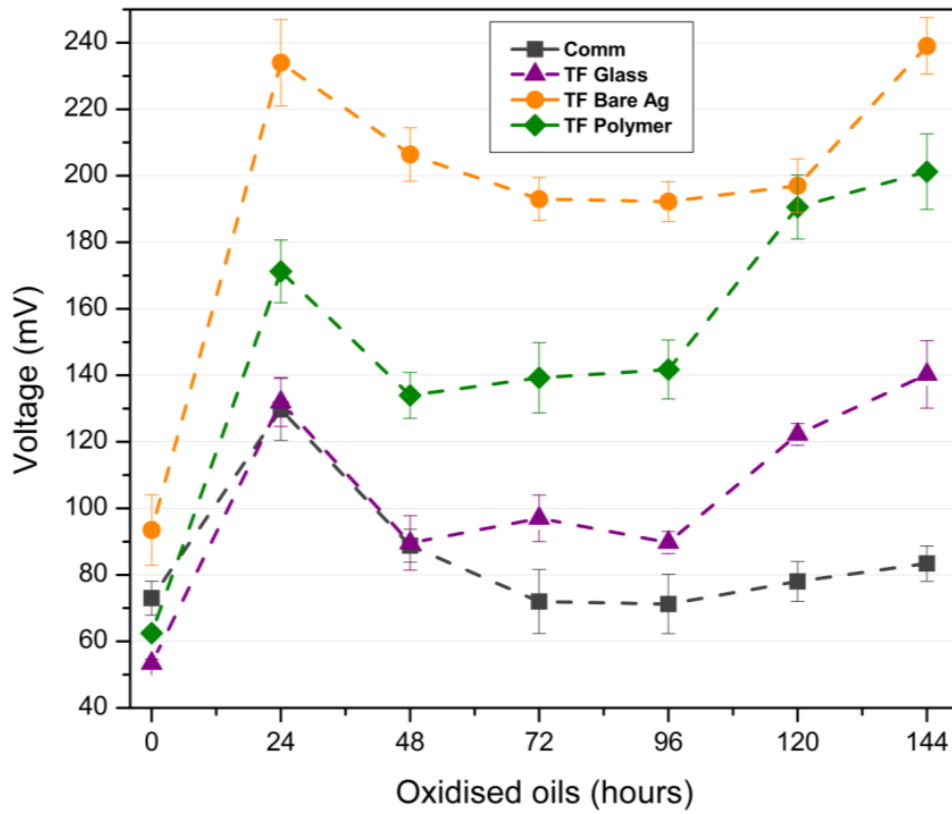


Figure 5-19: TF sensors output in oxidised fully formulated oil samples at 50 °C

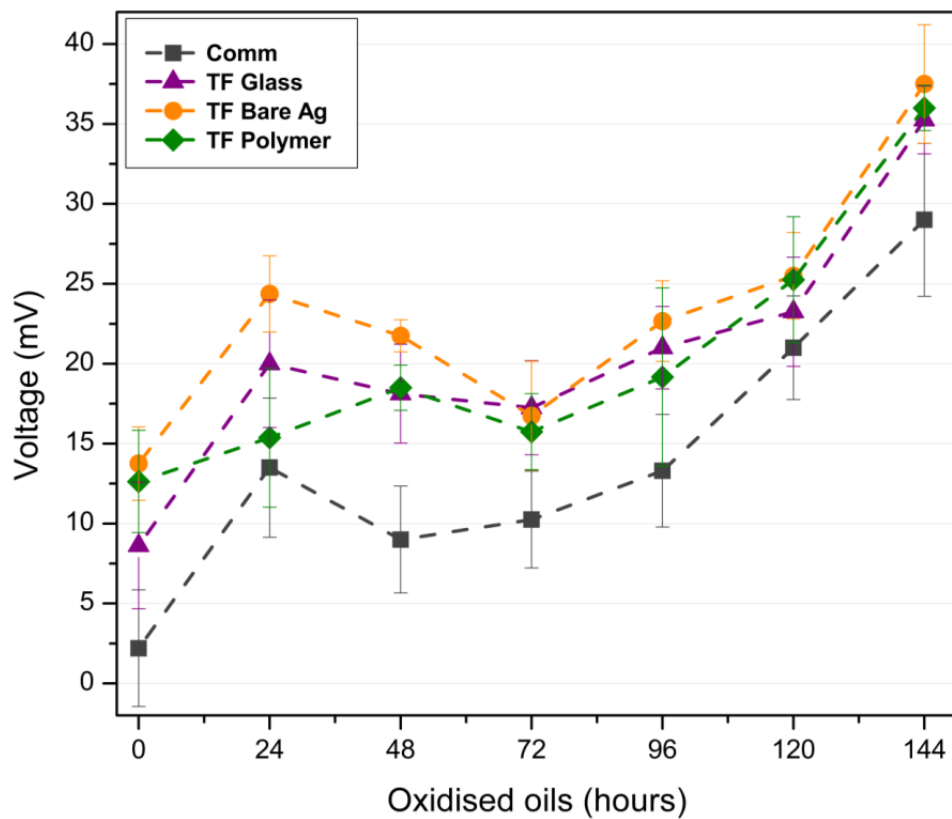


Figure 5-20: TF sensors output in oxidised fully formulated oil samples at 80 °C

5.4.2 AN, Viscosity and conductivity measurements

Figure 5-21 and Figure 5-22 show the acid number (at room temperature), conductivity and viscosity graphs of the oxidised oil samples at 50 °C and 80 °C, respectively. The acid number initially increased until 24 oxidation hours and stayed relatively constant thereafter until 96 hours before increasing to 3.4 mgKOH/g for the 144 hours. The initial increase in the AN can be due to the fact that at the same time as the additives are used, acidic constitutions are also formed. Additives and particularly anti-oxidants within the oil seem to be reacting to the oxidation steadily between 24 and 96 hours. The oxidation and its acidic by-products dominate after 96 hours increasing the acid number from 1.5 to 3.4 mgKOH/g.

Conversely, the conductivity of the oil samples primarily dropped for the 24 hours oil samples and continued to increase subsequently at both temperatures. The rate of increase in the conductivity plot also decreased and plateaued between 72 and 96 hours. This plateau might also be related to the oil additives as explained for AN plot. As can be seen in Figure 5-21 and Figure 5-22 for the 50 °C and 80 °C graphs, the conductivity trends for both temperatures are very similar but the initial drop and increase in the conductivity (absolute values range) of the oil samples were higher at 80 °C.

Viscosity of the oil samples did not change significantly until 96 oxidised hours and decreased slightly (~5 mPa.s) for the last 2 oil samples. It is generally expected to observe a slow increase in the viscosity with oil oxidation. In this case, the decrease in oil viscosity might be due to water formation as a result of oxidation.

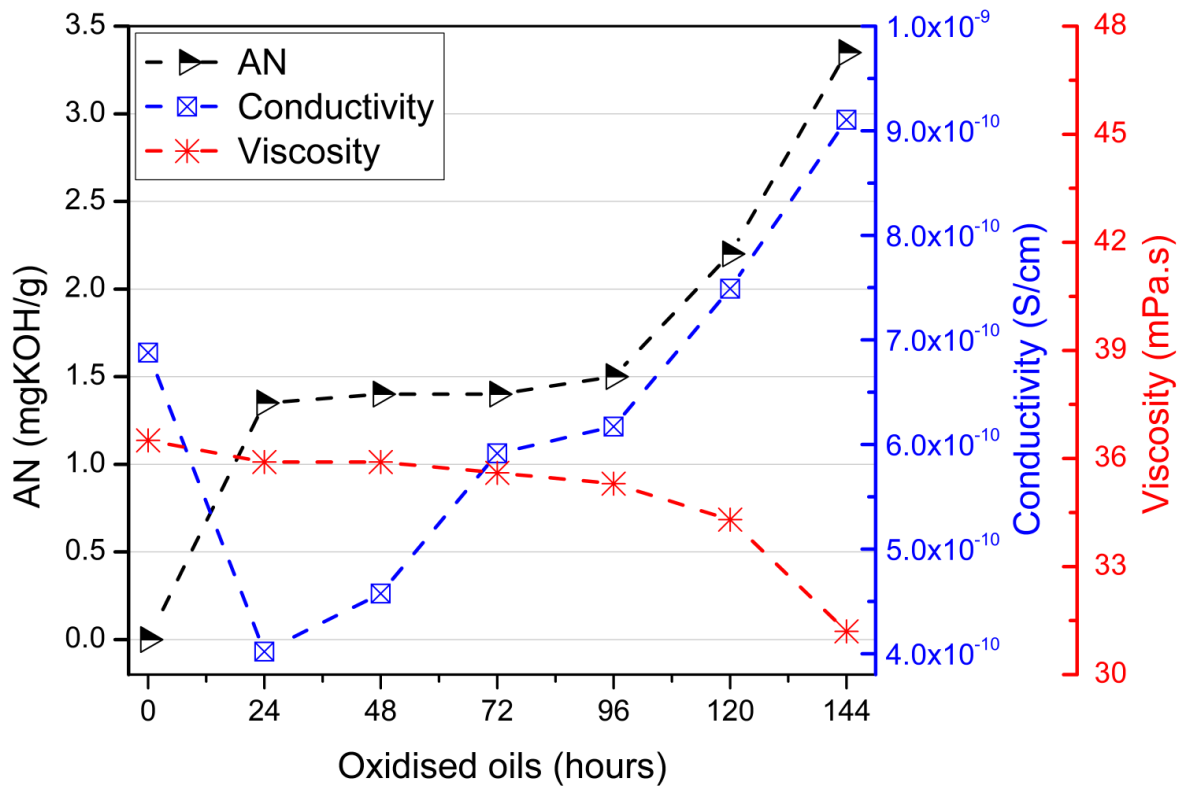


Figure 5-21: AN, conductivity and viscosity plots of the oxidised oil samples at 50 °C

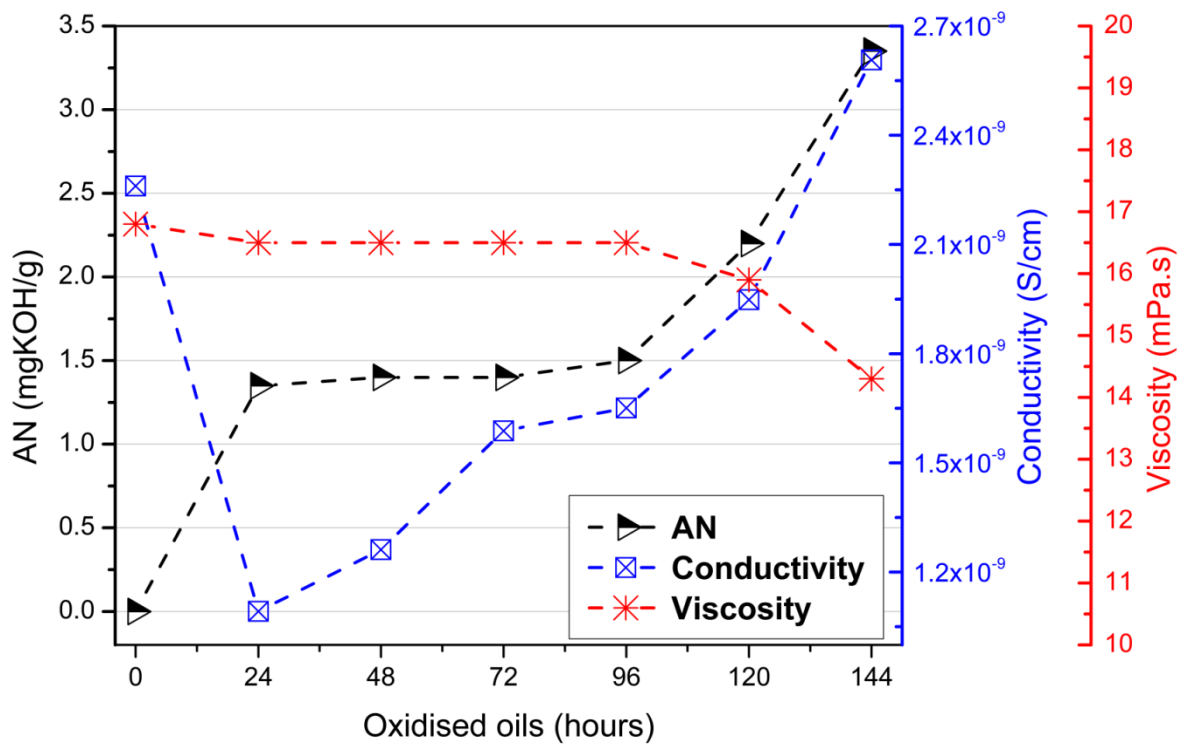


Figure 5-22: AN, conductivity and viscosity plots of the oxidised oil samples at 80 °C

5.4.3 Correlations between the TF sensors responses and AN, viscosity & conductivity

Figure 5-23 and Figure 5-24 compare the responses of the TF electrodes with the AN, viscosity and conductivity measurements of the oil samples at 50 °C and 80 °C respectively. Figure 5-23 can be divided into 3 regions and analysed separately. In the initial stage (0- 24 hours) the conductivity drops and the AN and TF electrode responses increase. It has been suggested⁵³ that the conductivity drop in oil degradation initially is due to the polar additive depletion. However, the increase in oil acidity (AN and TF electrode responses) is not fully understood and further investigation is required to explain this. This stage is also observed at 80 °C (Figure 5-24).

In the second region starting from 24 hours to ~84 hours, relatively steady state is observed in which AN and TF electrode responses do not change significantly. The conductivity increases by about 2×10^{-10} S/cm before plateauing at about 72 hours. In the first 2 regions the viscosity remains almost constant. As discussed in Chapter 2, antioxidants are the sacrificial additives which interrupt oil oxidation by reacting with free radicals and removing them via chain terminating reactions. Possible explanation to the increase in AN initially could be the fact that the anti-oxidants react with free radicals once they are formed, hence the initial increase followed by the plenteous. However, the important point is that the anti-oxidants mechanism in protecting the oil from oxidation is evident and highlighted in this region. Another point is that although the AN and viscosity remain almost constant, the oil conductivity increases showing that the conductive ion concentration which can be a combination of acidic compounds and other oxidation by-products such as water, is growing as a result of oxidation.

In the third region, oil oxidation accelerates once the antioxidants are depleted, increasing oil acidity and conductivity. The oxidation hour that the viscosity of the oil samples start decreasing is approximately the point in which the conductivity increases and similarly AN and TF sensor responses also rise. This is probably the start of ‘chain-branching’ phase during which oxidation accelerates as a result of additive depletion and oxidation by-products formation. Figure 5-25 shows the output of the TF electrodes versus Acid number at 2 temperatures. As can be seen, all of the TF electrodes responded to oil acidity changes in a linear fashion at both temperatures. This relationship does not occur for the output of the TF

electrodes versus viscosity and conductivity. Table 5-3 summarises the TF sensors performance and other oil properties.

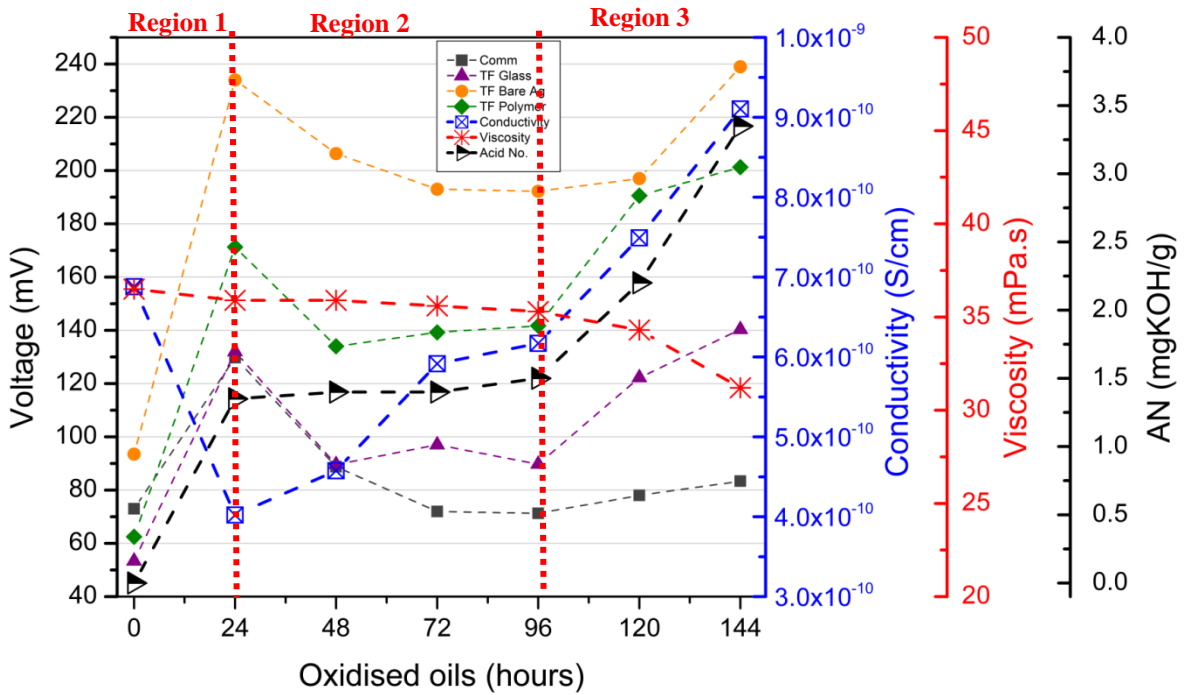


Figure 5-23: TF electrodes output alongside AN, viscosity and conductivity graphs at 50 °C

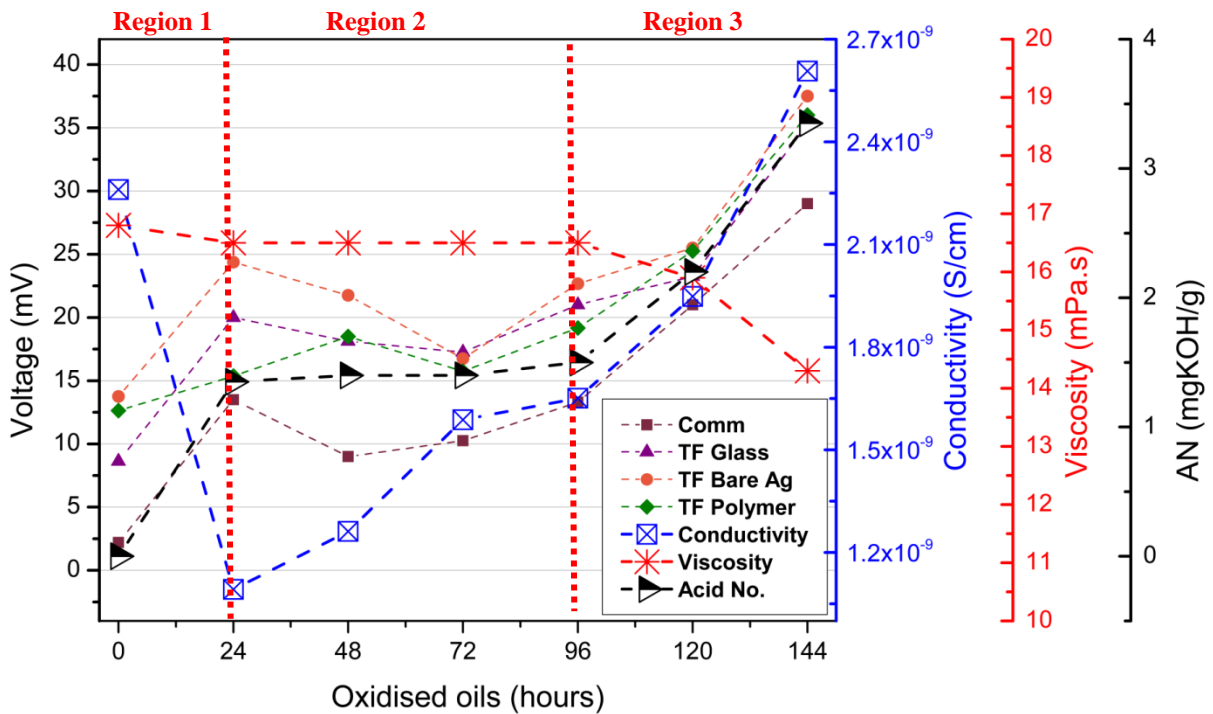


Figure 5-24: TF electrodes output alongside AN, viscosity and conductivity graphs at 80 °C

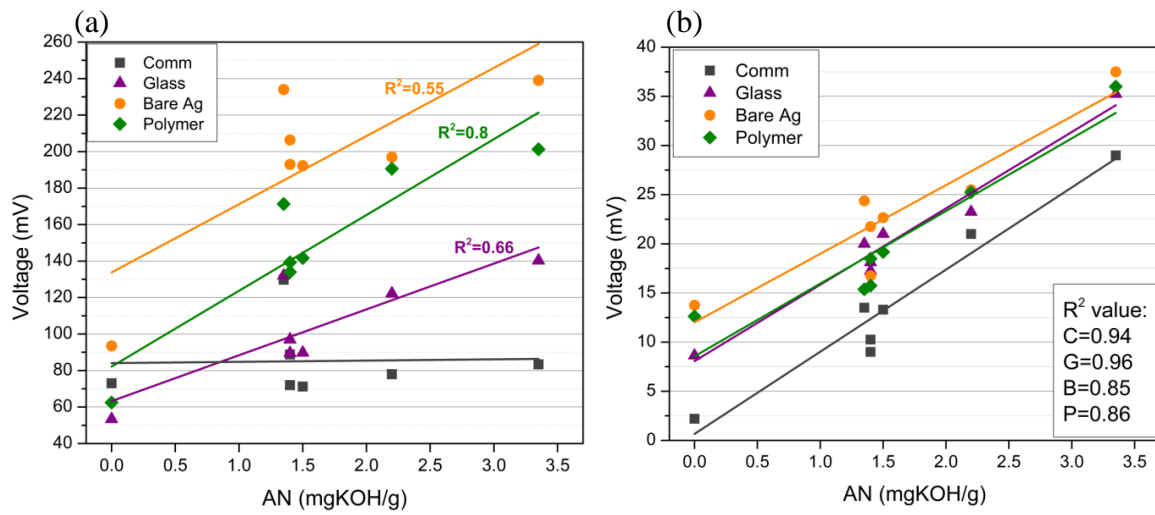


Figure 5-25: TF sensor responses vs. AN of the fully formulated oxidised oil samples, a) at 50 °C, and b) at 80 °C

Parameters measured		Reason	Range
TF sensors	At both temperatures: increase to 24h → reduction/plateaus → increase	Slow oxidation and acidity increase	50 °C: Increase of 60 mV (Commercial), 87 mV (Glass), 145 mV (Bare Ag), 138 mV (Polymer) 80 °C: Increase of 27 mV (Commercial), 26 mV (Glass), 24 mV (Bare Ag), 24 mV (Polymer)
AN	Increase to 24h → plateaus → increase	Plateaus probably because of acid neutralisation by anti-oxidants. Anti-oxidants depletion 96 hours onward hence AN increase	0 to 3.35 mgKOH/g at room temperature
Conductivity	Sharp reduce to 24h → increase	Sharp reduction due to polar additives consumption. Increase because of formation of polar oxidation by-products	2.23e-10 increase at 50 °C 3.461e-10 increase at 80 °C
Viscosity	Constant, reduced for the last 2 oil samples	Viscosity index improvers keep the viscosity constant. The decrease at the end can be due to the oxidation by-products (e.g. water) reducing the viscosity.	5.3 mPa.s reduction at 50 °C 2.5 mPa.s reduction at 80 °C
Interesting points:	<p>1. 24 hour oil sample in which conductivity drops, AN and TF acidity sensor responses increase.</p> <p>2. The point the viscosity of the oils decrease is exactly the same as the point in which the conductivity sharply increase and similarly AN and TF sensor responses rise.</p>		

Table 5-3: Summary of the oxidised fully formulated oil samples test

5.5 Oxidised base and fully formulated oil comparison

For the base oil test, samples were taken at six oxidation intervals: 2, 4, 8, 16, 20 and 24 hours. The same oxidation test was carried out for the fully formulated oil with the difference that it was oxidised for much longer since the oil samples contain additives, the oil was oxidised much slower. For the engine oil test, the samples were taken at 24, 48, 72, 96, 120 and 144 hours. For comparison purposes and in order to plot both set of oil samples on the same graph, the fresh oil (0 hours oxidised oil) is shown by '0' and each oxidised oil sample has been represented by the equivalent number in the series. The detail is shown in Table 5-4 below. In this section, different properties of the 2 sets of oxidised oil samples will be compared.

Oil samples	BO oxidation (hours)	FFO oxidation (hours)
0	0	0
1	2	24
2	4	48
3	8	72
4	16	96
5	20	120
6	24	144

Table 5-4: Oxidised base and fully formulated oil samples and their equivalent numbers

5.5.1 Conductivity

Figure 5-26 compares the conductivity of the oxidised base and fully formulated engine oil samples at 50 °C and 80 °C. Conductivity of both oil sets is higher at 80 °C compared to that at 50 °C due to lower viscosity and higher ion mobility. The conductivity trends of both oil sample sets are similar at 50 °C and 80 °C. As can be seen, the conductivity of the oxidised fully formulated engine oils is considerably higher than the base oil samples at both 50 °C and 80 °C which is probably due to the polar constituents such as additives. Therefore the initial decrease should essentially be involved with the neutralisation and reactions between additives and oxidation by-products. The conductivity of the first 4 base oil samples increased very slowly as base oils are extremely dielectric and non-conductive. However, the last 4 oil samples (i.e. 3, 4, 5 and 6) in both sets can be compared as the additive package within the fully formulated oil might have been depleted at high oxidation hours and it has

predominantly become base oil. Evidently, the conductivity of the last 4 oil samples of both sets increased almost linearly and by the same value of $3\text{e-}10$ S/cm at $50\text{ }^\circ\text{C}$ and $1\text{e-}9$ S/cm at $80\text{ }^\circ\text{C}$ probably due to free radicals formation.

The increase in the conductivity of the last 4 oil samples of both sets can also be an indication of increase in acidity of the oil samples which was also detected in the AN measurement and TF sensor responses.

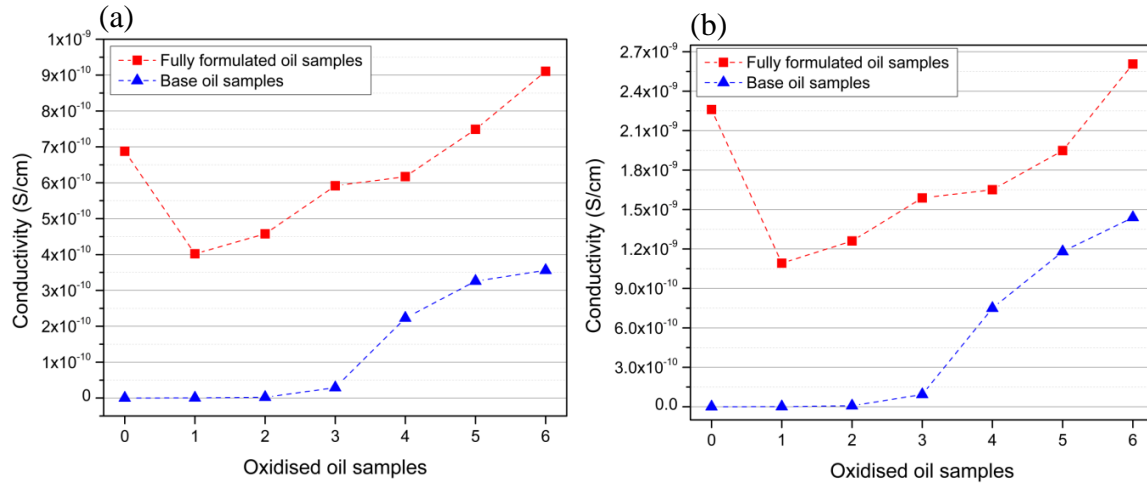


Figure 5-26: Conductivity of oxidised fully formulated and base oil samples, a) at $50\text{ }^\circ\text{C}$, and b) at $80\text{ }^\circ\text{C}$

5.5.2 Viscosity

Figure 5-27 compares the viscosity of the oxidised base and fully formulated engine oil samples at $50\text{ }^\circ\text{C}$ & $80\text{ }^\circ\text{C}$. As can be seen, the viscosity of the fully formulated oil samples stayed almost constant during the 144 hours of oxidation whereas the viscosity of the base oil increased significantly in only 24 hours. The increase in viscosity of the oxidised base oil samples is more than 560 % (from 25 to 166.8 mPa.s) at $50\text{ }^\circ\text{C}$ and almost 400 % (From 10 to 49.3 mPa.s) at $80\text{ }^\circ\text{C}$. This indicates the significant role of the additive packages such as anti-oxidants and viscosity modifiers in fully formulated oil samples in maintaining the viscosity of the oil throughout the degradation process.

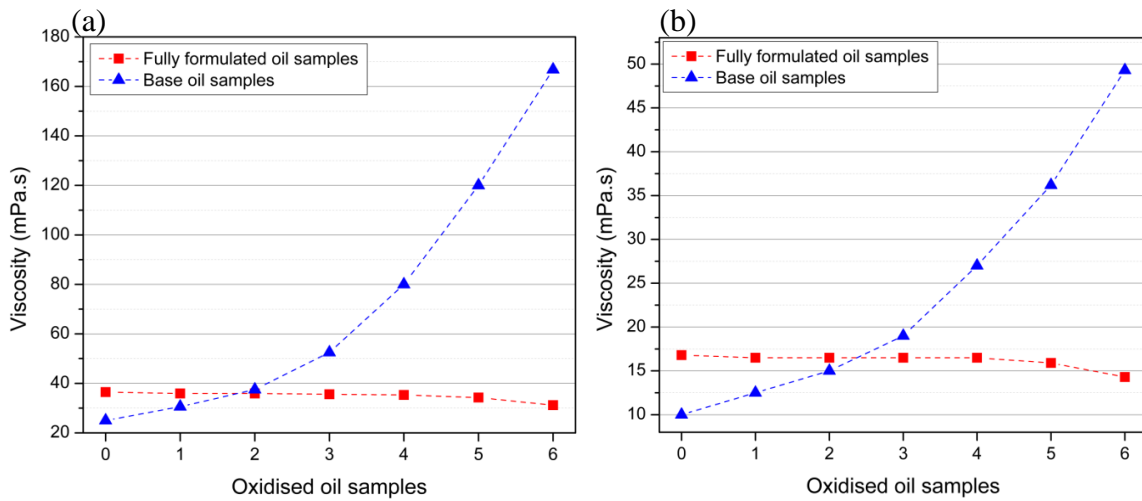


Figure 5-27: Viscosity of oxidised fully formulated and base oil samples, a) at 50 °C, and b) at 80 °C

5.5.3 Acid Number (AN)

Figure 5-27 compares the AN of the oxidised base and fully formulated engine oil samples at room temperature. As can be seen, the AN of the fully formulated oil samples stayed almost constant during the 144 hours of oxidation whereas the AN of the base oil increased significantly in only 24 hours. The AN of the oxidised base oil samples increased to 32 mgKOH/g after 24 hours compared to only 3.3 mgKOH/g after 144 hours oxidation. This again signifies the important role of the additives such as anti-oxidants in neutralising the formed acidic compounds as a result of oxidation within fully formulated oil samples.

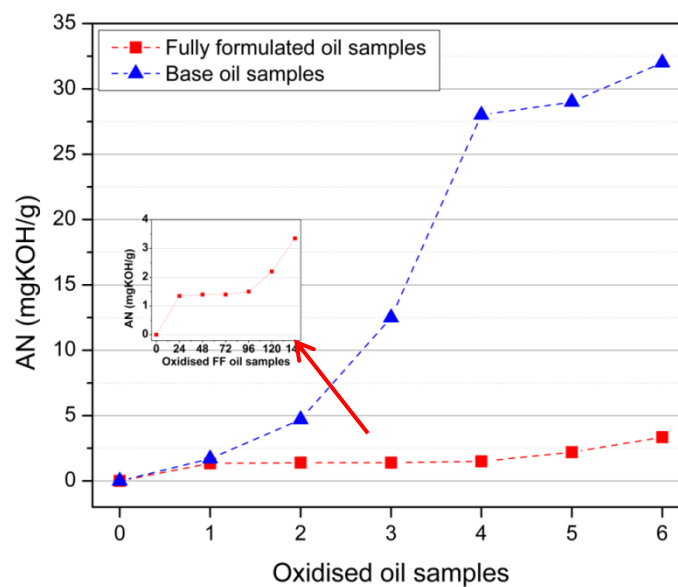


Figure 5-28: AN of the oxidised fully formulated and base oil samples at room temperature

5.6 Adding nitric acid into fresh engine oil

The TF electrodes were then tested in 13 oil samples prepared by adding nitric acid (at 30% v/v) to fresh off-the-shelf 5W30 engine oil at different acid concentrations (ppm).

5.6.1 Conductivity, Viscosity and AN measurements

Figure 5-29 demonstrates the conductivity graphs of the degraded oil samples at two temperatures (50 and 80 °C) alongside the AN of a number of oil samples. AN shows an initial increase to 1 mgKOH/g for the 200 ppm acid concentration and continues to increase to 1.7 mgKOH/g for the 1600 ppm acid concentration degraded oil followed by a decrease to 1.5 mgKOH/g for the last degraded oil sample (i.e. 2000 ppm). Conversely, the conductivity of the oil samples initially drops abruptly at both temperatures. This effect is more considerable at 80 °C in which the conductivity decreases by one order of magnitude when 200 ppm of nitric acid concentration is added to the fresh oil. After 200 ppm oil sample, the conductivity trends were almost flat at both temperatures. Overall, oil conductivity was higher at a higher temperature. Measurement of the oil viscosity showed little changes in oil samples as the content of added acid changes; hence the viscosity measurements are not presented.

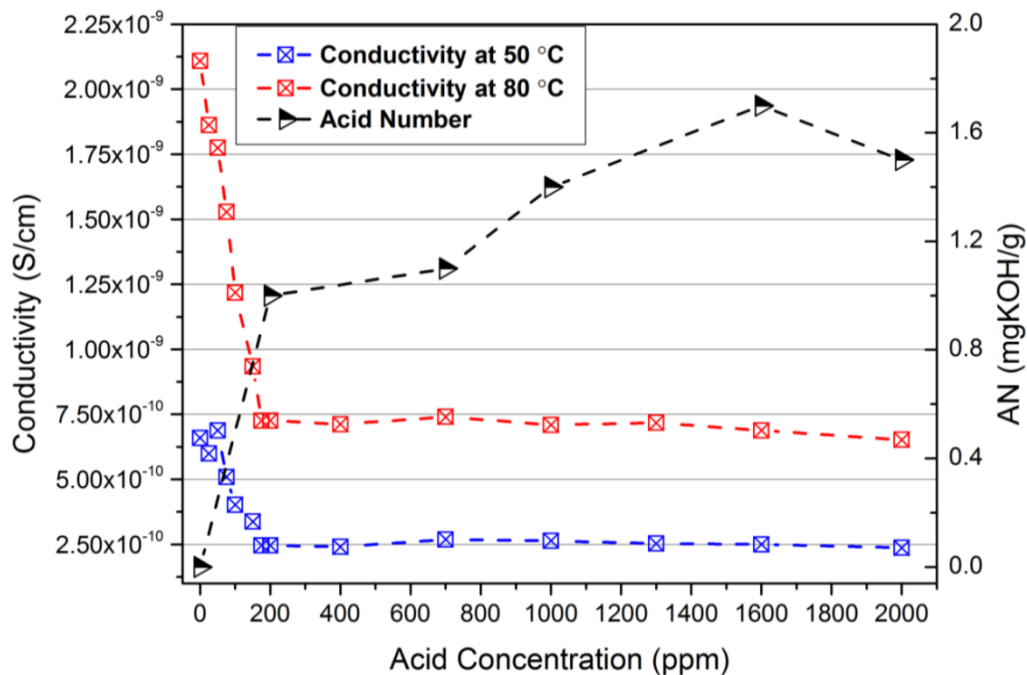


Figure 5-29 AN measurements of the degraded oil samples at room temperature combined with conductivity graphs at 50 and 80 °C

5.6.2 TF sensors responses

The measurement results of the TF electrodes in the degraded oil samples are presented in Figure 5-30 for 50 °C and Figure 5-31 for 80 °C oil samples. As can be seen, the overall performance of the 3 TF electrode pairs is similar (level and trend) at 50 °C in which the output potential initially increases sharply up to 200 ppm oil sample followed by slower increase and plateaus/decrease toward the end of the graph. The TF RuO₂ WE paired with silver/silver chloride (Ag/AgCl) electrodes (Glass and Polymer) responded to the oil acidity changes similarly but slightly different from the TF RuO₂ WE paired with bare silver RE in which this pair exhibited higher level of output voltage. The RuO₂ WE paired with commercial pH sensor primarily produced a decreasing trend (up to 100 ppm) followed by a continuous increasing trend and responded to acidity changes at lower voltages. At 80 °C, the output levels of the electrodes, i.e. actual measured voltage, are lower for all of the electrodes than those at 50 °C which is expected according to Nernst equation. Temperature dependency of the TF electrodes is discussed in details in Chapter 6.

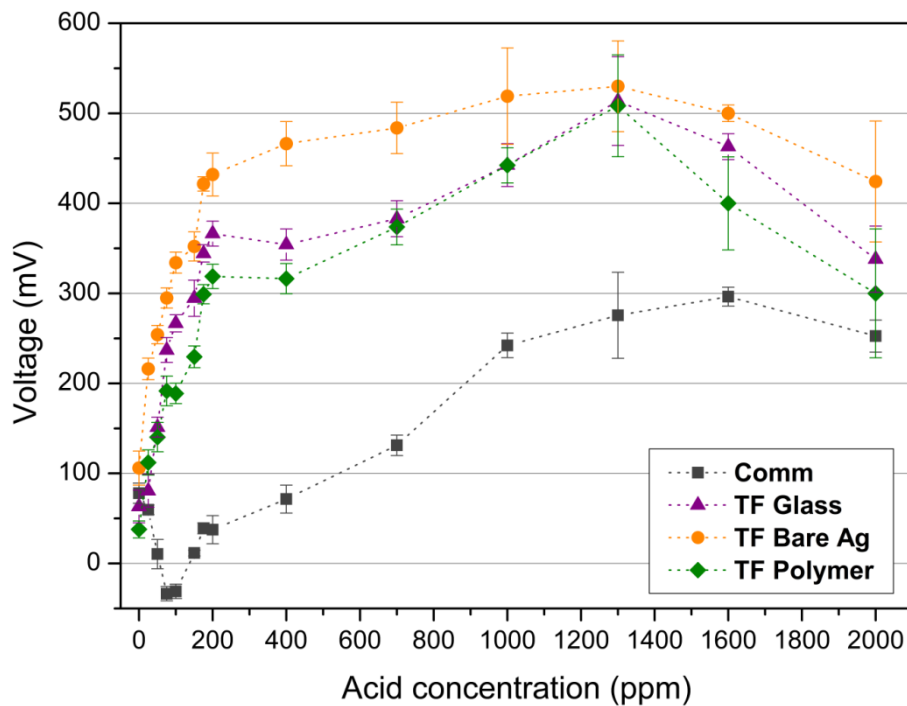


Figure 5-30: TF acidity sensors output in artificially degraded oil samples at 50 °C

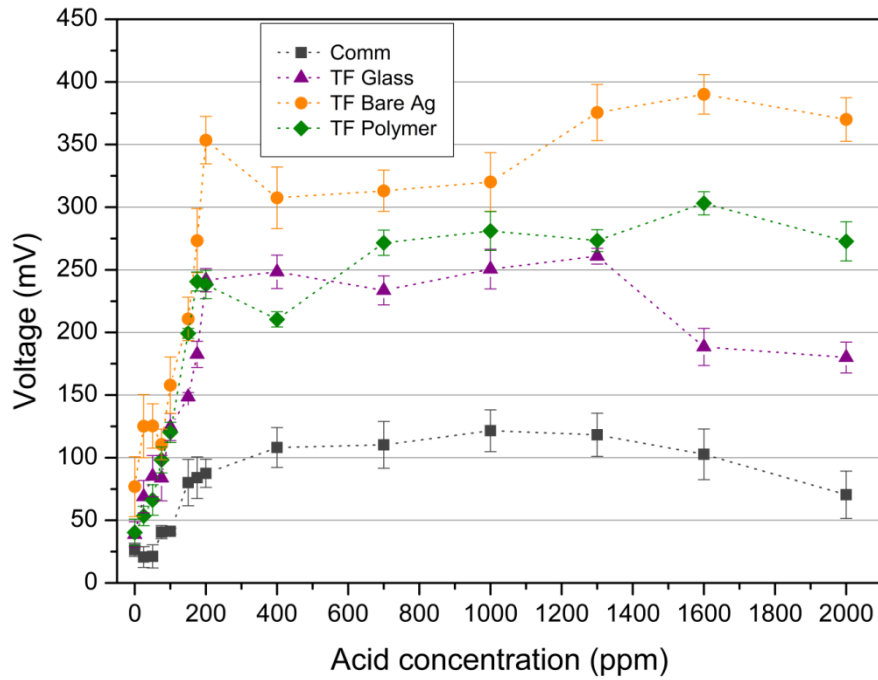


Figure 5-31: TF acidity sensors output in artificially degraded oil samples at 80 °C

Figure 5-32 and Figure 5-33 shows the TF acidity sensor responses together with the AN and conductivity graphs at 50 and 80 °C, respectively. As can be seen, two distinct trends are observed in both acidity and conductivity measurements which allow the x-axis range to be divided into lower, i.e. 0-200 ppm and higher, i.e. 200-2000 ppm acid concentration parts. Further discussions are provided in the following sections.

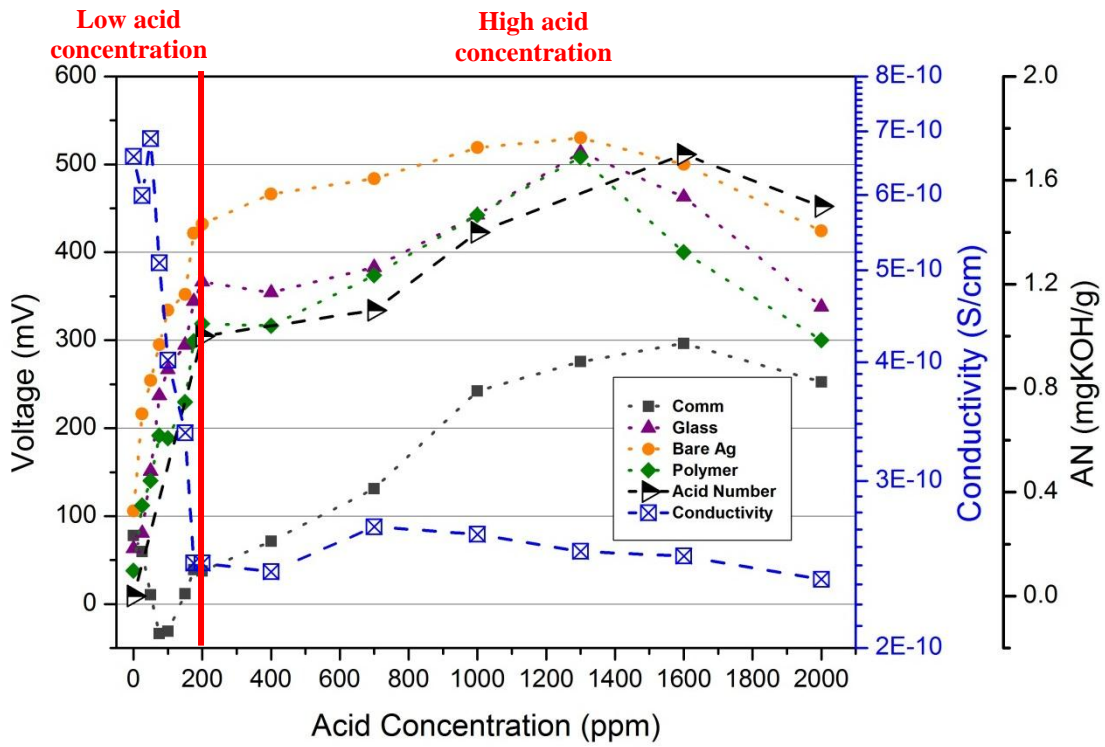


Figure 5-32: Acidity sensors output in oil samples (left y-axis) and the AN and conductivity of the oil samples (right y-axes)

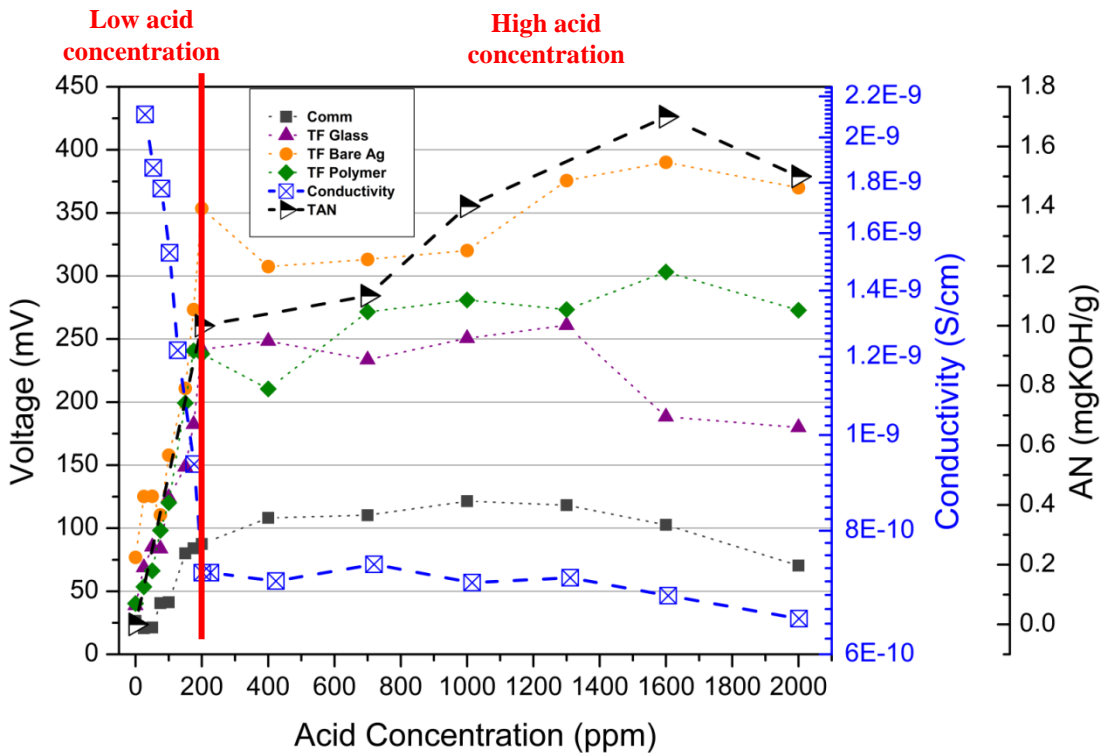


Figure 5-33: TF sensors output (left y-axis) and conductivity (right y-axis) of the oil samples at low acid concentration range.

5.6.3 Low acid concentration (0-200 ppm)

In the acid concentration range of 0-200 ppm, the TF sensors responded linearly to the increase of acid concentration at both 50 °C (Figure 5-34) and 80 °C (Figure 5-35). The calculated coefficients of determination (R^2 value) of the RuO_2 against the 3 TF REs at both temperatures are also shown. As can be seen in Figure 5-32, the AN of the oil samples increased to 1 mgKOH/g for the 200 ppm acid concentration oil. Similar results have also been reported^{102,103} in which the oil acid number (AN) increases from the onset of oil use in engine test which can be because of the additives not fully neutralising the formed acid in the oil.

Unlike oil acidity, the conductivity of the oil samples drops considerably in this range. This is thought to be a result of the consumption or transformation of the polar additives by the added acid. It has been reported⁵³ that the initial high conductivity of fresh engine oil is due to the calcium sulfonate (a common detergent in engine lubricants). The conductivity reduces from $6.5\text{E}-10$ for the fresh oil to $2.45\text{E}-10$ Siemens/cm for the 200 ppm acid concentration oil sample indicating additive depletion⁵³. The behaviour of the TF electrodes and the conductivity of the oil samples are similar at both temperatures.

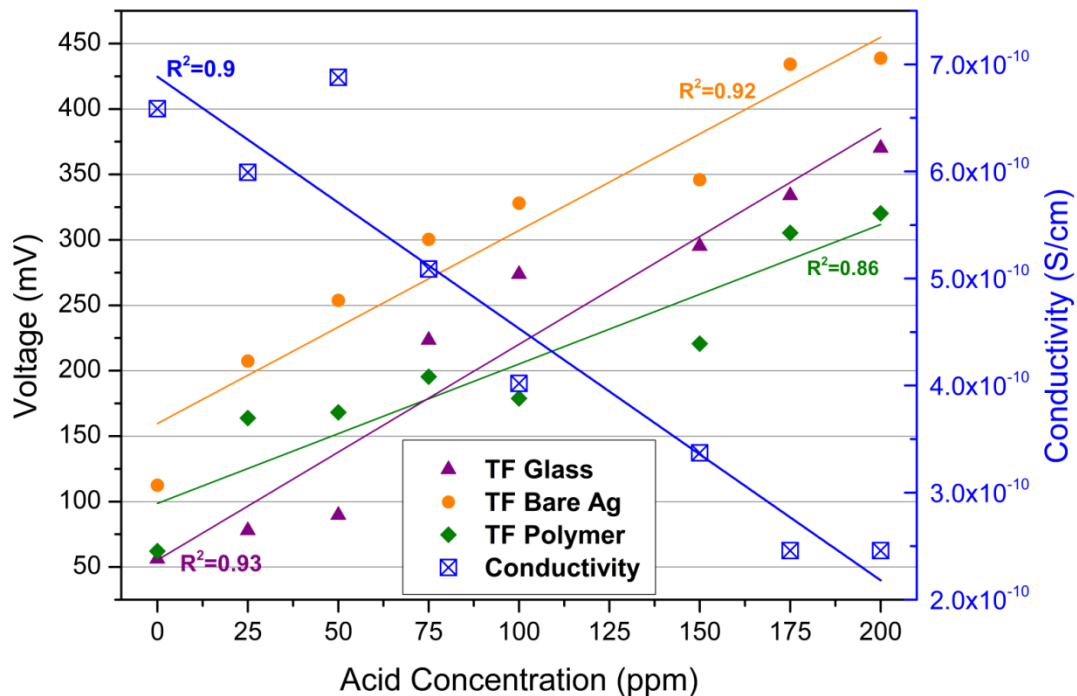


Figure 5-34: TF sensors output (left y-axis) and conductivity (right y-axis) of the oil samples at low acid concentration range at 50 °C

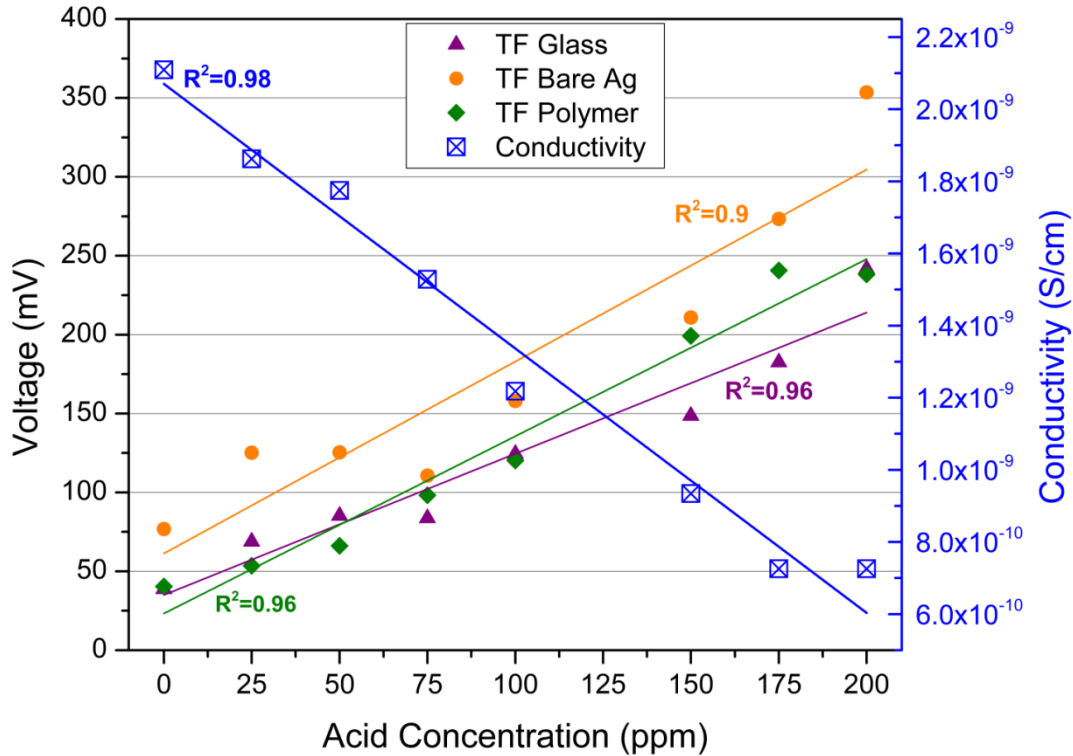


Figure 5-35: TF sensors output (left y-axis) and conductivity (right y-axis) of the oil samples at low acid concentration range at 80 °C

5.6.4 Higher acid concentration (200-2000 ppm)

When the acid concentration increased to above 200 ppm, the changes in TF sensor responses as well as other measurements (i.e. AN and conductivity) became relatively small. This could be due to the water (from the added acid) and oil emulsions rather than acid actually mixing with the oil.

Comparing the TF sensor responses with the AN measurements, a similar trend is observed, confirming the acidity of the oil slightly increased between 200 and 1300 ppm and decreased when the acid concentration was over 1300 ppm. Certain additives are weakly acidic¹⁰⁴ and the depletion of these additives can thus reduce oil acidity. The trend observed in the high acid concentration range may be related to this. However, further investigations are required to confirm this hypothesis.

Comparing the acidity measurements with the oil conductivity of the oil samples in the high acid concentration range, oil conductivity shows an opposite trend with an initial increase followed by a decreasing trend. Oil conductivity initially falls for oil samples with low acid concentration due to additive depletion whereas the acidity sharply rises as the acid

concentration mixed in oil is increased. This shows that the acidity sensors are detecting the hydrogen ions (H^+) from the nitric acid added to the fresh oil as expected. The conductivity continues to decrease after 700 ppm added acid which can be an indication of depletion of the remaining additives within oil. In real engine oil degradation, after additive depletion, oxidation process forms acidic by-products (e.g. weak acids such as carboxylic acid) accumulating acidic decomposition in oil which increases oil conductivity. Subsequently, acid accumulation rapidly elevates oil viscosity which decreases the conductivity. However, in this work, strong acid (nitric acid) has been used solely to investigate the TF acidity sensors response to the added acid and this does not affect the oil viscosity.

Comparing the performances of different TF reference electrodes in the linear region (0-200 ppm), WE against TF Bare Ag RE exhibited the highest sensitivity to the added acid concentration (163.1 mV per 100 ppm added acid ± 15 mV) followed by Glass (151.5 mv per 100 ppm added acid ± 12 mV), Polymer (140.5 mV per 100 ppm added acid ± 15 mV) and Commercial reference electrode (35.8 mV per 100 ppm added acid ± 9 mV) at 50 °C.

5.6.5 Summary

The acidity of artificially degraded oil samples by adding nitric acid concentration to fresh fully formulated oil was measured using TF chemical sensors and compared to AN and conductivity results of the oils. A summary of this test is shown in Table 5-6.

The results show that:

- The on-line TF sensors responded to the addition of nitric acid to oil which also increased the acid number (AN) and changed the oil conductivity
- The TF electrodes outputs displayed a good correlation with the oil Acid Number (AN)
- At low acid concentration range (0-200ppm): almost linear increase in TF acidity sensors with added acid to oil was observed at both temperatures
- Conductivity reduced considerably (sharper at 80 °C), probably due to additives consumption
- At high acid concentration range (200-2000ppm): slower rate of increase/plateaus were observed
- Sensor responses are influenced by oil temperature; the higher the temperature, the lower the sensor output voltage
- Oil sample with acid concentration of 200 ppm shows a 'turning point' in all measurements, indicating a significant change in oil properties. Similar changes also occurred in measurements for other oil types.

Table 5-5 summarises the TF sensors performance and other oil properties.

Parameters measured		Reason	Range
TF sensors	<ul style="list-style-type: none"> - Sharp increase to 200ppm - Slower increase, plateaus/decrease - Linear increase between 0-200 ppm at both temperatures 	See AN (below)	See Section 6-6.
AN	<ul style="list-style-type: none"> - Sharp increase to 200ppm - Slower increase up to 1800 ppm followed by decrease 	Sharp increase can be due to strong acid added. Also, additives may not fully neutralise the added acid. Plateaus might be due to water (from acid)-oil emulsion.	0 to 1.7 mgKOH/g (smaller than previous test with fully formulated oil, added acid not fully effective due to water-oil emulsion)
Conductivity	<ul style="list-style-type: none"> - Sharp fall up to 200 ppm - Plateaus thereafter at both temperatures 	<ul style="list-style-type: none"> - Sharp reduction can be due to polar additives consumption - Plateaus because of neutralisation process taking place or water (from acid)-oil emulsion. 	4.23e-10 decrease at 50 °C 1.458e-9 decrease at 80 °C
Viscosity	Constant at both temperatures	Added acid concentration did not affect the viscosity of the oil as the amount was neglectable.	Remained constant.
Interesting points:	- 200 ppm oil sample in which conductivity drops, AN and TF acidity sensor responses increase sharply.		

Table 5-6: Summary of the 'added acid to fresh engine oil' test

Chapter 6. Thick film sensors performance and mechanism

6.1 Introduction

In the previous Chapter, the results from acidity measurements of different oil samples using thick-film electrodes were presented and compared with the off-line measurements (i.e. viscosity, conductivity and AN). In this Chapter, the temperature effect on TF electrodes and other properties of the oil samples such as viscosity and conductivity are discussed in Section 6.2. The results from the stability and repeatability tests of the TF electrodes are presented in Sections 6.3 and 6.4 respectively. In Section 6.5, the sensing mechanism and the working principle of the TF electrodes in oil samples is presented. This Section also includes the factors affecting the responses of the TF electrodes. The discussion continues in Section 6.5 by comparing different REs performance in the tested oil samples.

6.2 Temperature effects

In this study, the TF electrodes and different properties of oil samples (e.g. conductivity and viscosity) have been tested at two temperatures (50 and 80 °C). These temperatures were chosen to represent engine operating temperatures within the oil sump¹⁰⁵. In this section, the temperature effects on thick film acidity sensors and oil properties such as conductivity and viscosity are investigated. This is carried out due to the fact that the sensors can be prone to temperature variances (in environments like car engine which experiences a range of temperatures) and the fact that the temperature can have a considerable influence on oil behaviour and main properties such as viscosity.

In this section, initially the performance of the TF electrodes in three buffer solutions (pH 4, 7 and 10) at different temperatures (25, 40, 60, 80 °C) is presented. Temperature effect tests on both oxidised base and fully formulated oils were carried out at room temperature (~20 °C), 30, 50, 70 and 90 °C. Two oil samples from each set (4 and 20 hours oxidised base oil samples alongside 48 and 120 hours oxidised fully formulated oil samples) were selected to investigate the temperature effects on the oil samples. The selected oil samples are from lower (i.e. 4 hours base and 48 hours oxidised fully formulated oil samples) and higher oxidised oil samples (i.e. 20 hours base and 120 hours oxidised fully formulated oil samples). The results from conductivity and viscosity measurements at these temperatures are also presented.

6.2.1 Aqueous buffer solutions

Figure 6-1, Figure 6-2 and Figures 6-3 illustrate the output potential difference (in millivolts) of the RuO₂ working electrode against different reference electrodes in aqueous buffer solutions at room temperature (~20 °C), 30, 50 and 70 and 90 °C. Generally, it is expected to see a reduction in the output of TF electrodes at higher temperatures according to Nernst equation¹⁷. This effect is observed in Figure 6-1 (RuO₂ WE vs. glass RE) for pH 7 and 10 but there is an increase in the output of the TF electrodes between 30 °C and 70 °C before reducing at 90 °C for pH 4. These trends were very similar for the RuO₂ WE vs. polymer RE (Figures 6-3 in which the TF response generally decreases with temperature except between 30 °C and 70 °C in pH 4 buffer solution. pH 4 buffer solution is an acidic solution and this effect might be due to higher acidic activities at higher temperatures which subsequently

increases the output potential of the TF electrodes. In this case, the reason for the reduction at 90 °C would be unknown. Bare Ag reference electrode produced more scattered results as initially (for the first three temperatures, i.e. 20 °C to 50 °C) the output of the electrodes reduced and thereafter increased for the last two temperatures.

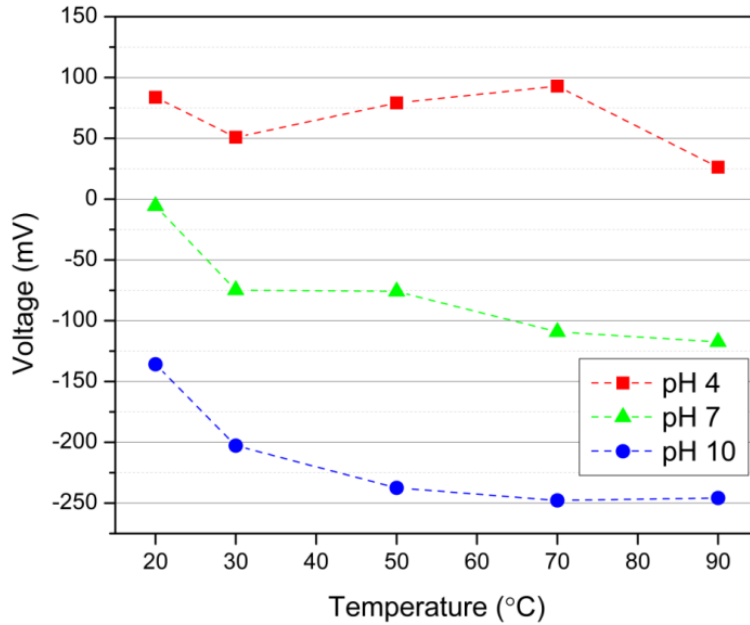


Figure 6-1: Temperature effects on thick film RuO₂ WE vs. Ag/AgCl glass reference electrode in pH 4, 7 and 10 buffer solutions

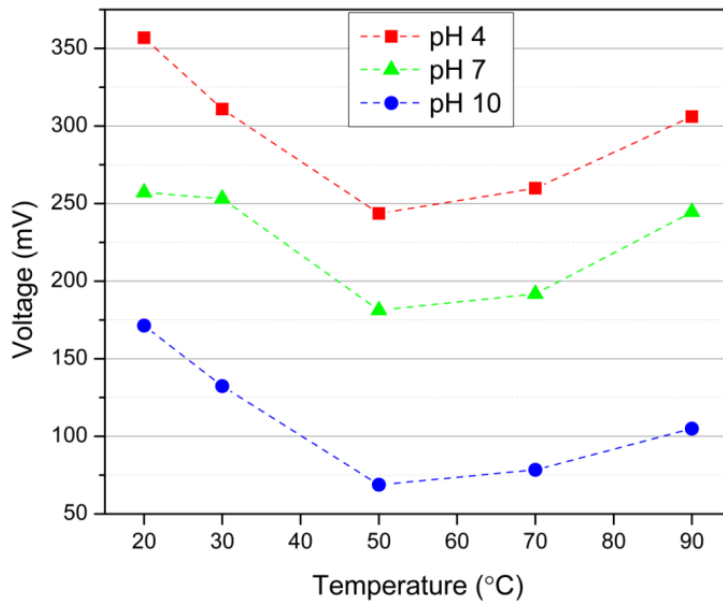
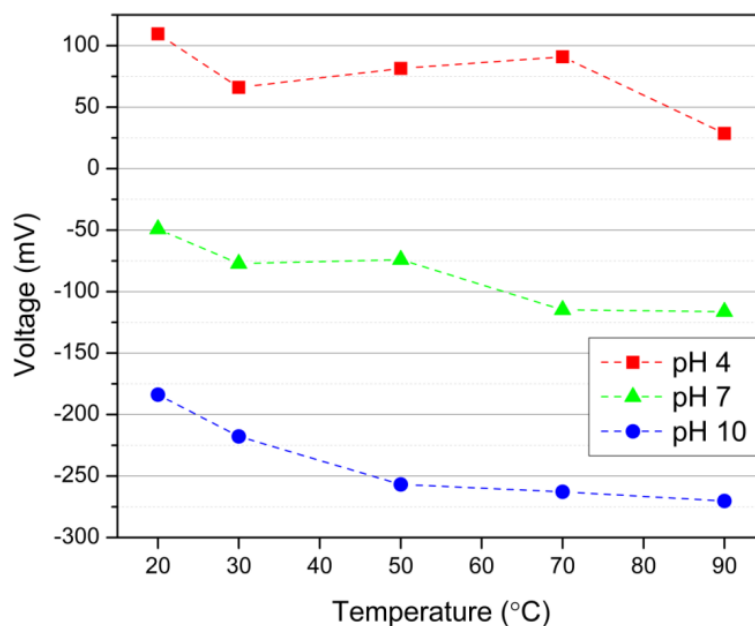


Figure 6-2: Temperature effects on thick film RuO₂ WE vs. bare Ag reference electrode in pH 4, 7 and 10 buffer solutions



Figures 6-3: Temperature effects on thick film RuO_2 WE vs. Ag/AgCl polymer reference electrode in pH 4, 7 and 10 buffer solutions

6.2.2 Oxidised base oil samples

Figure 6-4 illustrates the outputs of the TF electrode pairs (RuO_2 TF electrode paired with TF and commercial reference electrodes) in four hours oxidised base oil sample tested at five temperatures. As can be seen, there is an abrupt drop in electrodes output as the oil sample is heated up to 30 °C. The responses of the TF electrodes continued to decrease gradually until 70 °C whereas the RuO_2 TF electrode paired with commercial reference electrode slightly increased. For the last temperature (90 °C) the responses of all electrode pairs dropped. As discussed in the previous sections, according to Nernst equation it is expected to observe a decrease in electrode responses at higher temperatures.

Similar experiment was carried out with the 20 hours oxidised base oil. It was previously shown that above certain acidity the sensor shows an almost zero potential difference which is most probably because the conditions exceed the operating range of the TF sensors. This phenomenon is observed again in temperature test with different set of TF electrodes in which once the oil sample is heated to 30 °C the electrodes fail. The ruthenium oxide working electrode is probably being stripped/ reduced by the acidity of the solution, enhanced by the elevated temperature which could potentially leave only ruthenium (no oxide) or even the bare metal of the back contact (platinum/gold) on the substrate. In any case, this could then leave just a purely conductive electrode pair with no pH response. When that happens,

the sensor tends to short circuit because two conductors are present in the same oil having very similar electrode potentials. At that point the oil's conductivity has increased significantly responding as an electrical component, which results in an almost zero potential.

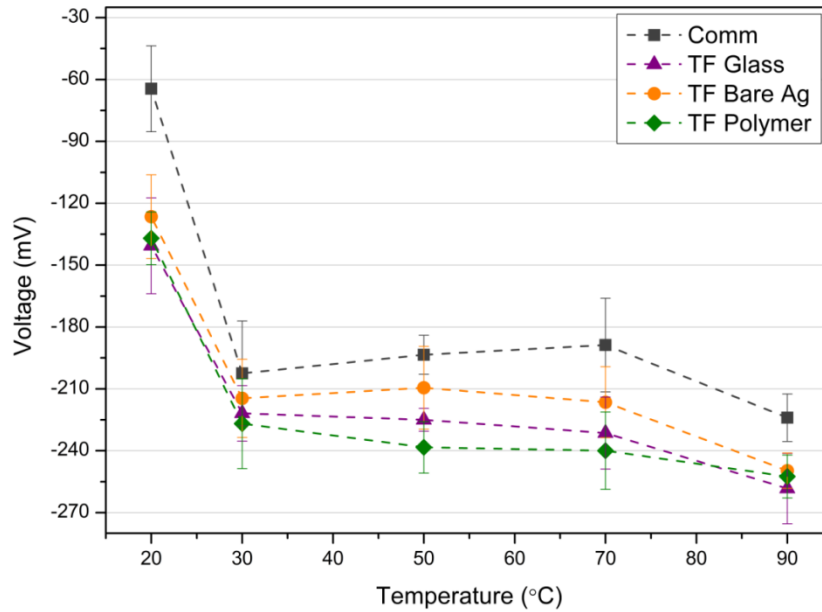


Figure 6-4: TF electrodes in 4 hours oxidised base oil sample tested at five temperatures

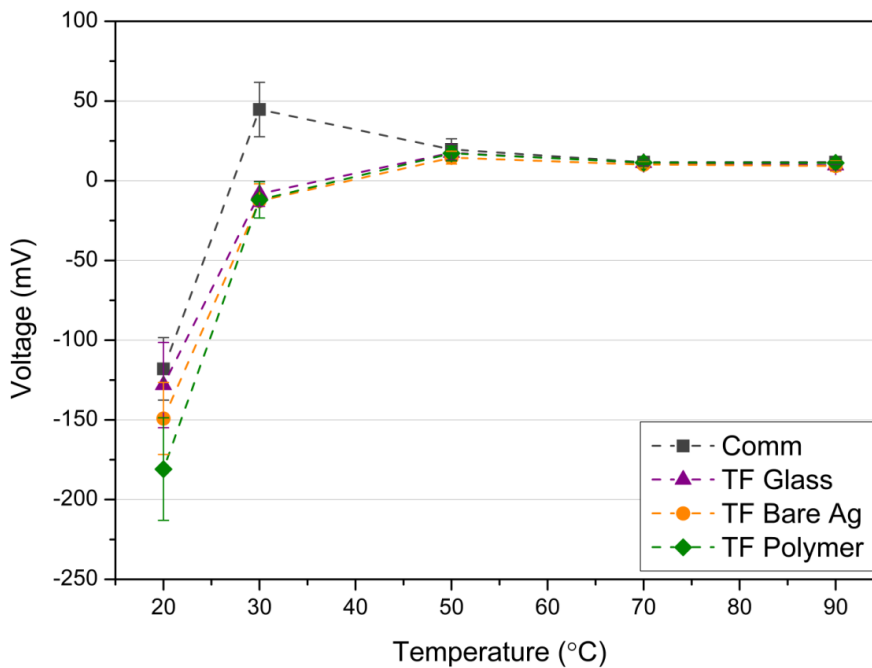


Figure 6-5: TF electrodes in 20 hours oxidised base oil sample tested at five temperatures

In order to analyse the temperature effect on oil conductivity, the 4 and 20 hours oxidised base oil sample were heated up to 90 °C and their conductivity was measured at the same temperature intervals (i.e. 20 °C, 30, 50, 70 and 90 °C). Figure 6-6 illustrates the conductivity

plots of the 4 and 20 hours oil samples at five temperatures. As can be seen, the conductivity of the 4 hours oxidised base oil sample does not change significantly with temperature whereas the conductivity of the 20 hours oxidised oil sample increased exponentially with temperature. Higher temperatures increase the oil viscosity and therefore ion mobility hence increased conductivity is expected. Conductivity of the oil depends on viscosity and mobile ion concentration from polar substances (e.g. oxidation by-products such as carboxylic acid) and evidently, the conductivity of the 4 hours oil sample did not increase considerably with higher temperatures (only 3.6×10^{-11} S/cm for 70 °C increase in temperature) as there is low ion concentration in the 4 hours oil sample.

Viscosity of the same base oil samples were also measured at the same temperature intervals (i.e. 20 °C, 30, 50, 70 and 90 °C) and is shown in Figure 6-7. The viscosity of both oil samples decreased with higher temperatures. The difference in the viscosity of the two oil samples is much higher at 20 and 30 °C and this difference decreases with temperature.

Figure 6-8 and Figure 6-9 illustrate the temperature effect on TF electrodes alongside conductivity and viscosity plots of the 4 and 20 hours respectively.

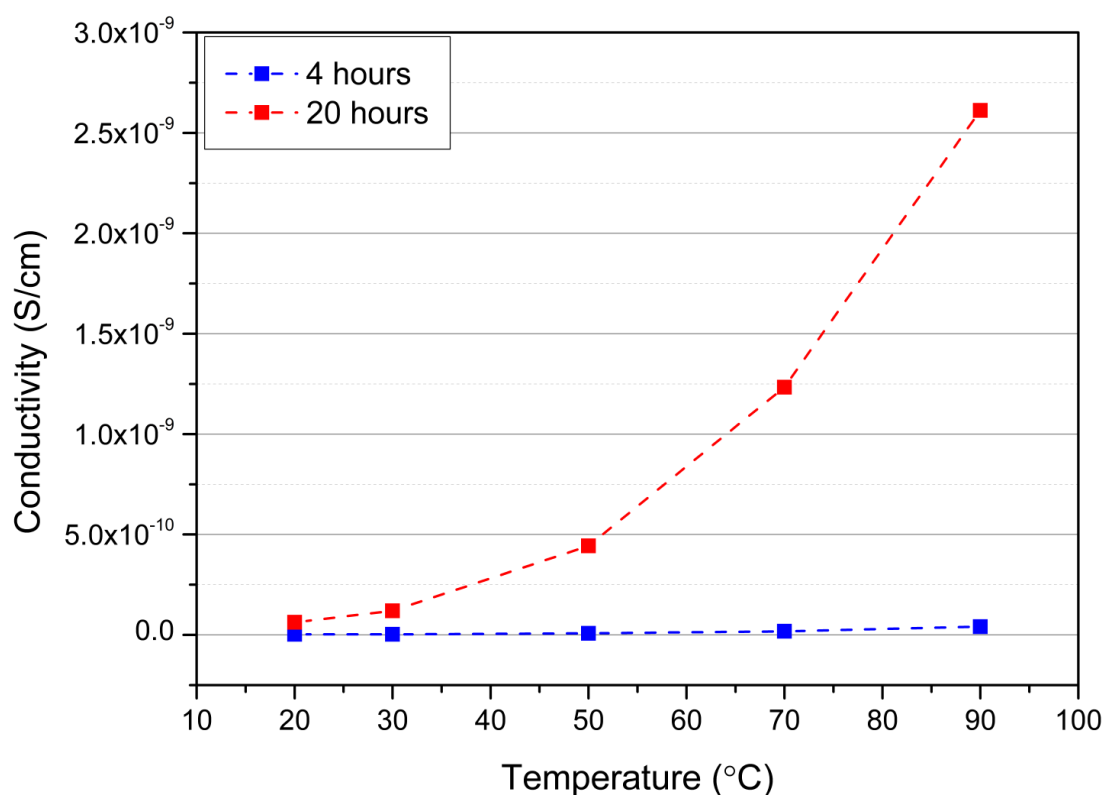


Figure 6-6: Temperature effect on conductivity of the oxidised base oil samples

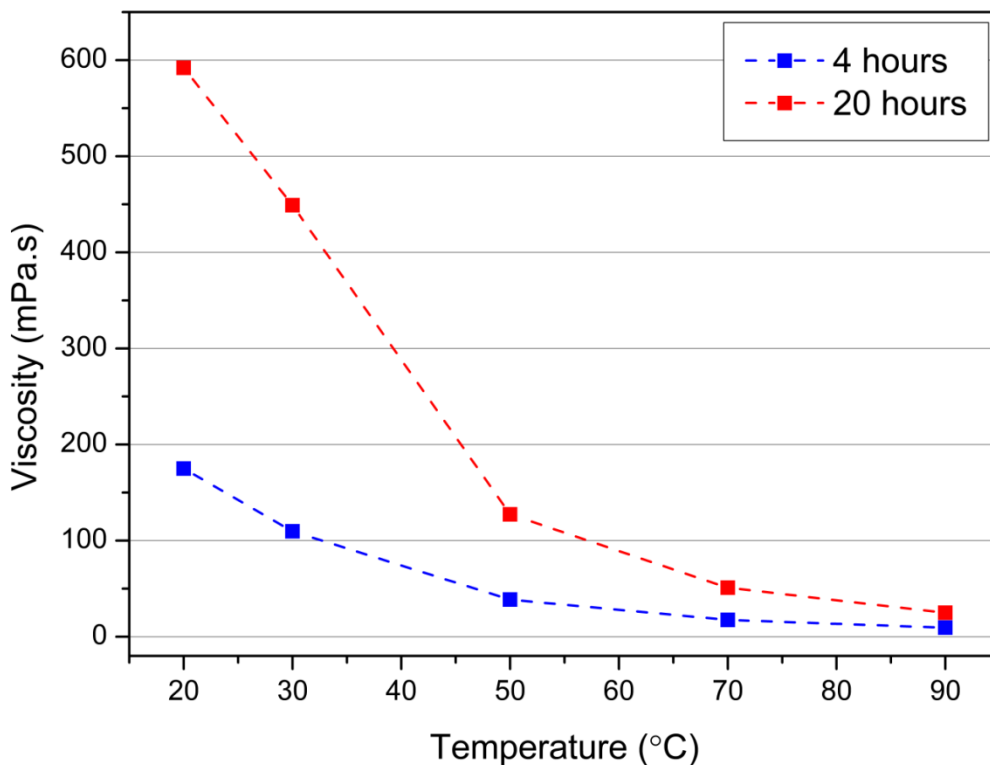


Figure 6-7: Temperature effect on viscosity of the oxidised base oil samples

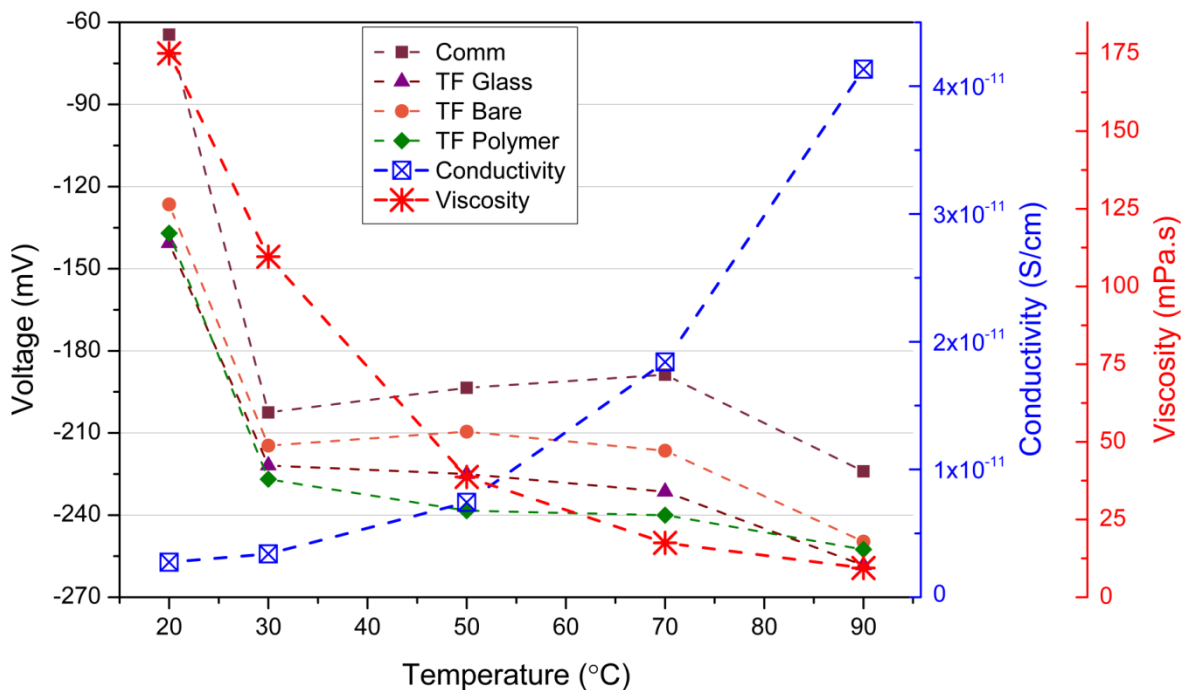


Figure 6-8: Temperature effect on TF electrodes, viscosity and conductivity of the 4 hours oxidised base oil sample

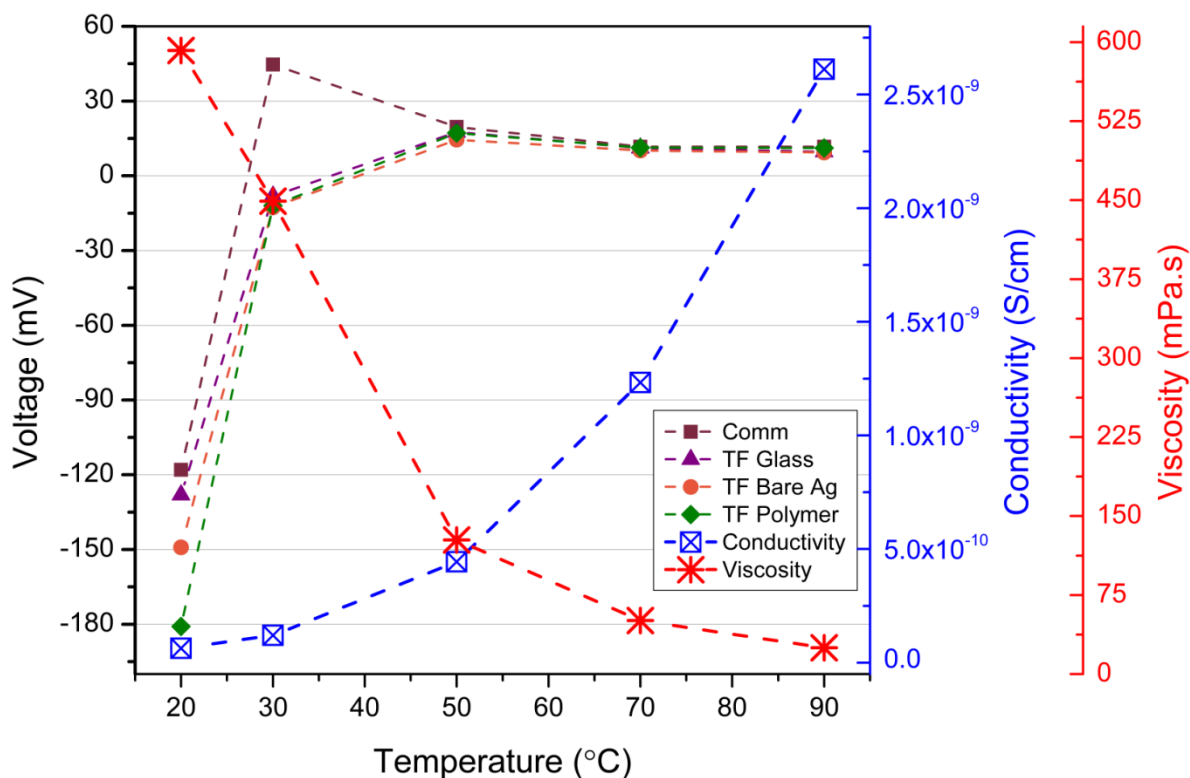


Figure 6-9: Temperature effect on TF electrodes, viscosity and conductivity of the 20 hours oxidised base oil sample

6.2.3 Oxidised fully formulated oil samples

Figure 6-10 demonstrate the output of the TF electrode pairs (RuO₂ TF electrode paired with TF and commercial reference electrodes) in 48 hours oxidised fully formulated oil sample tested at five temperatures. The TF electrode responses decrease exponentially with temperature in 48 hours oil while the decrease in 120 hours oxidised oil is less noticeable after 50 °C, as shown in Figure 6-11.

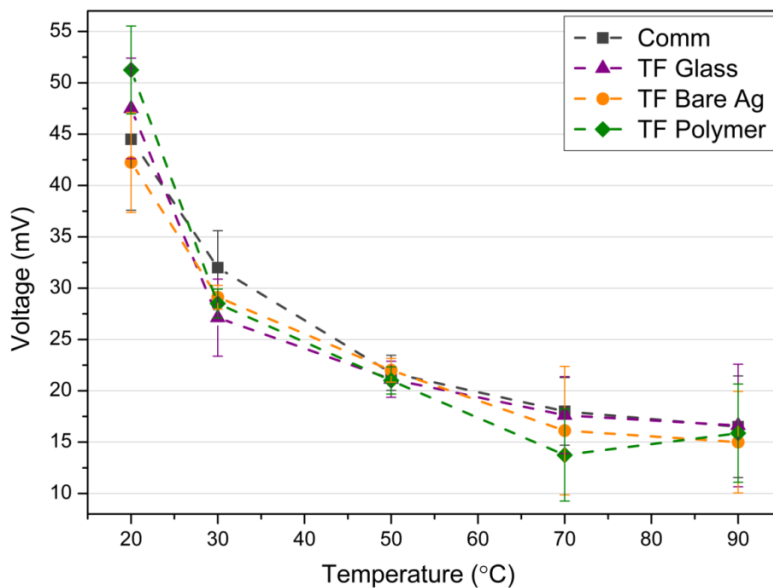


Figure 6-10: TF electrodes in 48 hours oxidised fully formulated oil sample tested at five temperatures

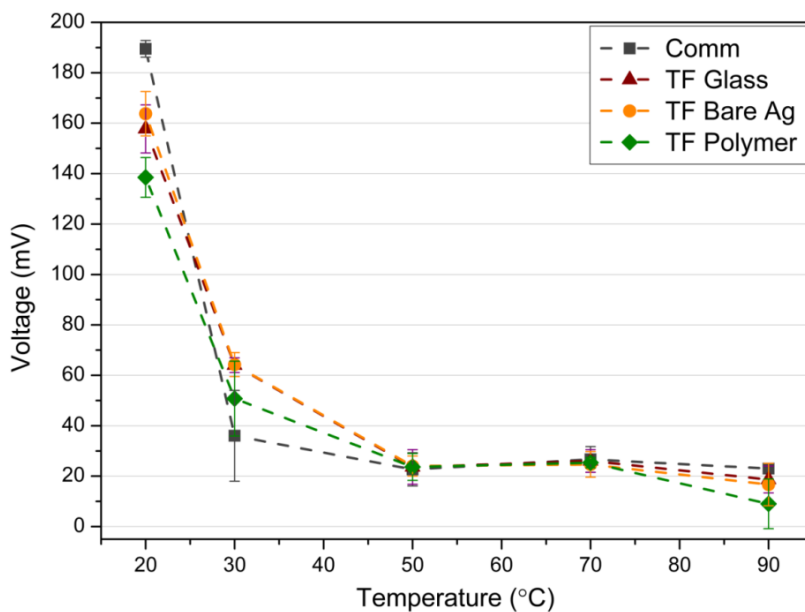


Figure 6-11: TF electrodes in 120 hours oxidised fully formulated oil sample tested at five temperatures

Figure 6-12 illustrates the conductivity plots of the 48 and 120 hours oxidised oil samples at five temperatures and as can be seen the conductivity of both oil samples increased exponentially with temperature as expected. The conductivity of the 120 hours oxidised oil sample is higher than that for the 48 hours oxidised oil at all temperatures. As can be seen, the difference between the conductivities of the two oil samples increases with temperature, for example the difference in the conductivities of the two oil samples at 20 °C is only 0.64e-

10 S/cm whereas this difference increases to $1e-9$ S/cm at 90 °C. This indicates the significant influence of temperature on oil conductivity.

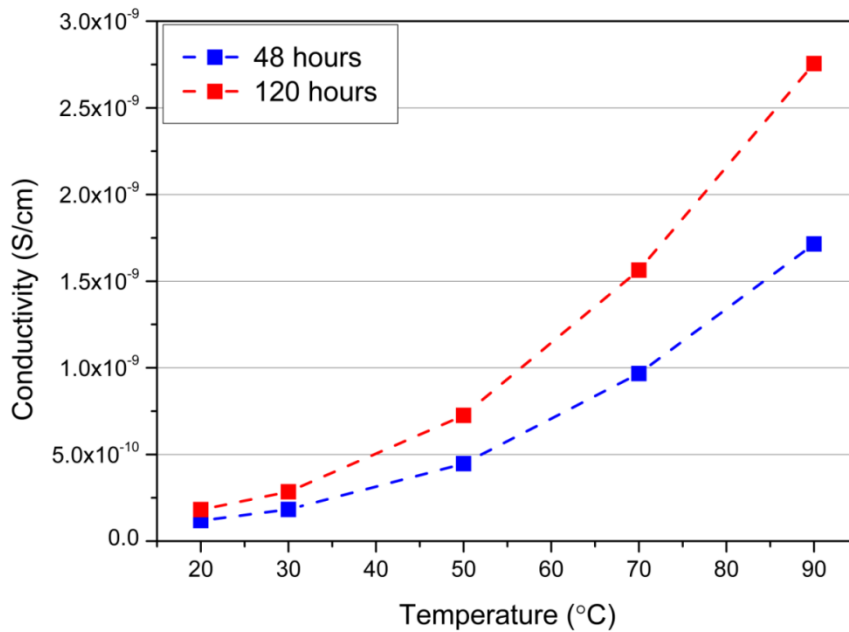


Figure 6-12: Temperature effect on conductivity of the oxidised fully formulated oil samples

Viscosity of the same oil samples were also measured at the same temperature intervals (i.e. 20 °C, 30, 50, 70 and 90 °C) and is shown in Figure 6-13. The viscosity of both oil samples decreased exponentially with higher temperatures. The viscosities of the two oil samples are almost identical and behave in the same fashion with changes in temperatures.

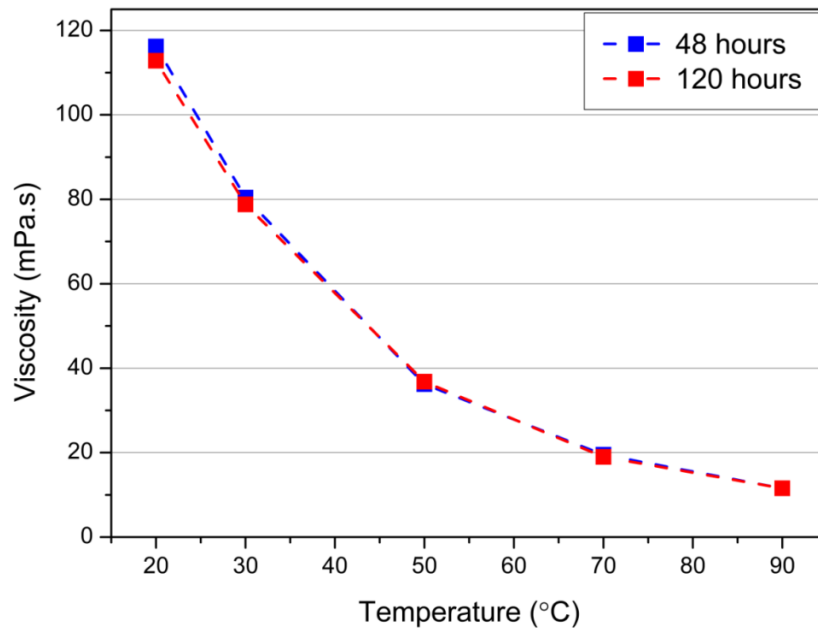


Figure 6-13: Temperature effect on viscosity of the oxidised fully formulated oil samples

Figure 6-14 and Figure 6-15 illustrate the temperature effect on TF electrodes alongside conductivity and viscosity plots of the 4 and 20 hours respectively.

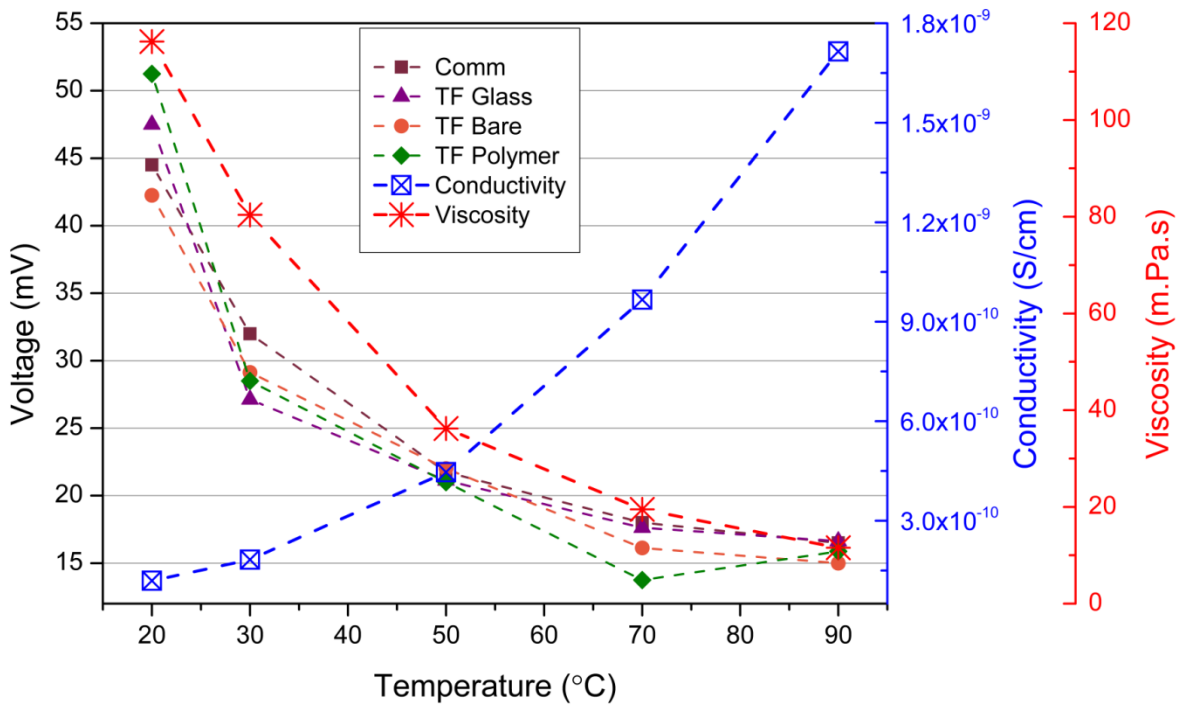


Figure 6-14: Temperature effect on TF electrodes, viscosity and conductivity of the 48 hours oxidised fully formulated oil sample

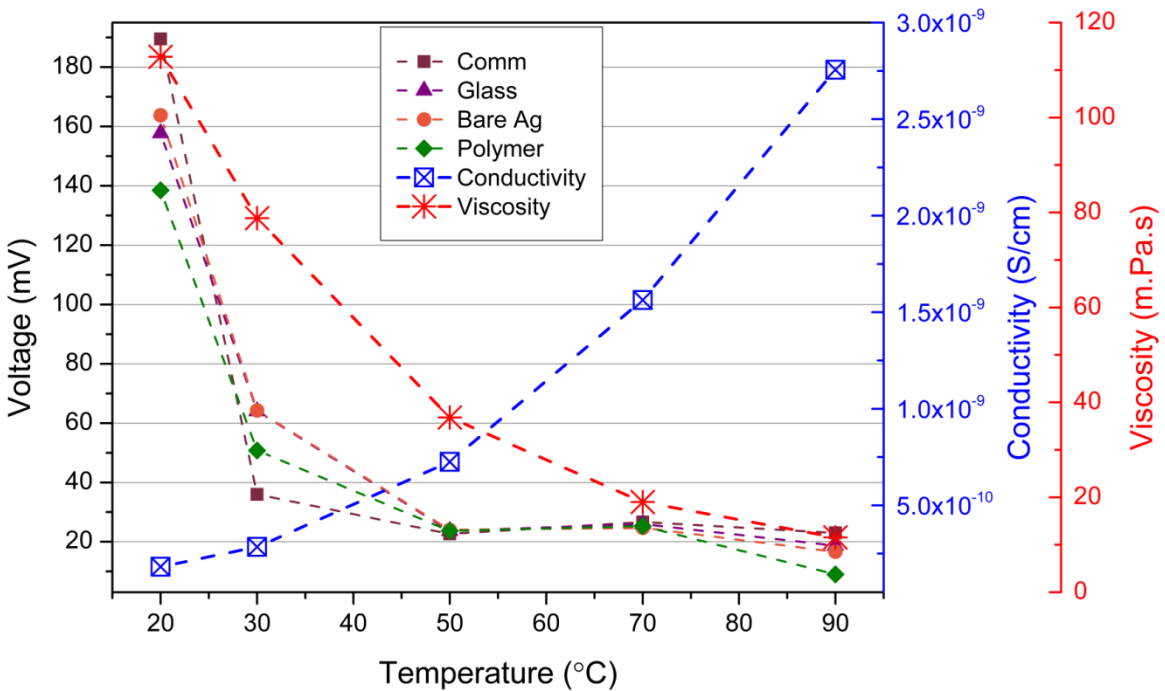


Figure 6-15: Temperature effect on TF electrodes, viscosity and conductivity of the 120 hours oxidised fully formulated oil sample

6.3 Stability test

The long term stability (drift) of the TF electrodes was investigated in 24 hours oxidised fully formulated oil sample. The TF electrodes were inserted in the 50 °C oil and the output voltage of the electrodes were recorded continuously every day for approximately one month. As shown in Figure 6-16, all the electrodes (TF and commercial) performed similarly and consistently for the duration of the test and only started scattering toward the end of the test, i.e. after 22 days.

This test proves the robustness and reliability of the electrodes for reasonably long time. It should be noted that the electrodes were submerged in the oil for the entire duration of the test. Practically, the TF electrodes are not required to be submerged in the oil permanently if utilised for monitoring the acidity of oil, for instance inside an engine sump, as the degradation/oxidation process of fully formulated oil is slow. Therefore, the number of readings (oil measurements) can be reduced for instance to every 3 days or every 100 miles, increasing the useful life of the electrodes. The electrodes can be replaced with a new set when the oil change takes place.

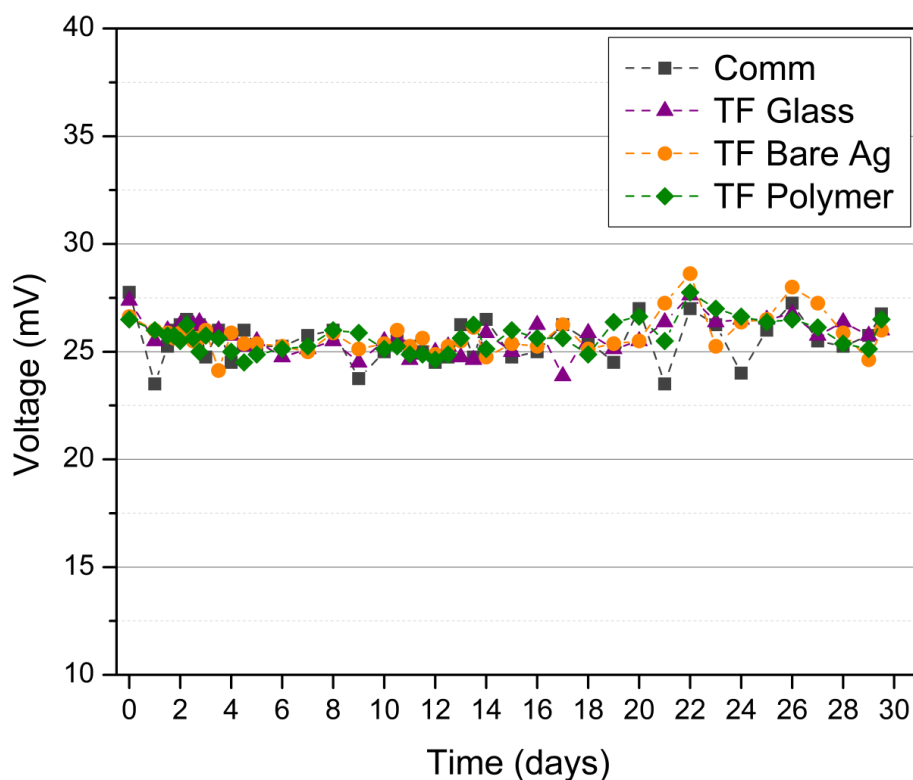


Figure 6-16: Long term stability test of the TF electrodes in 24 hours oxidised oil at 50 °C

6.4 Repeatability test

In order to confirm the repeatability of the TF electrodes, the oxidised base oil samples test was repeated with two different sets of TF electrodes, following the same procedure as explained in the previous Chapter and Section 5.3. Figure 6-17 illustrates the average responses of the two sets of electrodes (each with 4 WE and RE pairs) in the various oxidised base oil samples at 50 °C and 80 °C.

The performance of the 4 electrode pairs was similar at 50 °C and 80 °C to the results presented for the previous test in Section 5.3. However, at 50 °C plots, there is a glitch in the response of the TF electrodes in the fresh oil sample, more scattered outputs are observed in the 16 hours oil sample and there is a small drop for the last oil sample (24 hours). At 80 °C, the trends are approximately identical and the only difference is the range in which in the repeated test, the electrodes output changes from almost -650 to 20 mV in comparison to -450 to 0 mV for the previous test. At both temperatures, the absolute potential of the electrodes is different to the previous batch. This is most probably due to the fabrication process and layer thickness variations. More repeatability tests in different degraded oil samples are required to investigate this effect further.

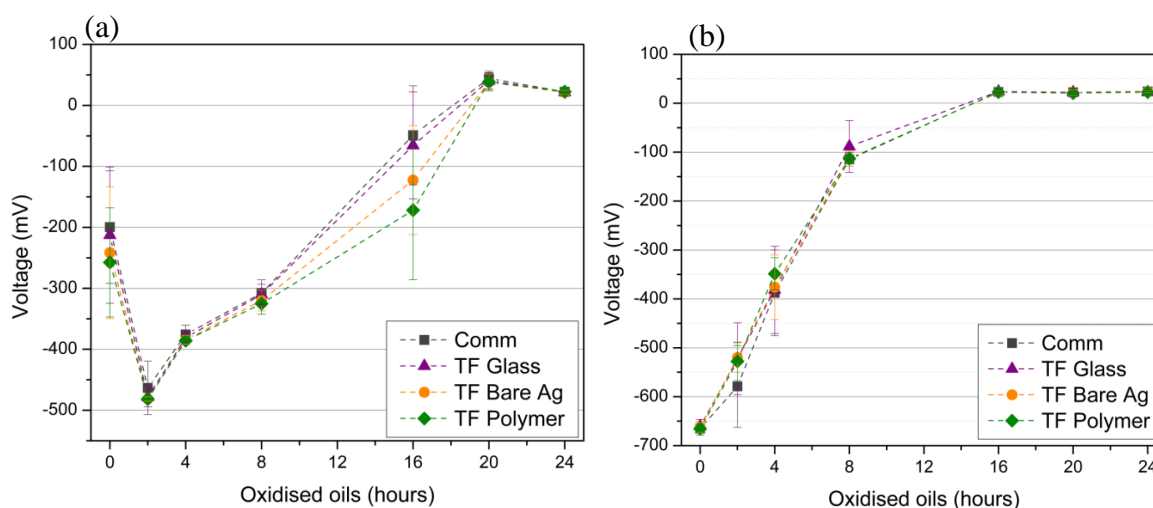


Figure 6-17: Repeatability test of the acidity sensors in oxidised base oil samples, a) at 50 °C, and b) at 80 °C

6.5 REs type and design influence

In this section, the three RE designs are compared and discussed based on the results shown in Sections 5.3, 5.4, 5.5 and 5.6.

In the oxidised base oil samples test, the responses of TF RuO₂ WE versus different TF and commercial reference electrodes were very similar. This is probably due to the fact that any changes in the potential of the reference electrodes are insignificant compared to the potential change of the working electrode. The output responses of the electrodes were negative apart from the last two oil samples (20 and 24 hours oxidised) at 50 °C and three oil samples (16, 20 and 24 hours oxidised) at 80 °C. The negative polarity from the electrodes indicates that the working electrode had a lower potential than the reference electrodes and this potential changed with oil oxidation hours. Table 6-1 summarises the output responses of different electrode pairs in the oxidised base oil samples. It should be noted that there are two columns for the sensitivity calculation in which one column contains the difference between highest and lowest output responses (Δ (Max & Min) in mV) of the TF electrodes whereas the other column comprises the first and last oil samples (fresh and 24 hours oxidised base oil samples) data. In the oxidised base oil test, these two columns are the same and the response range (sensitivity, calculated from the difference between the fresh and 24 hours oil samples) of the electrode pairs varies by approximately 311 mV at 50 °C and 418 mV at 80 °C.

Considering the oxidised fully formulated oil samples test, the responses of different WE and REs pairs were not the same. At 50 °C, the TF RuO₂ WE versus TF bare silver RE produced the highest output potential sensitivity (145.5 mV) followed by TF polymer RE (138.75 mV), TF glass RE (86.9 mV) and commercial RE (58.5 mV). At 80 °C, the electrode pairs performed similarly and had almost the same sensitivity range (25.2 mV). When compared to oxidised base oil samples, the output potential range of the electrode pairs were much higher for the oxidised base oil samples than that for the fully formulated oil samples. This is reasonable as the AN of the oxidised base oil samples were also much greater than the fully formulated oil samples generating higher potential difference. In terms of the output polarity, the electrode responses were positive in the oxidised fully formulated oil samples at both temperatures for all electrode pairs whereas it was negative in the oxidised base oil samples. Also, different electrode pairs had almost the same output values in the base oil samples whereas this was different in the oxidised fully formulated oil samples. In the oxidised base

oil samples test, it was concluded that the similarity in the electrode pairs output potential difference was due to the fact that any changes in the potential of the reference electrodes are insignificant compared to the potential change of the working electrode. The difference, in this sense, in the oxidised fully formulated oil sample test can be due to the electrochemically active additives which influence and react with the REs, not only shifting the output potentials, but also reducing the overall potential difference. In oxidised fully formulated oil samples the output potential difference is positive (negative in base oil) which can again be due to the additives influence in shifting the electrodes potentials. This effect needs further investigations.

Reference Electrodes	Sensitivity Δ (First & last oil) mV		Sensitivity Δ (Max & Min) mV		Notes
	50 °C	80 °C	50 °C	80 °C	
Commercial	313.25	408.25	313.25	408.25	All electrode pairs have similar responses at both temperatures.
TF Glass	311.5	413.87	312.62	413.87	Same as above.
TF Bare Ag	310.25	424.75	310.25	424.75	Same as above.
TF Polymer	309.25	424.87	309.25	426.25	Same as above.

Table 6-1: Performance of TF RuO₂ WE vs. different REs in oxidised base oil test

Reference Electrodes	Sensitivity Δ (First & last oil) mV		Sensitivity Δ (Max & Min) mV		Notes
	50 °C	80 °C	50 °C	80 °C	
Commercial	10	26.8	58.5	26.8	Commercial has the lowest potential difference at both temperatures.
TF Glass	86.9	26.63	86.9	26.63	TF Glass and TF Polymer have similar performances.
TF Bare Ag	145.5	23.75	145.5	23.75	has the highest potential difference at 50 °C.
TF Polymer	138.75	23.75	138.75	23.75	TF Glass and TF Polymer have similar performance.

Table 6-2: Performance of TF RuO₂ WE vs. different REs in oxidised fully formulated oil test

Reference Electrodes	Sensitivity Δ (First & last oil) mV		Sensitivity Δ (Max & Min) mV		Notes
	50 °C	80 °C	50 °C	80 °C	
Commercial	174.6	43.91	330	100.8	Commercial has the lowest potential difference at both temperatures.
TF Glass	274.7	141.2	450.3	222.1	TF Glass and TF Polymer have similar performances.
TF Bare Ag	318.3	293.1	424.1	313.2	highest change in the output response between first and last oil samples at both temperatures.
TF Polymer	262.2	232.4	470.5	262.8	TF Glass and TF Polymer have similar performances.

Table 6-3: Performance of TF RuO₂ WE vs. different REs in nitric acid added to fresh engine oil test

6.6 Effects on the sensitivities of the TF electrodes

Based on the experiments carried out, TF electrodes produced dissimilar results (polarity, level and sensitivity) in oxidised fully formulated and base oil samples. Additive packages in the fully formulated oil samples are probably the distinguishing feature of the fully formulated oils and it is assumed that the difference in the responses of the TF electrodes were caused by these additive packages. Different temperatures also changed the output response of the TF electrodes which will be discussed further below and in details in Section 6.2. In this study, one WE was used and paired with different types of reference electrodes. The behaviour of different types of reference electrodes was discussed in Section 6.5.

The sensitivity responses of the TF electrodes in the base oil and fully formulated oil samples were different. In the base oil samples, different TF electrode pairs produced very similar responses as the trends and absolute values were almost identical whereas the same electrode pairs had dissimilar responses in the fully formulated oil samples. Figures 6-2, 6-3 and 6-4 (RuO₂ paired with glass, bare Ag and polymer REs respectively) illustrate the responses of the TF electrode pairs versus AN in both oxidised base and fully formulated oil samples. As can be seen, in the oxidised base oil samples, the output potential of the TF electrodes increased by almost 310 and 424 mV at 50 °C and 80 °C respectively where the AN values increased by 32 mgKOH/g (sensitivity of 9.7 and 13.2 mV per AN at 50 °C and 80 °C). In comparison, in the oxidised fully formulated oil samples, the output potential of the TF electrodes (RuO₂ vs. bare Ag) increased by 145 mV as the AN values increased to 3.35 mgKOH/g (43.3 mV per AN) at 50 °C and approximately 25 mV (~7.5 mV per AN) at 80 °C. These values and the slope of the graphs (Figures 6-2, 6-3 and 6-4) show that the sensitivity of the TF electrodes is higher at 50 °C and lower at 80 °C in the oxidised fully formulated oils when compared to oxidised base oils. Also, the slopes of the output responses of the TF electrodes versus AN are similar in both sets of oil samples with high R^2 values (linearity) at 80 °C. However, the R^2 values of the TF electrode's responses versus AN in the fully formulated oil samples are lower (more scattered responses) at 50 °C. This may suggest that the TF electrodes perform better at 80 °C in fully formulated oil samples.

The dissimilarities observed in the TF measurements of the base and fully formulated oil samples, such as the sensitivity slope and polarity can be due to the additive packages. Additive packages are polar weak acid and base substances which may also react with the

surface of the RuO₂ affecting the output potential of the WE electrode and shifting the equilibrium. This effect can also occur at the surface of the TF reference electrodes which might be the explanation for the dissimilar responses of different pairs of TF working vs. REs. As a commercial lubricant, the details of the additive package were not available for this study and it is expected that particular additives within the package may dominate the effect on the equilibrium of the reactions at the interface of TF electrodes. This should be further investigated in a future study.

The temperature effect on the responses of the TF electrodes can be due to either temperature effects on the electrodes or the changes in the oil properties such as acidity, viscosity and conductivity. In the former case, the temperature can have possibly modified the structure of the pastes in different layers of the electrodes. In theory, metal oxide responses decrease at higher temperatures according to the Nernst equation due to the sensor potential¹⁸. In the latter (change in oil properties as a result of higher temperature), for example viscosity of oil decreases at higher temperatures which increase ion mobility. But it was shown previously that the responses of TF electrodes are not significantly affected by the changes in oil viscosity or conductivity. However, higher viscosities might have an influence on settling time of the electrodes, due to the reduced ion mobility in the oil samples, but this should not affect the steady state values.

6. Thick film sensors performance and mechanism

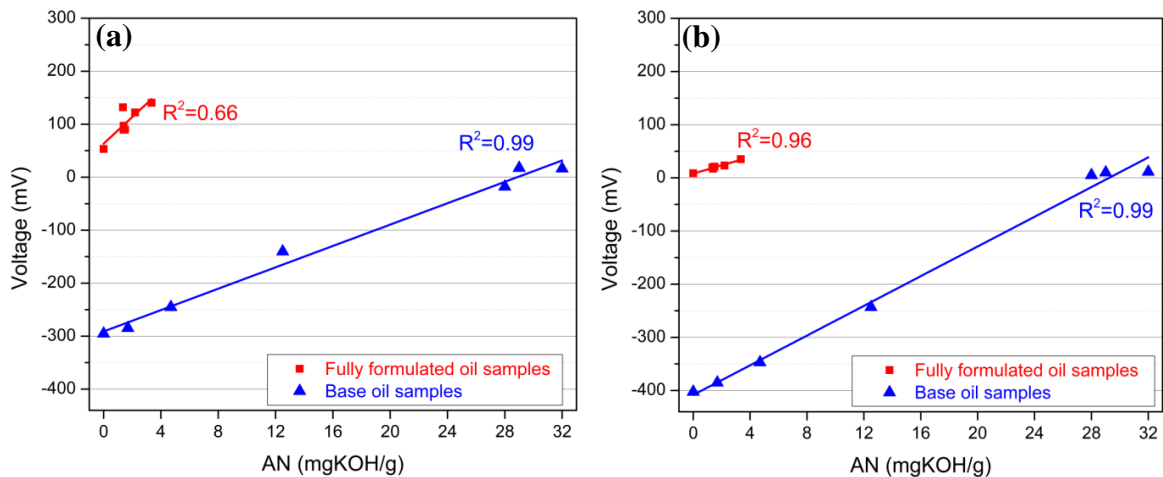


Figure 6-18: Response of TF RuO₂ WE vs. glass RE at: a) 50 °C and b) 80 °C

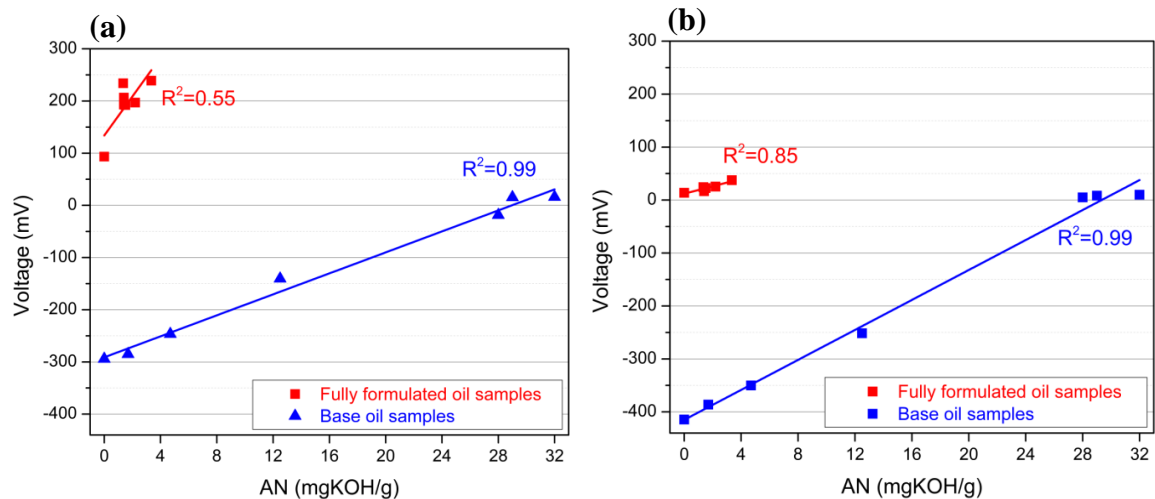


Figure 6-19: Response of TF RuO₂ WE vs. Bare Ag RE at: a) 50 °C and b) 80 °C

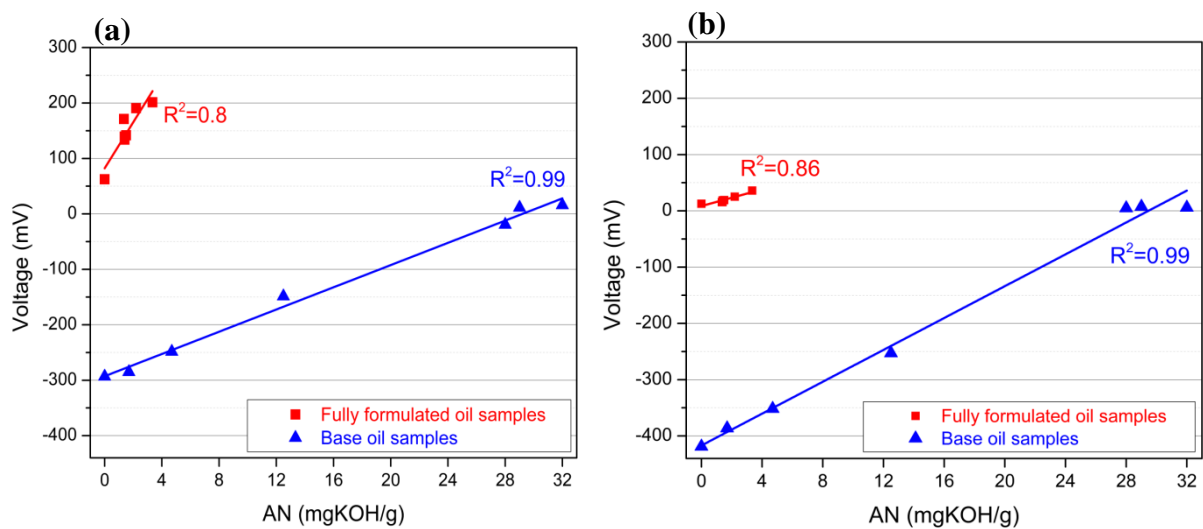


Figure 6-20: Response of TF RuO₂ WE vs. polymer RE at: a) 50 °C and b) 80 °C

6.7 Proposed sensing mechanisms of TF electrodes

In the previous Chapter, it was shown that the TF electrodes can detect the acidity increase as a result of oxidation or added acid in both base and fully formulated sets of oil samples. Fog and Buck⁸⁷ suggested five possible sensing mechanisms for the RuO₂ in aqueous solutions, including:

1. simple ion exchange in the surface layer of the WE containing OH groups which is observed in the commercial glass pH electrodes,
2. a redox equilibrium between two different solid phases, e.g. a lower and higher valence oxide, or an oxide and a pure metal phase,
3. a redox equilibrium involving only one solid phase, whose hydrogen content can be varied continuously by passing current through the electrode (also known as intercalation reaction),
4. similar to the previous mechanism, a single phase oxygen intercalation electrode may be envisaged,
5. lastly, a steady-state corrosion of the electrode might develop a pH-dependent potential in the WE.

McMurray et al.⁸⁵ consider the ‘oxygen intercalation’ to be the most probable mechanism (number 4 in the list above) in which the below equilibrium occurs:



Where RuO₂ is the higher metal oxide and RuO is a lower metal oxide. This then develops a potential difference of:

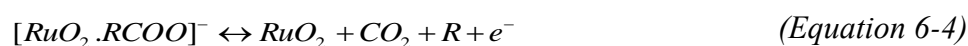
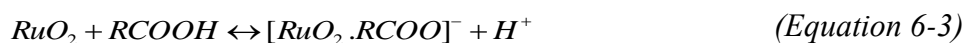
$$E = \text{‘constant’} + \left(\frac{RT}{F}\right) \ln a_{H^+}^l + \left(\frac{RT}{2F}\right) \ln a_o^s. \quad (\text{Equation 6-2})$$

Where $a_{H^+}^l$ is the proton activity in the liquid phase and a_o^s is the oxygen activity in the solid phase. The sensing mechanism of the RuO₂ in aqueous solutions was suggested to be the general reduction reaction taking place between the metal oxide electrode and the solution. This is probably due to the adsorption of H⁺ ions to the metal oxide electrode surface resulting in reduction reaction taking place. A conduction mechanism of charge transfer from front to the back of the electrode then takes place in the TF WE, based on an aggregated network of RuO₂ particles on top of the platinum/gold layer. Equilibrium between two solid

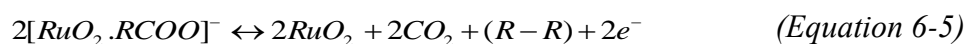
phases of the oxide or the intercalation of species into the oxide structure causes the potentiometric pH response in the WE^{82,87}.

The response characteristics of the TF electrodes in aqueous solutions and in oil samples followed a similar mechanism of interaction occurring between the electrodes and each solution. In aqueous solutions, output response of the TF electrodes increased with lower pH values (higher acidity) and in oil samples, the output potential followed the oil acidity number (AN) values.

Although the exact sensing mechanism of the TF electrodes cannot be determined from the presented experiments in this study, following reactions have been suggested as the possible behaviour for the interaction between TF metal oxide electrodes and the acids in the oil samples^{41,106,107}:



or



Where 'COOH' is carboxylic acid, R is a monovalent functional group such as hydrogen or an alkyl group (carboxylic acid is an oxidation by-product, see Section 2.2.5.2) reacting with the metal oxide electrode which then produces potential difference as a result of electrons transfer ('e⁻' in Equations 6-1 and 6-4). The produced potential depends on the number of transferred electrons and hence the carboxylic acid (and other oxidation by-products/acid) in the oil. In the experiments carried out, the output potential of the TF electrodes correlated with oil AN values. The measured AN values of the oil samples is a measure of acid concentration, which detects both weak organic acids and strong inorganic acids. In the case of experiments carried out in this study, the AN of the oil samples increased due to the presence of weak organic acids (e.g. carboxylic acid) in the oxidised oils and strong acids in the oil samples with added nitric acid. Therefore, the increase in output potential of the TF electrodes is an indication of the increased acidity in the oil samples. The proposed mechanism is based on the previous works, but this might not be the exact reactions occurring in this situation. Further chemical analysis should confirm the exact mechanism.

This page is intentionally left blank

Chapter 7. Conclusions and Further work

7.1 Introduction

The quality of oil decreases during the course of lubrication mainly due to oil oxidation and contamination from water, wear debris, fuel and coolant dilution etc. Among oil properties, chemical properties such as chemical composition and acidity/ alkalinity are true measures of oil oxidation and degradation. Thus far, there is no reliable commercially available on-line chemical sensor reported for oil chemical property monitoring probably due to the complexity of the chemistry of oils and their degradation processes. To achieve the overall aim of this project, i.e. to develop robust sensors for oil degradation detection, the performance of thick film chemical sensors in detecting oil acidity was investigated. From previous research, thick film RuO₂ working electrode had shown reliable performance in acidity measurements in aqueous solutions whereas reference electrodes face stability issues as they drift after certain amount of time depending on their construction. Therefore, ruthenium oxide (RuO₂) thick film sensor was chosen as the working electrode, while three different types of thick film reference electrodes (silver/silver chloride and bare silver) were studied. A commercial glass Ag/AgCl reference electrode was also tested in parallel for comparison. A number of well-controlled, artificially degraded oil samples were used to evaluate the feasibility of the TF sensors in oil acidity detection.

7.2 Conclusions

Initial testing in aqueous buffer solutions confirmed that the thick film electrodes, fabricated in this study, responded linearly to pH changes in aqueous buffer solutions, as expected. Then, the electrodes were tested in the degraded oil samples under two temperatures (50 and 80 °C) simulating the temperature of a conventional combustion engine sump. The oxidised base and fully formulated oil samples were prepared at the Shell Houston laboratories using a proprietary in-house blown NO_x (BNO_x) oxidation test, providing a series of oils with increasing ages. The oil samples with added nitric acid were prepared at the University of Southampton laboratories. The performance of the fabricated sensors was compared with laboratory-based measurements such as viscosity, titration (for AN determination) and impedance spectroscopy devices. In addition, tests were carried out to identify the parameters affecting the performance of the TF electrodes such as different temperatures, REs type, stability and reliability tests.

The main novelties in this study are:

- ❖ A series of base and fully formulated oil samples were artificially degraded under controlled conditions for testing the performance of the TF electrodes. For validating the responses of the TF electrodes, the physical (viscosity), chemical (AN) and electrical (conductivity) properties of the tested oils were measured and a relationship between different properties of oil samples during their degradation process, was established.
- ❖ For the first time, different types of miniaturised TF reference electrodes (bare silver and two silver/silver-chloride REs) were successfully developed and tested in oils.
- ❖ The oil acidity changes have been successfully detected using the miniaturised, low-cost chemical sensors. Linear correlation between the TF responses and the AN was found in the oxidised oils within certain ranges at the tested temperatures (50 °C and 80 °C). It was proved that TF sensors can detect oil acidity up to AN of 28 mgKOH/g.
- ❖ The effects of temperature and different properties of oil on the TF electrodes were explored. The repeatability and long term stability of the TF electrodes in oils were investigated and the sensing mechanism of the TF electrodes was proposed.

The main conclusions from this study are summarised below.

- This study investigated the feasibility of detecting acidity changes in oils by developing and testing TF electrodes in different types of artificially degraded oil samples. A valid test method was developed and conductivity, viscosity and AN of the oil sample were measured to validate TF sensor responses and identify their influence on the performance of TF electrodes.
- The conductivity of the oil samples changed with the degradation processes in different manners in base and fully formulated oils, due to the presence of additive packages. In fully formulated oils (oxidised and added acid) the conductivity trend initially decreased due to polar additive consumption and subsequently increased because of accumulation of polar oxidation by-products. However, in oxidised base oil samples the conductivity increased exponentially due to the formed oxidation by-products such as water and carboxylic acid. Oil conductivity can potentially affect the TF sensor responses, but no relationship was found.
- AN of the degraded oil samples increased with oxidation hours and added acid in both base and fully formulated oils. The AN of the oxidised base oils increased considerably to 32 mgKOH/g when oxidised for only 24 hours whereas oxidised fully formulated oil

samples increased to only 3.2 mgKOH/g after 144 oxidation hours and in the oil with added acid, the AN increased to 1.7 mgKOH/g after adding 2000 ppm of 30% concentrated nitric acid. AN displayed remarkable correlations with the TF sensor responses as linear relationships were found in both base and fully formulated oils. In overly oxidised oil samples (AN range higher than 28 mgKOH/g) the extreme acidity caused sensor malfunction. This effect was proved by SEM and EDX analysis of the TF WE electrode.

- Viscosity increased significantly in degraded base oils and did not change considerably in the fully formulated oils most probably because the additives neutralised the formed acids and prevented the viscosity increase. Viscosity of the oil samples did not seem to influence the response of the TF electrodes but higher viscosities might have an effect on settling time of the electrodes, due to the reduced ion mobility in the oil samples.
- Temperature affected the oil properties and the performance of the TF electrodes in aqueous buffer solutions and oxidised base and fully formulated oil samples. The output responses of the TF sensors decreased with higher temperatures according to Nernst equation. TF sensors displayed repeatable trends when different sets of electrodes were tested in the same oxidised oil samples at 50 and 80 °C. The absolute potential of the electrodes were different to the previous batch due to the fabrication process and layer thickness variations. The stability test confirmed the long-term performance of the TF electrodes in the 24 hours oxidised fully formulated engine oil which ran for one month at 50 °C. TF electrodes performed consistently for almost 22 days before starting to produce scattered responses.
- The performance of the three different reference electrodes did not vary significantly in different oil samples. Successful performance of the reference electrodes in this work was a key improvement in the electrochemical sensing of lubricating oil as previous attempts at making acidity sensors were flawed in that they did not pay attention to designing and testing a miniaturised reference electrode.
- The TF sensors developed in this study correlated remarkably with the oil AN in all types of oils for the first time. The output of the TF sensors increased linearly with oil AN in the oxidised base oil samples by 9.7 at 50 °C and 13.2 mV per AN at 80 °C. In oxidised fully formulated oils with additives, the TF sensors (RuO₂ WE vs. Bare Ag RE) increased linearly with oil AN (0 to 3.35 mgKOH/g) by 43.3 mV per AN at 50 °C and ~7.5 mV per AN at 80 °C. The sensitivity of the TF electrodes in the oxidised fully formulated oils was

higher and more scattered at 50 °C and lower at 80 °C when compared to oxidised base oils. The sensitivity responses of the TF sensors are similar in both sets of oxidised oil samples at 80 °C (also with higher R^2 values (linearity)) when compared to the measurements at 50 °C. This may suggest that the TF electrodes perform better at 80 °C in fully formulated oil samples. The difference in polarity and absolute values in the output responses of the TF electrodes in fully formulated oil samples is probably due to the additive packages which slow the oxidation process down and prevent AN increase. Additive packages may also have reacted with the surface of the TF electrodes affecting the output potential and shifting the equilibrium.

- The proposed sensing mechanism of the TF electrodes in oils is based on the chemical reactions taking place between the metal oxide (RuO_2) electrode and the formed acids due to oil degradation, e.g. oxidation, which then produces a potential difference as a result of the electrons transfer. The produced potential depends on the number of transferred electrons and hence the formed acid (such as carboxylic) in the oil.

7.3 Future work

This study proved the practicality of the TF acidity sensors in oil. However, further developments are required to enable its commercialisation. The future work aims to address the next steps for fully understanding and characterising TF electrodes in monitoring the acidity of lubricating oils. Following works is suggested for future investigation:

- Carry out tests in wider range of oil samples. This study tested limited types of base and fully formulated oil samples. In the future, it would be useful to test the TF electrodes in a wider range of oil samples from different manufacturer, base and fully formulated oils from different groups (i.e. I, II, III and synthetics) and oil samples with different additive packages. Tests in different artificially degraded oil samples such as oxidised, added acid (different soluble weak and strong acids at different concentrations) and with other contaminants such as metallic wear debris, water, soot and glycol as well as matrices of combined contaminants (e.g. added acid and soot, oxidised and added water).
- Other complementary properties analysis tests alongside TF electrodes, such as base number (BN), chemical analysis (e.g. infrared spectroscopy) etc. These tests provide more details on the oil samples and can be used to assess the sensors performance in different oil samples.
- Carry out further temperature, stability and repeatability tests in different oil samples at different temperature ranges. These tests can be employed to precisely define the sensors working range in terms of durability and lowest and highest temperatures they can correctly measure oil acidity.
- Data acquisition system is a key factor for successful implementation of on-line TF electrodes. Metrohm high input impedance meter was used in this study which is a manual, single channel meter, causing the experiments to become time consuming and laborious. An attempt to design and fabricate a miniaturised 10-channel on-line data logger was not successful and dismissed due to time constraints.
- Carry out tests in real-time engine environment. TF sensors to be installed on an engine (e.g. sump) and their output to be monitored over a certain period of time. A simple algorithm can also be developed on a microprocessor with defined thresholds to give signals on the oil condition.

The TF sensors used in this work can be enhanced and improved by customising and changing the design of the electrodes to meet the requirements of oil sensing. This includes

the use of other metal oxide pastes instead of ruthenium oxide (RuO_2) for fabricating the working electrode, such as iridium oxide (IrO_2) and Platinum oxide (PtO_2). Also, one reference electrode can be selected and used with the working electrode such as the glass Ag/AgCl as it is fired at higher temperature ($650\text{ }^\circ\text{C}$) rather than the other two reference electrodes tested. Furthermore, in order to avoid the fabrication errors which cause non-uniformity between different electrodes batches, more sophisticated printing machineries can be used with higher resolution and accuracy.

TF electrodes can be used on-line (e.g. inside an engine sump) or as a hand portable device (for instance in an automotive garage). An example of a portable or on-line deployment of the TF sensor is shown in Figure 7-1 (suggested by Atkinson et al.¹⁰⁸) whereby the TF sensor array is mounted in a probe assembly with a waterproofed connector. The TF sensors are protected inside a cup-like container with holes at the bottom through which the oil can flow. Furthermore, TF electrodes can be combined with TF temperature and conductivity sensors on a same substrate forming a robust inexpensive integrated sensor for oil sensing. This will also require further work to develop an algorithm which takes the various sensor outputs and gives a quantitative assessment of the remaining oil life. Such an algorithm, if accurate, would be very useful to customers and car/truck manufacturers.

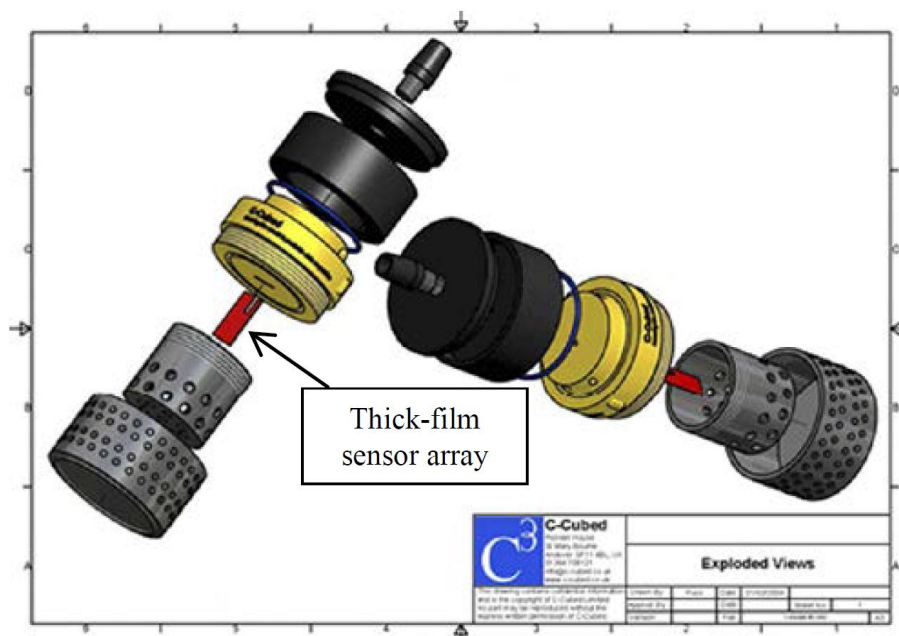


Figure 7-1: Design suggested for portable or on-line deployment of TF sensor¹⁰⁸

This page is intentionally left blank

References

- ¹ British Standards 3811. *Glossary of terms used in terotechnology*. British Standards Group, 2001.
- ² B. S. Dhillon, *Engineering Maintenance: A Modern Approach*, CRC Press. 2002.
- ³ K. C. Arora, *Production and Operations Management*, Laxmi Publications. 2005.
- ⁴ R. S. Beebe, *Machine Condition Monitoring: How to Predict Maintenance Requirements for Rotating and Stationary Plant*, MCM Consultants, 1st edition. 1993.
- ⁵ R. Barron, *Engineering Condition Monitoring: Practice, Methods and Applications*, Longman. 1996.
- ⁶ S. Gebarin, *On-line and In-line Wear Debris Detectors: What's Out There?*, 2003
[viewed; available online at: <http://www.machinerylubrication.com/Read/521/in-line-wear-debris-detectors>]
- ⁷ A. W. Batchelor and G. W. Stachowiak, *Engineering Tribology*, Elsevier-Butterworth-Heinemann. 2005.
- ⁸ A. R. Lansdown, *Lubrication and Lubricant Selection - A Practical Guide*, John Wiley & Sons. 2003.
- ⁹ W. Dresel and T. Mang, *Lubricants and Lubrication*, Wiley-VCH. 2007.
- ¹⁰ J. F. Rusling, *Electrochemistry in micelles, microemulsions, and related microheterogeneous fluids*, Electroanalytical Chemistry, A Series of Advances, vol. 18, New York: Marcel Dekker. 1994.
- ¹¹ R. H. Ottewill, et al., *Small-angle neutron-scattering studies on nonaqueous dispersions Part 5: Magnesium carbonate dispersions in hydrocarbon media*. Colloid. Polym. Sci., 270(6), 602-608, 1992.
- ¹² L. K. Hudson, J. Eastoe, P. J. Dowding, *Nanotechnology in action: Overbased nanodetergents as lubricant oil additives*, Adv. Colloid Interface Sci., 425(431), 123-126, 2006.
- ¹³ D. C. Hone, et al., *Acid-base chemistry in high-performance lubricating oils*, Can. J. Chem., 77, 842-848, 1999.
- ¹⁴ J. Booth, *The feasibility of using electrostatic charge condition monitoring for lubricant additive screening*, Ph.D. Thesis, University of Southampton, UK, 2008.
- ¹⁵ N. Canter, *Use of antioxidants in automotive lubricants*, special report, Tribology & Lubrication technology, STLE, 2008.
- ¹⁶ R. M. Mortier, M. F. Fox and S. T. Orszulik, *Chemistry and Technology of Lubricants*, Springer. 2010.
- ¹⁷ R. P. Buck, et al., *The measurement of pH. Definition, standards and procedures*, Pure Appl. Chem., 74 (11), 2169-2200, 2002.
- ¹⁸ A. Wahl, *A Short History of Electrochemistry*. Galvanotechnik, 96(8), 1820-1828, 2005.
- ¹⁹ J. Alexander, *Ruthenium dioxide thick film pH electrodes*, Ph.D. Thesis, University of Southampton, UK, 1997.
- ²⁰ D. D. Ebbing, S. D. Gammon, *General Chemistry*, (9th Edition), Houghton Mifflin Company. 2009.
- ²¹ F. J. Quail, J. Francis and A. Hamilton, *Detailed state of the art review for the different on-line/inline oil analysis techniques in context of wind turbine gearboxes*, ASME Journal of Tribology, 133(4), 1-17, 2011.
- ²² D. D. Ebbing, S. D. Gammon, *General Chemistry (9th Edition)*, Houghton Mifflin Company. 2009.
- ²³ R. J. Clark, *On-board monitoring of engine oil*, Master of Science thesis, Western Michigan University, 2011.
- ²⁴ P. Hedges, *Hydraulic Fluids*, John Wiley & Sons, Inc. 1996.
- ²⁵ Noria Corporation, *A Comprehensive Look At the Acid Number*, 2007
[viewed; available at: <http://www.machinerylubrication.com/Read/1052/acid-number-test>]
- ²⁶ S. Václav and V. Veselý, *Lubricants and Special Fluids*, Elsevier. 1992.
- ²⁷ J. W. Jewett, R. A. Serway, *Principles of Physics*, Brooks/Cole. 2005.
- ²⁸ W. M. Needelman, P. V. Madhavan, *Review of lubricant contamination and diesel engine wear*, SAE Technical Paper, 1988.
- ²⁹ S. Middelhoek and S. Audet, *Microelectronics and signal processing- Silicon sensors*, Academic Press, 1989.
- ³⁰ ASTM D445-09, *Standard Test Method for Kinematic Viscosity of Transparent and Opaque Liquids*, Annual Book of ASTM Standards, 2009.
- ³¹ V. M. Makarenko, L. V. Markova, M. S. Semenyuk and A. P. Zozulya, *On-line monitoring of the viscosity of lubricating oils*, Journal of Friction and Wear, 31(6), 433-442, 2010.
- ³² R. E. Kasameyer and W. Warren, *Fast-recovery viscometer*, US Patent 6584831, 2003.
- ³³ A. Buhrdorf, et al., *Multi parameter Oil Condition Sensor Based on the Tuning Fork Principle*, SAE Technical Paper, 2007.

- ³⁴ A. William, et al., *Acoustic viscometer and method of determining kinematic viscosity and intrinsic viscosity by propagation of shear waves*, US Patent 6439034, 2002.
- ³⁵ ASTM D974-12, *Standard Test Method for Acid and Base Number by Colour-Indicator Titration*, Annual Book of ASTM Standards, 2009.
- ³⁶ ASTM D664-09a, *Standard Test Method for Acid Number of Petroleum Products by Potentiometric Titration*, Annual Book of ASTM Standards, 2009.
- ³⁷ ASTM D2896-07, *Standard Test Method for Base Number of Petroleum Products by Potentiometric Perchloric Acid Titration*, Annual Book of ASTM Standards, 2007.
- ³⁸ ASTM D4739-08e1, *Standard Test Method for Base Number Determination by Potentiometric Hydrochloric Acid Titration*, Annual Book of ASTM Standards, 2008.
- ³⁹ S. Nakamura. *pH Measurement using the Harned Cell*, National Institute of Advanced Industrial Science and Technology (AIST), 2005, [Viewed; available at: http://www.ami.ac.uk/courses/topics/0255_tft/index.html]
- ⁴⁰ N. F. Sheppard, A. Guiseppi, *pH Measurement*, 2000.
[Viewed; available at: <http://dsp-book.narod.ru/MISH/CH71.PDF>]
- ⁴¹ V. F. Lvovich and M. F. Smiechowskia, *Iridium oxide sensors for acidity and basicity detection in industrial lubricants*, Sens. Actuators, B, 96(1), 261-267, 2003.
- ⁴² J. P. Bentley, *Principles of Measurement Systems*, Prentice Hall, 2005.
- ⁴³ T. Katafuchi and H. Kanamori, *Development of an apparatus to evaluate oil deterioration and oil life based on a new principle for environmental conservation*, Part J: Journal of Engineering Tribology, Vol. 225, 359-367, 2011.
- ⁴⁴ A. Geach, *Infrared Analysis as a Tool for Assessing Degradation in Used Engine Lubricants*, Wearcheck Technical Bulletin, 2008.
[viewed; available at <http://www.wearcheck.co.za/downloads/bulletins/bulletin/tech2.pdf>]
- ⁴⁵ A. W. Koch, K. Kudlaty, A. Purde, *Development of an Infrared Sensor for On-line Analysis of Lubricant Deterioration*, Proceedings of IEEE Sensors conference, 903-908, 2003.
- ⁴⁶ A. Agoston, et al., *An IR-Absorption Sensor System for the Determination of Engine Oil Deterioration*, Proceedings of IEEE Sensors conference, 1, 463-466, 2004.
- ⁴⁷ J. R. Macdonald, *Impedance spectroscopy*, Annals of Biomedical Engineering Vol. 20, 289-305, 1992.
- ⁴⁸ V. F. Lvovich and M. F. Smiechowski, *Non-linear impedance analysis of industrial lubricants*, Electrochimica. Acta., 53(25), 7375-7385, 2008.
- ⁴⁹ H. S. Lee and S. S. Wang, *The application of A.C. impedance technique for detecting glycol contamination in engine oil*, Sens. Actuators, B, 40(2), 193-197, 1997.
- ⁵⁰ F. Björefors, et al., *Simultaneous estimation of soot and diesel contamination in engine oil using electrochemical impedance spectroscopy*, Sens. Actuators, B, 127(2), 613-618, 2007.
- ⁵¹ Wear Check, *Effects of temperature on engine lubricating oil*, Technical bulletin, Issue 43, 2008.
[viewed; vailable at: <http://www.wearcheck.co.za/downloads/bulletins/bulletin/tech43.pdf>]
- ⁵² V. F. Lvovich and M. F. Smiechowski, *Electrochemical monitoring of water-surfactant interactions in industrial lubricants*, J. Electroanal. Chem., 543(2), 171-180, 2002.
- ⁵³ H. S. Lee and S. S. Wang, *The development of in situ electrochemical oil-condition sensors*, Sens. Actuators, B, 17(3), 179-185, 1994.
- ⁵⁴ V. F. Lvovich, *Impedance Spectroscopy- Applications to Electrochemical and Dielectric Phenomena*, John Wiley & Sons, USA, 2012.
- ⁵⁵ S. S. Wang, *Road tests of oil condition sensor and sensing technique*, Sens. Actuators, B, 73(2), 106-111, 2001.
- ⁵⁶ P. J. Voelker, J. D. Hedges. *Oil quality sensor for use in a motor*, US Patent 5789665, 1998.
- ⁵⁷ U. Latif and F. L. Dickert, *Conductometric Sensors for Monitoring Degradation of Automotive Engine Oil*. Sensors, 11(9), 8611-8625, 2011.
- ⁵⁸ Machinery lubrication, *Predict Navigator- A Portable Oil Screening Tool*, 2010.
[viewed; available at: <http://www.machinerylubrication.com/Read/74/predict-navigator-oil-screening>]
- ⁵⁹ S. Raadnui, S. Kleesuwa, *Low-cost condition monitoring sensor for used oil analysis*, Wear, 259(7), 1502-1506, 2005.

-
- ⁶⁰ C. J. Collister, *Electrical measurement of oil quality*, US Patent 6459995, 2002.
- ⁶¹ A. Mujahid and F. L. Dickert, *Monitoring automotive oil degradation: analytical tools and on-board sensing technologies*, Anal. Bioanal. Chem. Volume 404, pages 1197–1209, 2012.
- ⁶² M. A. Lace, *Engine oil condition monitoring apparatus*, US Patent 3723964, 1973.
- ⁶³ H. Kubo and H. Hashimoto, *Engine oil degradation detector*, US Patent 6449538, 2002.
- ⁶⁴ J. K. Duchowski and H. Mannebach, *Novel Approach to Predictive Maintenance: A Portable, Multi-Component MEMS Sensor for On-Line Monitoring of Fluid Condition in Hydraulic and Lubricating Systems*, Tribol. T., 49, 545-553, 2006.
- ⁶⁵ S. Chee, et al., *Oil sensor systems and methods of qualitatively determining oil type and condition*, US Patent 5274335, 1993.
- ⁶⁶ T. Kita, H. Kobayashi, H. Saito and S. Yasuhara, *Oil deterioration detector method and apparatus*, US Patent 4646070, 1987.
- ⁶⁷ R. H. Hammerle, *Resistive oil quality sensor*, US Patent 5332961, 1994.
- ⁶⁸ D. Langervik, *Oil maintenance indicator*, US Patent 6484127, 2002.
- ⁶⁹ S. Lunt, *Recent Developments in Online Oil Condition Monitoring Sensors and Alignment with ASTM Methods and Practices*, J. ASTM Int., 8(7), 2011.
- ⁷⁰ E. Irion, K. Land, M. Klein, *Oil-Quality Prediction and Oil-Level Detection with the TEMIC QLT-Sensor*, SAE Tech. Pap., 1997.
- ⁷¹ L. F. Matsiev, *Application of Flexural Mechanical Resonators to Simultaneous Measurements of Liquid Density and Viscosity*. Proc. IEEE Ultrason. Symp., 1, 457-460, 1999.
- ⁷² J. C. Andle, *Measurement, Compensation and Control of Equivalent Shear Rate in Acoustic Wave Sensors*. US Patent 7181957, 2007.
- ⁷³ J. D. Turner and N. M. White, *Thick-film sensors: past, present and future*, Meas. Sci. Technol., 8(1), 1997.
- ⁷⁴ M. Tarr, *Thick film technology*, 2011.
[viewed; available at: http://www.ami.ac.uk/courses/topics/0255_tft/index.html]
- ⁷⁵ J. E. Brignell, A. Cranny and N. White, *Sensor applications of thick film technology*, IEEE Proceedings on Solid-State & Electron Devices, 135 (4), 77-84, 1988.
- ⁷⁶ A. Cattaneo, R. Dell'Acqua, F. Forlani and L. Pirozzi, *Low-cost thick-film pressure sensor*, SAE Technical Paper, 45, 49–54, 1980.
- ⁷⁷ D. Crescini, V. Ferrari, D. Marioli and A. Taroni, *Triaxial thick-film load cell*, Sensors Mater., 5, 45-55, 1993.
- ⁷⁸ J. K. Atkinson, R. P. Siona and J. D. Turnera, *A novel accelerometer using thick-film technology*, Sens. Actuators, B, 37, 348-351, 1993.
- ⁷⁹ M. G. Norton, Q. M. Reynolds, *Thick-film platinum temperature Sensor*, Microelectronics International, 2, 31-44, 1985.
- ⁸⁰ A. Alberigi-Quaranta, et al., *Magnetoresistive properties of Ni-based thick-films*, J. Mater. Sci.- Mater. Electron., 1(2), 118-122, 1990.
- ⁸¹ B. Morten, G. De Cicco, M. Prudenziati, A. Masoero and G. Mihai, *Magnetoresistive thick-film sensor for linear displacements*, Sensors Actuators A, 46-47, 261-5, 1995.
- ⁸² J. K. Atkinson and J. A. Mihell, *Planar thick-film pH electrodes based on ruthenium dioxide hydrate*, Sens. Actuators, B, 48, 505-511, 1998,.
- ⁸³ P. J. Holmes, R. G. Loasby, *Handbook of Thick Film Technology*, Electrochemical Publications, 1976.
- ⁸⁴ R. E. Belford, A. E. Owen and R. G. Kelly, *Thick-film hybrid pH sensors*, Sens. Actuators, B, 11, 387-398, 1987.
- ⁸⁵ H. N. McMurray, P. Douglas and D. Abbot, *Novel thick-film pH sensors based on ruthenium dioxide-glass composites*, Sens. Actuators, B, 28, 9-15, 1995.
- ⁸⁶ R. Koncki and M. Mascini, *Screen-printed ruthenium dioxide electrodes for pH measurements*, Analytica Chimica. Acta., 351(1), 143-149, 1997.
- ⁸⁷ A. Fog and R. Buck, *Electronic semiconducting oxides as pH sensors*, Sens. Actuators, B, 5, 137-146, 1984.
- ⁸⁸ D. J. Ives and G. Janz, *Reference Electrodes: Theory and Practice*, Academic Press, 1961.
- ⁸⁹ A. W. J. Cranny & J. K. Atkinson, *Thick film silver–silver chloride reference electrodes*, Meas. Sci. Technol., 9, 1557-1565, 1998.

-
- ⁹⁰ D. Desmond, et al., *Evaluation of miniaturised solid state reference electrodes on a silicon based component*, Sens. Actuators, B, 44, 389-396, 1997.
- ⁹¹ A. Mroz, *Disposable reference electrode*. Analyst., 123(6), 1373-1376, 1998,.
- ⁹² A. Simonis, et al., *New concepts of miniaturised reference electrodes in silicon technology for potentiometric sensor systems*. Sens. Actuators, B, 103(1-2), 429-435, 2004.
- ⁹³ A. Kisiel, et al., *All-solid-state reference electrodes based on conducting polymers*, Analyst., 130(12), 1655-1662, 2005.
- ⁹⁴ R. Martínez-Máñez, et al., *A multisensor in thick-film technology for water quality control*, Sens. Actuators, A, 120(2), 589-595, 2005.
- ⁹⁵ Ł. Tymecki, E. Zawierkowska and R. Koncki, *Screen-printed reference electrodes for potentiometric measurements*, Analytica. Chimica. Acta., 526, 3-11, 2004.
- ⁹⁶ T. M. Lee, *Over-the-Counter Biosensors: Past, Present, and Future*, Sensors, 8, 5535-59, 2008.
- ⁹⁷ A. Gac, J. K. Atkinson, Z. Zhang, and R. P. Sion, *A comparison of thick-film chemical sensor characteristics in laboratory and on-line industrial process applications*, Meas. Sci. Technol., 13, 2062-2073, 2002.
- ⁹⁸ ASTM D341, *Standard Practice for Viscosity-Temperature Charts for Liquid Petroleum Products*, Book of Standards Volume: 05.01, 2009.
- ⁹⁹ A. Cranny, J. K. Atkinson, *Thick film silver-silver chloride reference electrodes*, Science and Technology 9:1557-65, 1998.
- ¹⁰⁰ Kittiwake online resource, *TAN testing helps to Significantly Reduce Downtime*, 2013.
[viewed; available online: <http://www.kittiwake.com/total-acid-number-drop-test>]
- ¹⁰¹ R Wurzbach, *Lubricant Oxidation Analysis and Control*, Practicing Oil Analysis, Machinery lubrication, 2000.
- ¹⁰² Basu, A., et al., *Smart sensing of Oil Degradation and Oil Level Measurements in Gasoline Engines*, SAE Technical Paper Series 2000-01-1366. SAE World Congress Detroit, 2000.
- ¹⁰³ Kauffman, R.E., *Rapid Determination of Remaining Useful Lubricant Life*, Handbook of Lubrication and Tribology, Volume III, CRC Press, 1994.
- ¹⁰⁴ Noria Corporation, *A Comprehensive Look At the Acid Number Test*, 2013.
[viewed; available online; <http://www.machinerylubrication.com/Read/1052/acid-number-test>]
- ¹⁰⁵ Wear Check Africa, 'Effects of temperature on engine lubricating oil', Technical bulletin, Issue 43, 2008.
[viewed; available online: <http://www.wearcheck.co.za/downloads/bulletins/bulletin/tech43.pdf>]
- ¹⁰⁶ A. Capon, R. Parsons, *The oxidation of formic acid on noble metal electrodes. II. A comparison of the behaviour of pure electrodes*, J. Electroanal. Interf. Chem. 44, 239-254, 1973.
- ¹⁰⁷ S. Ogano, *Electrochemical Control of Friction and Wear*, University of London, London, 1998.
- ¹⁰⁸ J. K. Atkinson, M. Glanc, M. Prakorbjanya and M. Sophocleous, *Thick film screen printed environmental and chemical sensor array reference electrodes suitable for subterranean and subaqueous deployments*, Microelectronics International: 30, 2, pages 92-98, 2013.